



“Internal Combustion Engine”

Final Design Report

Instructor:
John Fabijanic

Sponsor:
Joseph Mello

Mechanical Engineering Department
California Polytechnic State University
San Luis Obispo

Jason Wu
jwu73@calpoly.edu

Philippe Daniel Habets
phabets@calpoly.edu

Sam S. Flood
ssflood@calpoly.edu

Paing Htet Lin
Plin06@calpoly.edu

Ricardo Cuevas
Rcueva01@calpoly.edu

Table of Contents

Executive Summary	7
Introduction	7
 Competition	8
 Existing Designs.....	9
Competition Winners.....	9
Previous Cal Poly Engines.....	9
 Technology Research.....	9
Intake and Exhaust.....	9
Thermodynamics	11
Compression Ratio	15
Bore to Stroke Ratio.....	16
Air Starting Systems	17
Customers	18
 Summary of Meetings/Interviews.....	18
Dr. Mello Interview – April 11 th , 2019.....	18
Will Sirski Interviews	18
Dr. Lemieux Interview – April 24 th , 2019	19
Objective.....	19
 Problem Statement	19
 Customer Needs.....	19
 QFD	20
 Final Product Specifications	21
 Concept Generation	22
 Concept Evaluation	24
Thermal Management Structure Evaluation	25
Insulation Material Evaluation.....	26
Intake/Exhaust Evaluation	28
Electric Starting System	31
 Preliminary Concept Design	32
Thermal Management	33
Intake and Exhaust.....	35
Compression Ratio	36
Electric Starting System	37
Final Design.....	38
 Post-CDR Change Summary	39
Thermal Management System.....	39
Intake and Exhaust.....	39
Dynamometer Fixture.....	39
Electric Starting System	39
Electronic Fuel Injection.....	40

Thermal Management System	40
Intake and Exhaust	42
Resonator.....	42
Exhaust.....	43
Lotus Engine Simulation.....	44
Safety and Maintenance	46
Manufacturing Plan	47
Design Verification Plan	47
Bill of Materials	48
Dynamometer Fixture	49
Reduction Power Train	49
Engine Mount	55
Safety and Maintenance	56
Manufacturing Plan & Report	57
Design Verification Plan & Report	60
Bill of Materials and Cost Summary	61
Electric Starting System	62
Motor	62
Clutch & Reduction Systems	64
Mounting Bracket	66
Safety	68
Packaging, Repair, and Maintenance.....	68
Manufacturing Plan & Report	70
Design Verification Plan & Report	73
Bill of Materials and Cost Summary.....	74
Electronic Fuel Injection	75
Design Overview	75
Safety	76
Repair and Maintenance.....	76
Manufacturing Plan	77
Design Verification Plan	78
Preliminary Testing	78
Testing Results	79
ECU Software	80
Preliminary Data & Conclusions.....	82
Scope of Work.....	83
Roles and Responsibilities	84
Project Management.....	84
Design Process	85
<i>Conclusion & Recommendations</i>	<i>85</i>
Engine Mechanical Design	85
Dynamometer Fixture	86
Electric Starting System	86
Intake System	86

Electronic Fuel Injection	87
Closing Statements.....	88
References.....	89
Appendices.....	91

Table of Figures

Figure 1: Intake with In-Series Resonator	10
Figure 2: Rel. Vol. Eff. vs. Exhaust length [m] for a 500cc Engine	11
Figure 3: Exhaust Temp vs. Exhaust Length for a 500cc Engine	11
Figure 4: Efficiency of a Spark Ignition Engine vs Nominal Compression Ratio [Ferguson & Kirkpatrick Fig. 13.13].	12
Figure 5: Predicted Efficiency Ratio of an Over-Expanded Engine (Over a Standard Otto Cycle) vs. Expansion:Compression Ratio [Ferguson & Kirkpatrick Fig 2.8].	13
Figure 6: Power Ratio (Over Expanded over Otto) vs. Expansion:Compression Ratio [Ferguson & Kirkpatrick Fig 2.9].	13
Figure 7: A qualitative PV plot of a typical Otto cycle (1-2-3-4 _{Hot}), and one for a cold engine (1-2-3-4 _{Cold}). The reduction in net work is shaded in yellow-green and is the area enclosed by (4 _{Cold} -3-4 _{Hot}).	14
Figure 8: Average BSFC vs. Average Engine Temperature (Calculated from Data Reported by Will Sirski).....	15
Figure 9: Plot of Net Indicated Efficiency at Three Different Bore to Stroke Ratios.....	17
Figure 10: Clockwise from the top left: 1. An exhaust pipe wrapped around the cylinder head, 2. A modular insulation design, 3. A hot oil pumping system, and 4. An active heat transfer controller.	22
Figure 11: Honda GX35 Clutch Mechanism.	23
Figure 12: Radar plot associated with material selection decision matrix	27
Figure 13: Heat Rejection by Convection and Conduction from Equivalent Surface Areas Using Reported Aluminum Material Properties and a Horizontal Fin Convection Coefficient.....	28
Figure 14: Intake with In-Series Helmholtz Resonator.....	29
Figure 15: Volumetric Efficiency Curves for Different Volume Ratios.....	29
Figure 16: Plot of Torque and Horsepower vs. RPM	30
Figure 17: Assembly of the Concept Design Model.....	32
Figure 18: Preliminary concept model for the ICE thermal management system	33
Figure 19: The lower thermal management box features a thermal insulation to retain monoblock heat, unimpeded output shaft, a retaining/sealing lip for the upper half, and a low emissivity coated surface.....	34
Figure 20: The upper thermal management box features a thermal insulation to retain monoblock heat, semi-sealed intake and exhaust ports and a low emissivity coated internal surface.....	34
Figure 21: Preliminary design of the intake system with a Helmholtz resonator	35

Figure 22: Preliminary design of exhaust pipe	36
Figure 23: Secondary Exhaust Cam Lobe in the Fully Deactivated (Left) and Activated (Right) Positions.....	37
Figure 24: ICE Honda Clutch Drum.....	37
Figure 25: Early Starter Bracket Prototype.....	38
Figure 26: Revised Electric Starting System	40
Figure 27: Engine covered in thermal shroud.....	41
Figure 28: Isometric Section View of Initial Design of Resonator.....	42
Figure 29: Schematic of Exhaust with Components.....	44
Figure 30: Volumetric Efficiency Curves of the Honda GX35 from Lotus Simulation	45
Figure 31: Volumetric Efficiency Curves from Helmholtz Theory.....	46
Figure 32: Intake/Exhaust Valve Operation.....	48
Figure 33: Gear Train Reduction and Dynamometer Concept	50
Figure 34: Decision Matrix for Reduction System Selection	50
Figure 35: Set up of the Pre-CDR Belt Drive Reduction System.....	51
Figure 36: Assembled View of the Dynamometer Fixture (Post CDR)	52
Figure 37: Bearing Rating Calculator	53
Figure 38: Large Pulley Subassembly	53
Figure 39: Engine Flywheel and Small Pulley Assembly.....	54
Figure 40: Bearing Plate Subassembly	54
Figure 41: Tensioner Subassembly.....	55
Figure 42: Exploded View of the Engine Mount.....	56
Figure 43: Engine, Engine Mount and Coupler Assembly	58
Figure 44: Dynamometer Fixture Assembly.....	58
Figure 45: Undersized Bearing Plate End.....	59
Figure 46: Oversized Bearing Bore Issue	59
Figure 47: Dynamometer Reduction Fixture Final Assembly (During Testing)	60
Figure 48: Electric Starting System	62
Figure 49: Comparison of Simulated Work vs. Crank Angle for the Yamaha and Honda.....	63
Figure 50: Starter motor mounting hole angle.....	64
Figure 51: Clearance Requirements for Starter Gear.....	65
Figure 52: Proposed Alternative Manufacturing Method for the Original Starter Bracket	66
Figure 53: Measuring the mounting hole and crankshaft locations of the GX35 on the Mustang 60 CMM	67
Figure 54: The new bracket design.....	67
Figure 55: Packaging of Starter and Engine Assembly in SMV Chassis.....	68
Figure 56: Starter Bracket Mounting	69
Figure 57: Exploded Diagram of Starting System	70
Figure 58: The gear with the remains of the outer race in the bore (left). Marring on the face of the gear was from the vise while attempting to remove the race with a drift. The pieces of the race after	

slicing and removal (right).....	71
Figure 59: The custom groove cutting tool.....	71
Figure 60: The finished gear and adaption shaft threaded onto the engine.....	72
Figure 61: The gear and adaption shaft with the retaining c-clip.....	72
Figure 62: The finished bracket with starter motor attached before fastener trimming.....	73
Figure 63: RPM plot used for estimating cranking speed.....	74
Figure 64: Wiring Diagram for EFI system.....	78
Figure 65: Engine Configuration as coupled to the dynamometer	79
Figure 66: Ecotrons ECU software illustrating live-data variables.....	80
Figure 67: Engine Performance Data plotted with Ecotrons Data Analyzer for a sample dynamometer run.	81
Figure 68: Lookup tables for advanced injection tuning within the Ecotrons software.....	82
Figure 69: Wiring Pinout for Stock EFI ECU.....	88

Table of Tables

Table 1: Design Parameter Targets with their Associated Tolerances, Risks, and Method of Compliance	21
Table 2: Decision Matrix for Thermal Management Structure.....	26
Table 3: Decision Matrix for Thermal Insulation Material Selection.....	27
Table 4: Intake and Exhaust decision matrix	30
Table 5: Starter Engagement Decision Matrix.....	31
Table 6: Starter Reduction Type Decision Matrix	32
Table 7: Engine Configurations of the Honda GX35 for Lotus Simulation	45
Table 8: Summary of Manufacturing Plan for Intake and Exhaust.....	47
Table 9: Intake and Exhaust Bill of Materials	49
Table 10: Bill of Materials for the Dynamometer Fixture	61
Table 11: Cold-Air Model Estimates of Compression Work for Yamaha and Honda	63
Table 12: Engine Package Location.....	69
Table 13: Electric Starting System Bill of Materials	75
Table 14: EFI Bill of Materials	76
Table 15: Preliminary Power & Torque Test Data	82
Table 16: Individual Roles and Responsibilities.....	84
Table 17: AGMA Input Factors	111
Table 18: Bearing Calculation Input Factors	111
Table 19: Starter Calculation Results.....	111

Executive Summary

The ICE Team was tasked with the selection of an internal combustion engine for use in the Supermileage Shell ECO-Marathon competition. In addition to selecting the engine, the team designed and developed a series of modifications to the existing engine to adhere to the rules and regulations of the competition. The team also allocated significant resources to the design and manufacture of a dynamometer adapter that will allow the Supermileage team to continue the work and tune an extremely efficient fuel-injected internal combustion engine. The modifications and subsystems developed by team ICE are outlined below:

- Design and manufacture an intake piping system to minimize pumping losses.
- Design and manufacture a dynamometer mount for engine testing with in-house equipment.
- Design and manufacture a starting system which complies with Shell Eco-marathon rules.
- Select and install components required for Electronic Fuel Injection (EFI).
- Design a thermal management system for future development by the Supermileage team.

The manufacture of the exhaust piping system has been postponed until Ricardo Cuevas returns to Cal Poly.

Testing was delayed by the extensive development required for the dyno adapter. This meant that data needed to fully evaluate the efficacy of the thermal, intake, and starting systems was not collected. However, the dyno adapter and engine systems are now fully operational, paving the way for future development by the Supermileage and future senior project teams.

The engine and all associated components developed by team ICE are discussed in the following sections. Each system is designed to be stand-alone, such that future development on each subsystem may be completed independently without a great effect on the other systems. We at ICE believe that this division will allow the Supermileage team to optimize the engine for greater effect in competitions to come.

Introduction

The goal of this project is to modify a Honda GX35 engine to improve its fuel efficiency and maximize its competitiveness in the Shell Eco-marathon competitions. This competition has tight restrictions on the type of fuel used to power the engine, but otherwise has very few rules limiting the type of modifications which may be made. Our primary goals are to maximize volumetric efficiency and maintain an efficient operating temperature. Future work might pursue more advanced technologies such as pseudo-atkinson cycle operation.

Team members:

Ricardo Cuevas: Secretary, Testing Co-Coordinator

Sam Flood: Testing Coordinator, Co-Editor

Philippe Habets: Project Planner, Co-Editor

Paing Htet Lin: Manufacturing Lead

Jason Wu: Point of Contact, Treasurer

Background

The Cal Poly Supermileage team is responsible for the design and development of a hyper-efficient internal combustion engine vehicle. Each year, the team designs and fabricates a car capable of achieving over 1000

miles per gallon. With this vehicle, the team competes in the Shell Eco-marathon competition and has historically performed very well. Since beginning the competition, The Cal Poly team has consistently placed within the top ten and repeatedly within the top three.

Supermileage car gets 2,752 MPG

JON - APRIL 30, 2008



Ryan Chartrand

In the day and age in which car dealers exclaim over the efficiency of an automobile that gets 40 miles per gallon, the Cal Poly Supermileage Team will sit back and laugh at their enthusiasm.

After all, the team just built a car that gets 2,752.3 miles per gallon. No, that's not a typo.

Since 2006, the Cal Poly Supermileage team (hereafter SMV) has entered into the Shell Eco-marathon competition. Five years ago, the team changed from a Honda GX35 engine to a 50cc Yamaha out of a scooter. The predicted advantages of this new engine have not been realized. While it is much more powerful and has a 3 valve cylinder head, it is also larger, heavier, and less fuel efficient. Therefore, the ICE team will develop an initial set of modifications to produce a competitive and reliable Honda GX35.

Competition

The relevant Shell Eco-marathon rules state that [2]:

- The fuel will be 87 octane [Section 4A, Article 53, Subsection a]
- The engine may consume only the fuel provided by the event organizers (and must not consume engine oil). [Section 4B, Article 59]
- Electric fuel pumps are not permitted. [Section 4B, Article 60, Subsection a]
- Fuel tanks may be pressurized. [Section 4B, Article 60, Subsection b]
- Auxiliary energy sources (chemical, latent energy from phase changes, etc.) are not permitted. [Section 4B, Article 60, Subsection c]
- The external regulation temperature of the engine by external heating devices is limited to 100°C (212°F). [Section 4B, Article 60, Subsection f]
- Fuel injection must be used. [Section 4B, Article 62, Subsection e]
- The fuel system may not be heated or cooled beyond ambient temperatures.
- Air filters are prohibited. [Section 4B, Article 62, Subsection f]
- Blow by gases must be captured and may not be recirculated. [Section 4B, Article 62, Subsection f]
- An electric starter must be used. Manual hand starting is prohibited. [Section 4B, Article 64, Subsection a]
- An electric starter must never be capable of providing any forward propulsion to the vehicle. [Section 4B, Article 64, Subsection b]

In addition, through interviews with the SMV team we have determined that the team often warms up the engine in the pits before the race, and that they operate the vehicle on a "burn and coast" cycle. This method involves running the engine at full-throttle for a short period, and then shutting it off and coasting the

vehicle. This process is repeated again and again until the race is complete.

Existing Designs

Competition Winners

There is little published information on our competitor's engine designs. Through research into the winning teams' websites, talking with faculty, and reading publications from these teams certain information has been gleaned.

According to the lead of the Lavol team, much of their success is rooted in an extremely small bore diameter and associated piston. The team currently downbores their engine to match with a 35cc Honda piston. In addition to the extremely constricted bore, the Lavol engine has been fitted with a custom cylinder head. The head has a unique design that allows the compression ratio to change based on the thickness of an intermediary plate between the cylinder block and the head. This intermediary plate can be changed based on the modifications running on the engine at any given moment.

BYU has developed an engine that rivals Lavol in terms of efficiency. Research has indicated that in order to achieve the efficiency out of the much larger Briggs and Stratton engine (~200cc in original specification), they have used an extremely large bore-to-stroke ratio of 1:4. According to their research, this allows for the complete combustion of the fuel in the cylinder while producing the maximum amount of rotational energy out of a miniscule amount of fuel. In addition to the reduced bore-stroke ratio, BYU developed a custom cylinder head.

Previous Cal Poly Engines

The Cal Poly Supermileage team has been competing in the Shell Eco-marathon for the last 13 years. In order to learn from previous development, we examined the engines that the Cal Poly team has used at the Eco-marathon previously. Dr. Mello stated that the previous Honda 35cc engine was very competitive compared to the current Yamaha 50cc. He reported that the major motivation for moving to the Yamaha engine was the 3 valve head (vs. 2 valves on the Honda engine), but it does not appear that the possibility for reduced pumping losses has resulted in an increase in fuel economy. Other specifications of the current Yamaha engine are a bore:stroke ratio of 1.2:1, a compression ratio of 13:1, and a redline of 5000 RPM. A stock Honda GX35 has a bore:stroke ratio of 1.35:1, a compression ratio of 8:1, and 7000 RPM redline.

Technology Research

In addition to examining current and previous engine designs, we wanted to see what strategies were used in the industry in order to achieve an increase in engine efficiency. In order to accomplish this goal we consulted with experienced faculty, Cal Poly Supermileage team members, and research documentation. Based on these results, and our personal knowledge of engines, we selected several key research areas to focus on. The results of our research and interviews are summarized here.

Intake and Exhaust

One of the major components of any internal combustion engine is the intake. The intake brings air (and more importantly oxygen) into the engine to combust with the gasoline to power the vehicle. During the combustion cycle, the inflow of air must be controlled through an intake to create the perfect ratio of fuel to air that will provide total combustion of the injected fuel.

The main goal of intake tuning is to improve the volumetric efficiency of the engine, which is the actual amount of air that fills the cylinder over the theoretical amount that it can actually hold. Higher volumetric efficiency translates to better power output, meaning less fuel is needed to achieve the same power. In short, volumetric efficiency has a direct relation to fuel efficiency.

The method investigated for improving volumetric efficiency comes from the Helmholtz resonator theory, an approach well investigated by H.W. Engelman. The theory is applied by inputting an in-series Helmholtz resonator (V2) onto the intake, which is modeled by Figure 1. The Helmholtz resonator acts on the theory of harmony and wave phenomena. As a charge of air flows into the resonator through the neck, the air will expand to fill up the chamber, resulting in an increase of pressure. In addition, the expansion cavity will cool the incoming air, allowing it to become denser.

As the air progressively fills the cylinder, its speed increases because of the increase of pressure inside the cavity. When the piston reaches bottom dead center, the valve will close but the air flowing through the manifold will still have velocity. This air will hit the closed valve and its pressure wave, which is the result of a pressure difference due to flow interruption caused by the closed valve, will back bounce in the opposite direction towards the resonator. Since there is a pressure differential in the resonator due to the expansion of the incoming air, the resonator will act as a spring for the pressure wave and cause it to proceed forward towards the valve again with the second set of incoming air. If the intake parameters are properly tuned to its appropriate RPM, this combined pressure wave will hit the valve right when it is open.

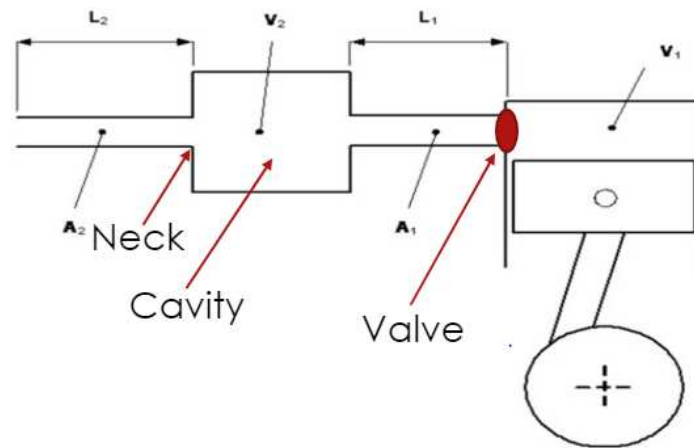


Figure 1: Intake with In-Series Resonator

Relative to intake tuning, exhaust tuning is more sensitive to changes with its pipe length. Small changes in its pipe lengths contribute to positive and negative efficiencies as seen in Figure 3. Intake tuning exhibits positive contributions for a wide range of intake lengths at a given RPM range. Exhaust tuning on the other hand, has positive and negative contributions with a potential increase in volumetric efficiency of up to 5% compared to 12% from the intake. The objective of the exhaust is to remove the toxic gases as soon as the exhaust valve opens. To simplify this, exhaust tuning is a little more sensitive due to scavenging. Scavenging is the process of removing the exhaust gas out of the cylinder and drawing in fresh charge of air through the intake. As the piston is at bottom dead center (BDC) the pressure in the cylinder is at its highest and as the piston moves toward top dead center (TDC) the pressure inside the cylinder will decrease

and as it reaches TDC the pressure difference between the gases inside the cylinder and the gas that is flowing through the exhaust will be minimal. As we know exhaust gas flows from high to low pressure and if the pressure inside the cylinder and the exhaust are the same, the exhaust will not want to evacuate. If this happens, the next combustion cycle will be less effective and the tuning of the intake would have been in vain.

Exhaust tuning is highly dependant on its temperature and RPM range which can be seen in Figure 3, with an inverse relationship between the two. Unfortunately, exact temperatures of the exhaust will not be obtained until the engine gets dynoed in the upcoming Fall quarter. The figures shown are reference to a single piston, 4-stroke, 500cc engine.

As can be seen in Figure 2, small changes in pipe length contribute to sudden changes in volumetric efficiency.

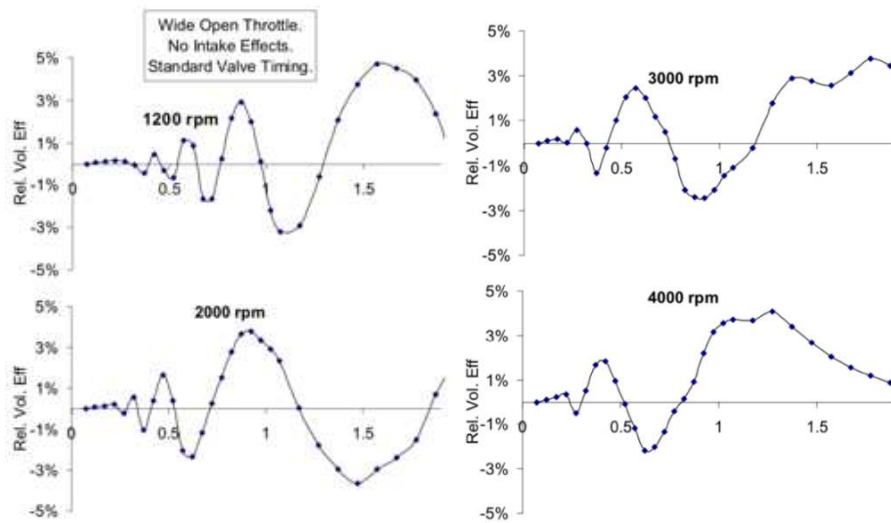


Figure 2: Rel. Vol. Eff. vs. Exhaust length [m] for a 500cc Engine

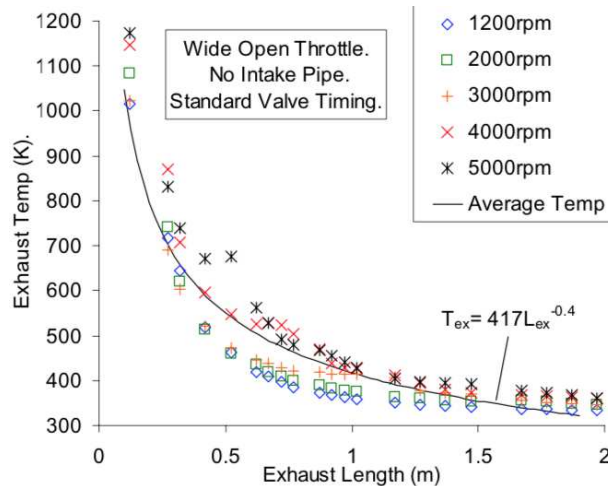


Figure 3: Exhaust Temp vs. Exhaust Length for a 500cc Engine

Thermodynamics

Both of the textbooks used in Cal Poly's Combustion Engine Design class (ME 444) [Ferguson][Heywood] show that efficiency improvements can be made by making to modifications the thermodynamic cycle. The amount of heat transfer from the combustion chamber is also expected to have an impact on the engine's efficiency. These two concepts are explored in detail below.

Large changes in engine performance through the manipulation of compression ratio, expansion ratio, and type of combustion (compression vs. spark ignition) are well documented. Of these, we consider only the compression and expansion ratio because of the difficulty of controlling gasoline compression ignition.

Compression Ratios (see [Compression Ratio](#)): The compression ratio is the volume of the cylinder at the end of the intake stroke divided by the volume at the end of the compression stroke. Increased compression ratios lead to increased efficiency. For example, a compression ratio of ~17:1 results in a brake thermal efficiency of ~40% compared to ~35% at 9:1. The theoretical (Otto), realized (Indicated), and realized less frictional losses (Brake) efficiencies are plotted in Figure 4 (reproduced from Ferguson and Kirkpatrick).

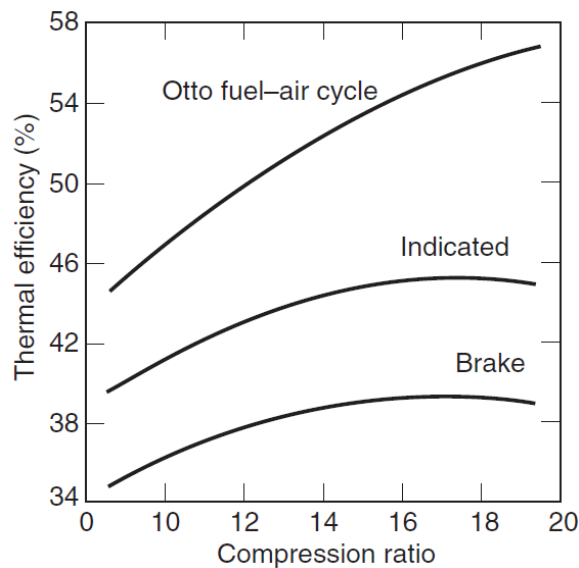


Figure 4: Efficiency of a Spark Ignition Engine vs Nominal Compression Ratio [Ferguson & Kirkpatrick Fig. 13.13].

The realized efficiency curves differ from the idealized Otto cycle for several reasons including:

- Mechanical friction – various sources for mechanical friction exist, chief among them are the piston rings. The magnitude of this loss increases with increasing engine speed.
- Pumping inefficiencies – the engine cannot completely fill the cylinder with fuel air mixture due to the finite time and valve area available.
- Finite time – heat addition and rejection cannot happen instantly at constant volume, therefore some efficiency is lost.

Additionally, increasing the compression ratio can lead to issues such as uncontrolled combustion, increased frictional and heat losses, an increased compression work input. These issues can be partially counteracted by more advanced engine technologies such as exhaust gas recirculation [4] but they still have limitations and ICE does not have sufficient design resources to pursue these options.

Expansion Ratios: The expansion ratio is the volume of the cylinder at the end of the exhaust stroke divided by the volume of the cylinder at the end of the compression stroke. An engine with a larger expansion than compression ratio is described as being “over-expanded.” As seen in Figure 5 an expansion:compression ratio of 2.5:1 netted a 25% efficiency gain over a 1:1 ratio.

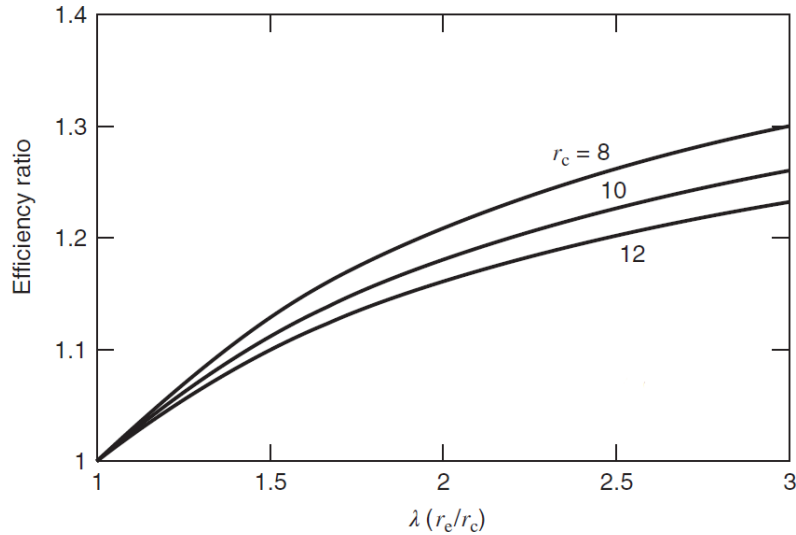


Figure 5: Predicted Efficiency Ratio of an Over-Expanded Engine (Over a Standard Otto Cycle) vs. Expansion:Compression Ratio [Ferguson & Kirkpatrick Fig 2.8].

However, increased expansion ratios reduce power production for a given cylinder volume. The same 2.5:1 expansion:compression ratio engine produced ~45% less power than one operating at a 1:1 ratio. This is because the effective volume of the cylinder – that is, the volume of air combined with fuel and combusted – is substantially reduced.

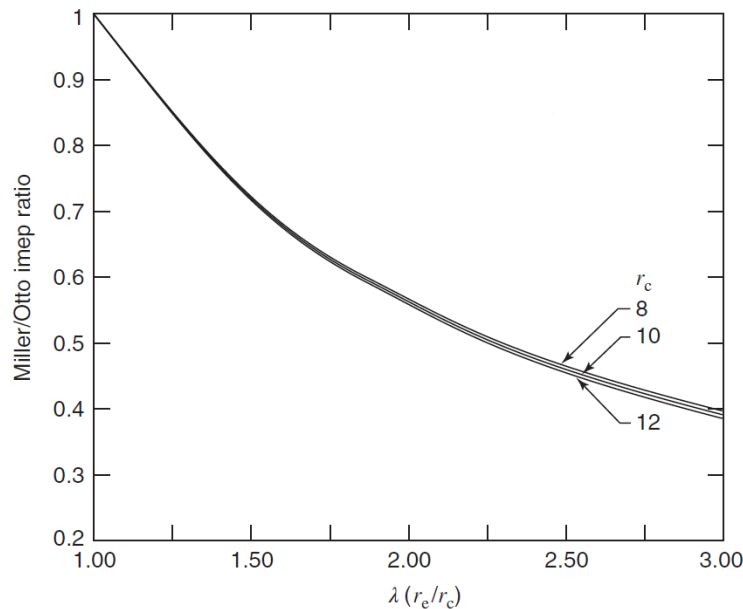


Figure 6: Power Ratio (Over Expanded over Otto) vs. Expansion:Compression Ratio

[Ferguson & Kirkpatrick Fig 2.9].

These types of engines operate on the “Atkinson” or “Miller” cycle (the later employing some kind of forced induction in order to restore power density). These cycles are being emulated by some manufacturers through the use of modified valve timing (e.g. Toyota closes the intake valve after the beginning of the compression stroke on some engines) but we are not sure if the associated power density (power per engine weight) penalty is worth the increase in efficiency. If the power density is too low, then a larger engine will be needed to provide sufficient power. The larger engine will mean a heavier vehicle, which will need more power to get to the speed required, which will require a larger engine. This positive feedback will settle out eventually, but if we can have a smaller engine, then we will need less fuel. We anticipate that there will be a local minimum of the trade off between power density and expansion ratio, and suggest exploring these trends through the use of simulation tools.

Heat Transfer: Additional efficiency can be gained by reducing heat transfer from the combustion chamber. This heat transfer represents an energy loss which could otherwise be used to accelerate the vehicle. As can be seen from the 2D equation for convective heat transfer, the rate of heat transfer is affected by the surface area:volume ratio of the cylinder, the engine operating temperature, and the time required for complete combustion.

$$\dot{Q} = hA(T_f - T)$$

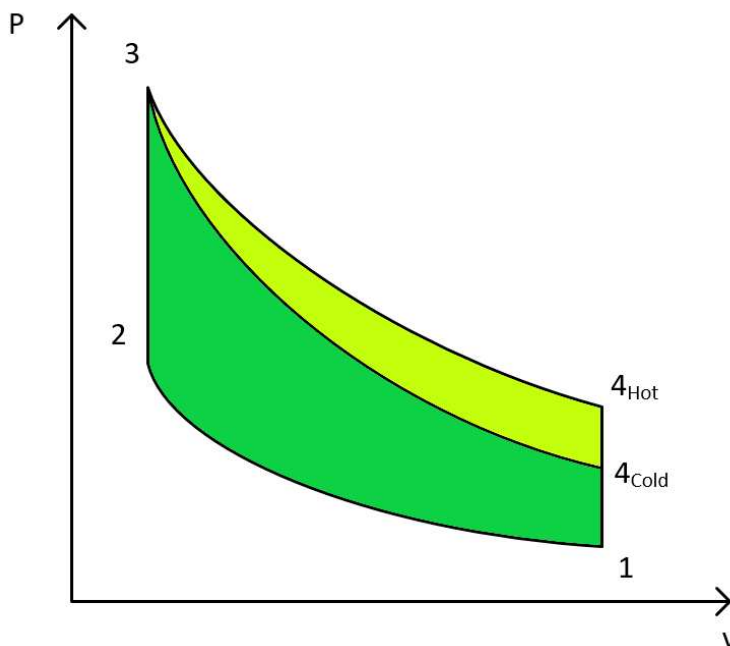


Figure 7: A qualitative PV plot of a typical Otto cycle (1-2-3-4_{Hot}), and one for a cold engine (1-2-3-4_{Cold}). The reduction in net work is shaded in yellow-green and is the area enclosed by (4_{Cold}-3-4_{Hot}).

- *Area:Volume ratio* (see [Bore:Stroke](#)): Note that the amount of fuel burned is proportional to the cylinder volume, but heat transfer is related to the surface area. Therefore a small area:volume ratio is preferred.
- *Engine temperature:* A higher engine temperature will reduce the $(T_f - T)$ term (and therefore the

heat transfer). Will Sirski's dyno testing investigated this effect. During interviews with our team he reported that efficiency was highly correlated with cylinder head temperature. Team ICE saw the same trend in the data (see Figure 8), but would like to collect additional data.

- *Time:* If the combustion can occur rapidly less heat will be lost. However, the flame speed of combustion is dependent on complex fluid dynamics.

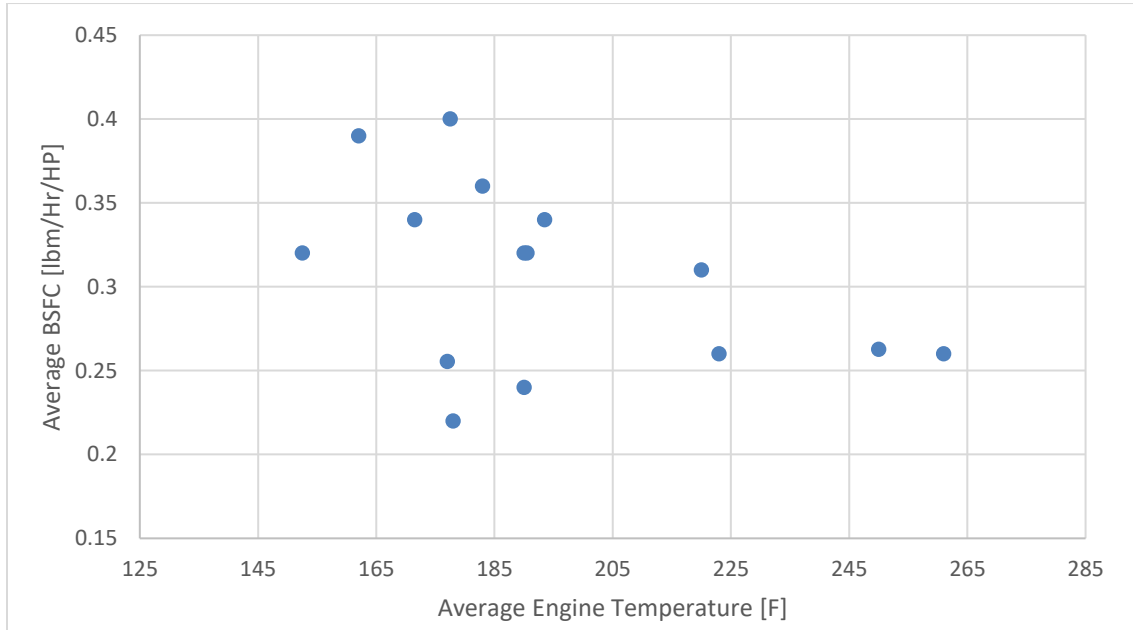


Figure 8: Average BSFC vs. Average Engine Temperature (Calculated from Data Reported by Will Sirski)

However, it is important to realize that fundamental thermodynamics requires that a certain percentage of the energy must be rejected as heat. Team ICE anticipates that, on top of this lower limit, additional energy will be lost to engine warm-up. This additional loss is caused by increased heat transfer when the engine is cold (and therefore a high $T_f - T$ term). This heat transfer will lead to a reduced cylinder pressure and reduced net work. A qualitative plot of this process vs. a typical Otto cycle process is presented in Figure 7. In order to minimize these losses and others, we will design and construct a system to maintain the engine temperature at its optimum over the anticipated burn-coast cycle.

To conclude, there are numerous methods for improving an engine's efficiency through manipulation of its thermodynamic cycle and parameters relating to heat transfer. Many of these manipulations can be made by carefully selecting the engine's geometry.

Compression Ratio

In the automotive racing industry, obtaining a relative high compression ratio is one of the ideal objectives for manufacturers. A compression ratio is a ratio where the maximum cylinder volume is compressed into the minimum cylinder volume. With a piston moving up and down inside of the cylinder, the lowest point of the piston is called the Bottom Dead Center where the cylinder volume is the highest. The highest point of the piston in the cylinder is called the Top Dead Center, where the cylinder volume is the lowest. Comparing the two volumes will output the compression ratio.

Air and fuel get compressed in the cylinder. Having an engine with a high compression ratio means that a given volume of air and fuel is being squeezed into a much smaller space than an engine with a lower compression ratio. Engine power is generated when combustion exerts a force on the piston, causing the piston to go down the cylinder during the expansion stroke. The higher the piston is in the bore when combustion starts, the greater the force that will be exerted. As the compression ratio increases, the piston travels higher in the bore at the top dead center meaning there is additional force for the same amount of fuel which equates to higher efficiency.

During the interview with Dr. Lemieux, he stated that there is a point of diminishing returns for an increased compression ratio; can't increase it without bound. In an actual engine other processes which affect engine performance and efficiency will vary with changes in compression ratio, such as: combustion rate and stability, heat transfer, and friction. While the geometric aspect of compression ratio (ratio of maximum to minimum volume) is well defined, the actual compression and expansion processes in engines depend on multiple factors. These factors include valve timing details and the importance of flow through the valves while they are opening or closing (which depends on engine speed). While obtaining higher compression ratios is great, there are limits to how high compression ratios can be before efficiencies and mean effective pressures start to decrease in engines. In addition, the ability to increase the compression ratio is limited by the octane quality of available fuels and knock.

Bore to Stroke Ratio

During the interview with Will Sirski and Dr. Mello, we discussed several possible parameters that could affect the engine fuel efficiency based on the lessons learned from the competition. One of the parameters that have a significant impact on the fuel efficiency is engine's bore to stroke ratio and therefore, the team decided to do background research on that topic.

Bore to stroke ratio is the ratio of the cylinder bore diameter and the length of the piston stroke. Smaller bore to stroke ratios reduces the surface area to volume ratio when the piston is at the top dead center. This reduces the heat loss from the combustion and improve the engine thermal efficiency. Smaller bore to stroke ratio also minimizes the flame travel distances and reduces heat release duration. These results will lead to a low performance but high fuel efficiency for the engine.

Moreover, based on the research, the team discovered that the reduction of the bore to stroke ratio will not lead to the direct increase in engine efficiency. A study conducted by Hyundai Motor Company states that the effect of efficiency increase was saturated near the bore to stroke ratio of 0.83.

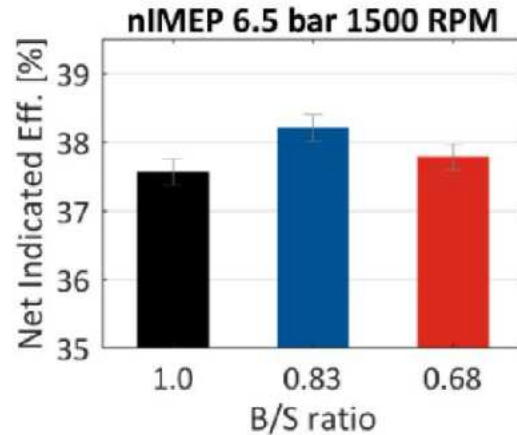


Figure 9: Plot of Net Indicated Efficiency at Three Different Bore to Stroke Ratios

Significant improvement in efficiency occur when it is reduced from the bore to stroke ratio of 1 to 0.83, but when the ratio is further reduced to .68, the data showed no further improvement. Although the flow enhancement is obtained from the additional decrease in bore to stroke ratio, this could lead to a greater cooling loss and hence no further increase in engine efficiency.

Air Starting Systems

During the Preliminary Design Review, Mr. Fabijanic brought up the possibility of using an electrically activated air starting system. We are concerned that this may be interpreted as not complying with the rules: “Article 64: Starter a) An electric starter must be used during the competition.”[Shell Eco-Marathon Rules]. We believe that it would be prudent to bring a back-up, electric only system to competition if an air-system is selected. In any case, we decided to take a preliminary look at air-starting.

Injecting compressed air into the cylinder is used in multi-cylinder engines, but we don’t see that as a viable strategy for this engine. There is only one cylinder, so it is foreseeable that it would be difficult to build enough momentum in the flywheel by only pressurizing on the downstrokes. And pressurizing the crankcase to drive upstrokes would require additional valving (which carries a weight penalty), and likely a redesign of the crankcase seals and oil circulation pipe to tolerate the higher pressure.

Alternatively, an air-motor could be used in place of an electric starter. Air motors offer a high power density, which is certainly attractive. However, we think that the main issue with an air-starting system would be onboard compressed air storage. Modern batteries have achieved very good power densities, and we believe that a metal air tank would not compare well. Of course, if bump-starting would be used, then not much energy would need to be stored, and the power density of the air-starter may offset the losses in the tank. Another option to consider would be a composite tank.

However, we consider the risks of not complying with the Shell rules too high, and will therefore continue with a traditional, electric starting system.

Customers

The customers for this project are as follows:

1. Cal Poly Supermileage
2. Dr. Joseph Mello
3. ICE team Members

Cal Poly Supermileage team is the most important customer because the team is going to be the end user our engine selection. Our team had a meeting with Will Sirski, who was the engine lead for the Cal Poly Supermileage in 2019. After the interview, we learned about current engine related needs and available testing equipment. Another important customer for our team is Dr. Mello, who is our project sponsor as well as the faculty advisor for Cal Poly Supermileage team. Based on the interview with Dr. Mello, we were able to determine the project scope and the expectations from the sponsor regarding this project. Lastly, we also consider ourselves as customers because all team members will be working on the stages of designing, implementing and testing for this project. Using the information collected from these interviews, the team will come up with the list of needs that this project has to fulfill. The detailed list of the customer needs is attached as Appendix 1:.

Summary of Meetings/Interviews

Dr. Mello Interview – April 11th, 2019

Efficiency and reliability were the main concerns that Dr. Mello brought up during our first meeting. He mentioned that the current Yamaha engine was not providing the same level of efficiency as the Honda engine (which the Supermileage team used previously). He wanted our team to research parameters that could affect the engine efficiency. He suggested possible research areas and what he learned from this year's competition. With regards to the intake system, he mentioned that no other teams were using throttle bodies, and suggested that we investigate this and other intake and exhaust design choices. From this project, he expected that our team would be able to come up with a more efficient engine selection that could be handed off to the future engine subsystem for the Cal Poly Supermileage club.

In addition to some general guidelines, Dr. Mello made recommendations to the team about potential engines. The most discussed was the Briggs and Stratton Junior 206, which both Lavol and NIU are using to great effect. This also would allow the team to compete in the SAE Supermileage Competition. Mello also spoke of development into the Honda GX35, and suggested that the smaller displacement and much lower mass might offset some of the power constraints with such a small engine. The compromise between the large and small engines is the current 50cc Yamaha engine being used by the team. All parties agree that this engine is overpowered and ineffective for the present vehicle and competition.

Will Sirski Interviews

During our first meeting with Will Sirski on April 16th 2019, he pointed out the key improvements that he made to the current engine and the result of those modifications. He stated that he was able to achieve 53% efficiency on this current engine. He also explained the testing set up at the dynamometer and the possible sensors that could be useful for our engine testing. In addition, he mentioned about possible research areas such as pressure relief and adjustable cam shafts which could be implemented for the engine to improve the efficiency. He also advised the team to be aware of the manufacturing limitations for the project.

In a subsequent interview with Will, he mentioned that the officials at the Shell EcoMarathon like to see clear starter disengagement from the engine.

Dr. Lemieux Interview – April 24th, 2019

We consulted with Dr. Lemieux to make sure we did not miss any major areas of analysis and to get his impression of the areas with the biggest potential for gains to be made. Dr. Lemieux believes that the largest improvements will be made by managing the heat rejection from the engine. He recommended that we determine the steady state and transient (burn and coast) temperature distribution of the engine in the stock and modified configurations. Finally, he recommended that we avoid making a custom piston or cylinder head, and thinks that modifying the connecting rod is a more realistic goal. If we wanted to change the displacement of the engine, he thought a 'Frankenstein' approach (where components from one engine would be made to fit another) would have numerous advantages with regards to reliability and parts availability.

Objective

In this section, we present the problem statement and customer needs. Based on the customer needs, a QFD was created to scope out the project and brainstorm the possible modifications for the engine. Final product specifications were then generated to create a product that would be feasible and fulfill the customer needs.

Problem Statement

Team ICE strives to select and perform modifications which will result in an efficient and reliable engine that will compete in the Shell Eco-marathon. Our team will focus on improving efficiency without sacrificing reliability. To this end, we will design and build a thermal management system to maintain a selected engine temperature (which we will determine via dyno testing). Additionally, we will design and build intake and exhaust piping to minimize engine pumping losses, develop an electric starting system, and select and install an EFI/ESC system. We will also work with the new Cal Poly Supermileage engine team so that they are familiar with the engine and can continue development after the conclusion of our senior project. Finally we will work in the engines lab to benchmark the original engine and measure our progress from it.

Customer Needs

Team ICE met with customers and conducted interviews to determine their needs for our project. Using the customer statements from the interviews, the team came up with a list of requirements that this project has to satisfy. The list of requirements is tabulated and presented as [Appendix 1](#). The requirements are sorted into similar categories that the team used as “Whats” for our QFD. A summary of the top three categories are described below:

Efficiency: The main goal of Cal Poly Supermileage is to win the Shell Ecomarathon competition. In this competition, the team is judged on their vehicle’s fuel efficiency. Therefore it is essential that the engine used in the vehicle can provide the minimum power needed with the least fuel consumption. Moreover, the engine also needs to be compliant with the rules and regulations for each competition. The Cal Poly team and other teams appear to have had good success with the Honda GX35 engine, and it offers sufficient power in a lightweight, compact, small displacement package. Upon further discussion with Dr. Mello and

the SMV, Dr. Mello directed Team ICE to select the Honda GX35 as the development platform.

Weight: Since the vehicle needs to go around the track, it is also important that it has the least weight since it will lead to lower fuel consumption. Moreover, a lighter engine will be easy to transport and assemble. This means that when designing components for the engine, our team needs to select materials and designs which accomplish the design goals with minimum weight.

Reliability: One of Dr. Mello's main expectations is that our engine selection and modifications must be able to be passed onto the future engine subsystem team of Cal Poly Supermileage. Therefore, Team ICE needs to make the engine reliable as well as easy to operate and test.

QFD

ICE began developing the specifications for the new Honda GX35 engine by first completing a standard Quality Function Deployment (QFD). Refer to [Appendix 2](#) for QFD. ICE used a number scale for the "Who vs. What" sections to identify the important relationship between the two. The scale is as follows: 5 for very important, 3 for neutral, and 1 for weak. ICE determined that the customers ("Who") in this case are the Supermileage Assembly, Drivetrain, Chassis/Aero, Engine teams, the Supermileage Driver, and Dr. Mello. We have considered Dr. Mello's and the Engine team's priorities first, and will aim to satisfy the other customers when possible. For the needs/wants ("What") we identified the following list as the most important: powerful, easy to install, small/compact, light, efficient, quiet, vibration, and reliable.

From the "Who vs. What" section we concluded that Dr. Mello wants a reliable, efficient, and sufficiently powerful engine. In addition to those parameters, the engines team is somewhat interested in a quiet, and light engine which does not vibrate excessively. In general, all of the "Whats" had strong support amongst a few "Whos".

Our next step in the QFD was to examine the competition's and Cal Poly's engine designs. This proved to be difficult because competitors are not required to publish any information about their designs. We were able to find two papers: one covering an overhead cam cylinder head published by the Laval team, and a design overview from Northern Arizona University. Unfortunately these papers did not have all the information we needed. Fortunately, we were able to find more information in their marketing videos and material, but were unable to completely fill out the "Now" section of the QFD.

We moved on to the "How" and "How Much" sections in order to develop measurements of a successful engine design. Laval, BYU, and Canada UBC all run high compression ratios (from 12:1 to 17:1), low bore:stroke ratios (1:1.58 to 1:4) and low rpm (3000-5000RPM). This provided some confirmation of the trends we expected from our background research. The 1:4 bore:stroke ratio seems excessively high - we suspect that that engine runs on an over-expanded, Atkinson type, engine cycle.

In summary, the QFD provided some potential design targets (higher compression ratio, low bore:stroke ratio, and low rpm) and confirmed the effectiveness of these modifications which was predicted by our background research.

Final Product Specifications

Table 1: Design Parameter Targets with their Associated Tolerances, Risks, and Method of Compliance

	Parameter Description	Stock	Modified	Risk	Compliance
1	Brake Specific Fuel Consumption	0.6 lb/hr/HP	0.44 lb/hr/HP	H	A, T
2	Engine Power	1.3 HP	1 HP	H	A, T
3	Starter Reliability (# of Starts)	N/A	120	M	A, T
4	Volumetric Efficiency	80% (Estimate)	90%	M	A, T
5	Engine Control	Carburetor and Fixed Timing	EFI / ESI	M	I
6	Weight	7.6 lb	< 9.5 lb	L	A, T
7	Engine Temperature	Cold	170 °F	M	T

Modifying the compression ratio is tempting, but because the Shell Eco-marathon only allows for 87 octane fuel, we expect this avenue to be severely knock limited. We have developed a test plan to rapidly evaluate this limit, and will thereafter determine whether the efficiency gain is worth the development time. Similarly, we expect that modifying the bore:stroke ratio will be difficult due to the limited availability of parts in the required sizes and their specialized alloys and construction. Therefore, we propose to modify the engine in order to reduce energy loss by heat transfer and pumping inefficiencies, and to maintain an efficient operating temperature over the burn-coast drive cycle. These modifications will result in an engine specification better suited for the Shell Eco-marathon competitions (specifically: higher fuel efficiency).

In addition, we will make several quality of life modifications including an electric starting system. We evaluated the risk of each of these modifications and have considered how we would predict and test their results. The modifications, risks, and method of compliance determination are listed in Table 1. Concept Design

Our design process will include concept generation and evaluation, detailed design, testing, and validation phases. To date, we have made significant progress in the concept generation and evaluation phases, and look forward to beginning the detailed design and testing phases first this next quarter. The results of the concept generation and evaluation are presented in the following subsections.

Concept Generation

To avoid mental blocks during our initial ideation, we started with very general design goals. For the thermal system, we began with the idea of keeping warm items warm, but not too hot. Among others, we considered the techniques used in travel coffee mugs, winter athletic gear, and camping equipment. We then examined the engineering principles at work in each of the technologies. Each of the thermal systems limited heat transfer by conduction and convection in some way. Additionally, camping and athletic gear often provided some way to modulate the heat transfer through the use of vents, zippers, flaps, and other adjustments. We also noted that radiation might be an important heat transfer pathway due to the relatively high engine temperature.

Since the intake and exhaust have limited roles of inputting and outputting air to and from the engine, we generated ideas based on providing the best air flow. Starting with a stock intake we considered the curvature of its pipe, whether we wanted it to be curved or linear based on the RPM range we wanted to work at. The next step was to incorporate a resonator to help resonate the frequencies of the incoming flowing air and the opening and closing of the intake valve to further increase the volumetric efficiency. Again, since the role of the intake is to input air, we generated concepts of the resonator based on the organ pipe analysis and helmholtz resonance analysis. For the exhaust, we considered a similar approach as the intake, but after more research it was determined that adding a resonator will be a little more difficult and the increase in volumetric will not be noticeable and in fact if it was not properly tuned, it will create a negative efficiency impact. We decided to go with a straight pipe that would be tuned to a certain length depending on the best operating temperature and RPM.

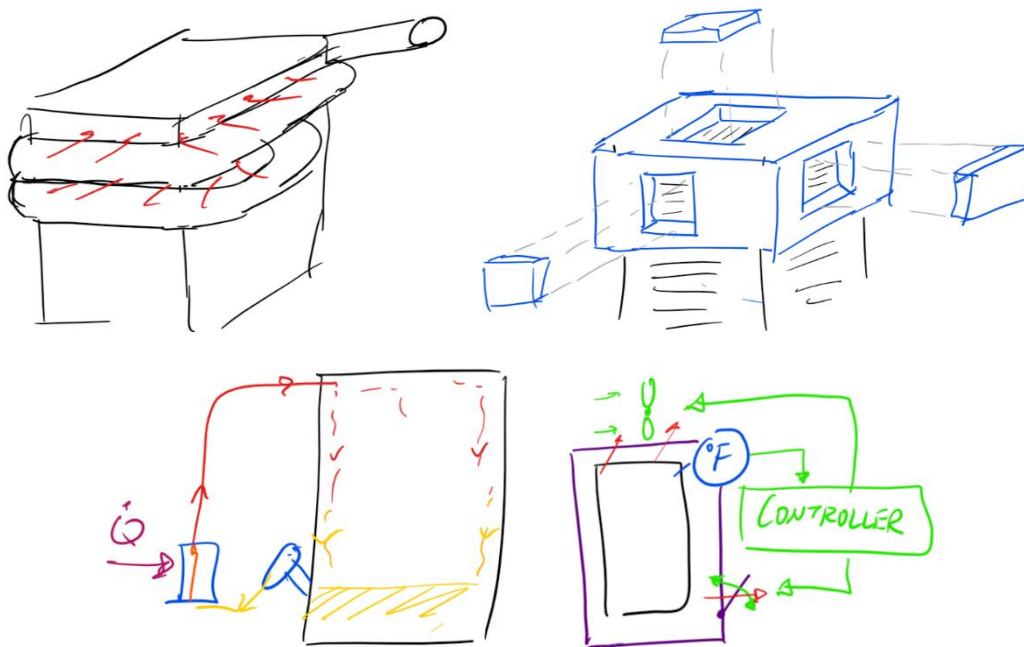


Figure 10: Clockwise from the top left: 1. An exhaust pipe wrapped around the cylinder head, 2. A modular insulation design, 3. A hot oil pumping system, and 4. An active heat transfer controller.

Our initial brainstorming session resulted in many interesting concepts (shown in Figure 9) including:

- An exhaust pipe which wrapped around the engine
- Custom made vacuum insulation
- Actively controlling heat transfer
- Hot oil pumping system
- Modular systems of rigid insulation panels

With regards to the engine starting system, we started our concept generation process after reading the competition rules and speaking with the SMV team. This directed our brainstorming session towards starting systems powered by electric motors. We also wanted to avoid the losses of constantly free-wheeling the starter motor. Some options we considered were:

- Solenoid starters (like those found in modern automobiles)
- Bendix starters (like those found in older automobiles and motorcycles)
- Centrifugal or plate clutches
- Sprag or one-way bearings
- The Honda OE clutch

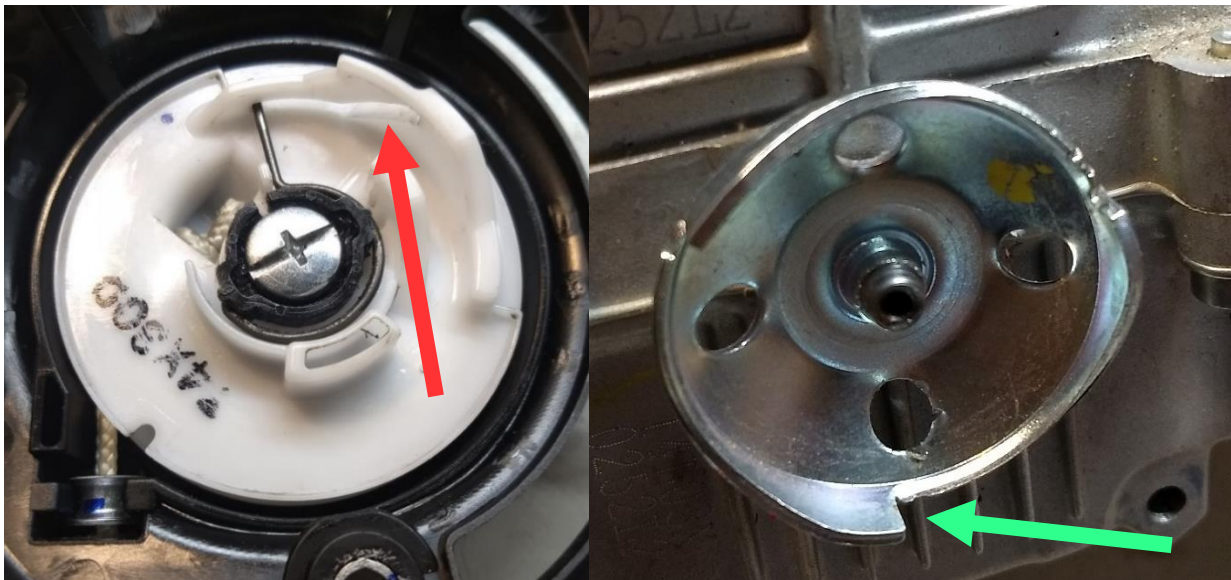


Figure 11: Honda GX35 Clutch Mechanism.

Referring to Figure 11, the white plastic drum (left image) is driven by the pull-cord (visible in the bottom left) and the black peg slides in the slot (red arrow) up and into the plane of the tooth on the crank (right image, green arrow). The black peg then transmits the torque input from the cord into the crank. Once the engine starts the ramps on the crank (right) allow the engine to ride over the black peg, and once the drum is driven backwards by the clock spring the black peg returns out of the crank tooth plane.

We also spent some time investigating the different materials available for thermal management and gas piping. Some of the options we considered for the thermal system were:

- Aerogel
- Mylar
- Aluminum Foil
- Fiberglass Exhaust Wrap
- Ceramic Coatings

And for the gas piping systems we considered using:

- 3D printed plastics
- Aluminum
- Steels

Ideas for modification of the main engine parameters such as compression and expansion ratio were also considered.

A simple way to increase the compression ratio would have been to shave a head or block as one would in an automotive application. However, the Honda GX35 has a single piece head and block, so this option is not available to us. Other possibilities we raised include: offset grinding the crankshaft journals, making a custom connecting rod, piston, or crankshaft, or raising the crankshaft centerline up towards the valves. After doing some additional research, we discovered some online forum posts that claimed that a GX31 piston shared the same bore and wrist pin design as the GX35 but had a longer wrist pin to crown dimension. If true, this would be a low-cost way to increase the compression ratio.

Modifying the expansion ratio was also an attractive possibility. Major automotive manufacturers such as Toyota and Volkswagen accomplish pseudo-Atkinson cycles by varying the valve timing of the intake or exhaust valves. By holding them open part of the way through the compression stroke, they can reduce the effective compression ratio while holding the expansion ratio constant. Another possibility is to close the intake valve earlier than normal. A simple way to accomplish this might be through adjusting the cam timing, otherwise a custom camshaft, mid-operation cam timing variation, or some kind of camless valve actuation (Koeinsegg freevalve?) would be needed.

Concept Evaluation

In order to evaluate our initial concepts, we developed a list of functions that our final design must accomplish. We then selected quantitative and qualitative measurements with which we could judge our concept's effectiveness.

The thermal management system's primary function is to maintain the engine's temperature within a range at which it's brake specific fuel consumption (BSFC - a measure of the amount of fuel required to produce a unit of output power) is minimized. We anticipate that an engine which is too cold will reject excess heat (and thus produce less output power), and an engine which is too hot will suffer from increased likelihood of knock. Furthermore, excessively high temperatures might risk exceeding material temperature limits.

Additionally, the thermal management system must not excessively interfere with maintenance and troubleshooting tasks, should incorporate functions which allow for engine pre-heating before the competition runs, and should be as light as possible.

The intake and exhaust systems must minimize the engine's pumping losses. The exhaust system must also duct its gases to a place where they do not pose a hazard to the driver. Due to the intake port having a fixed diameter, increasing the manifold diameter was not an option so the design of the resonator was the main priority in providing more air flow. The change in airflow into the cylinder occurs from the resonator to the cylinder so the length of the piping before the resonator depended on the design of the chassis and does not have an effect on the change of airflow.

The electric starting system should reach a good balance of efficiency, power, and lightness. Increasing the frictional losses of the engine is the antithesis of this project. Furthermore, if the starter can more quickly bring the engine to speed, fuel use during cranking might be reduced. Finally, the vehicle must also carry the starter with it. So a very heavy but efficient starter is not a good trade off, as the combustion engine will have to expend more fuel to accelerate it to speed.




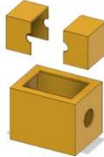
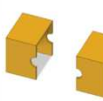
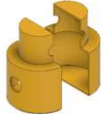
All of the systems must withstand the vibrations transmitted from the road and engine, be affordable, and should be able to be purchased or manufactured within 15 weeks at Cal Poly.

From these functions we were able immediately set aside some of our initial concepts. An engine wrapped in an exhaust pipe would likely make maintenance difficult, be heavy, and may reduce the engine's volumetric efficiency. Among other shortcomings, a fully controlled heat transfer system would be heavy when the control, power, and actuation systems are included. A sprag clutch or one-way bearing constantly meshed starter would increase frictional losses. Finally, many of the compression and expansion ratio changes would require advanced manufacturing and design which may not be feasible in the time remaining.

Thermal Management Structure Evaluation

The structure of our thermal management is important because it needs to be rigid and contain all the insulation material. The team conducted brainstorming sessions to determine several designs of the structure for our thermal management systems. From those ideas, we chose the following 5 potential concepts and created a decision matrix that would allow us to compare the advantages and disadvantages our potential designs. One of the main limitations for the design of the structure is that it needs to be able to accommodate all the other connecting components such as the drive shaft, intake and exhaust.

Table 2: Decision Matrix for Thermal Management Structure

Criteria	Weight	Concept A 	Concept B 	Concept C 	Concept D 	Concept E 	Concept F 
Easy to Assemble	3	DATUM	-	S	+	-	S
Weight	3		+	+	+	+	+
Manufacturability	3		-	-	-	-	-
Space Efficiency	3		+	+	+	+	+
Maintenance	3		S	S	S	+	S
Air Tightness	3		S	S	+	-	S
Adjustability/ Flexibility	3		+	+	+	+	+
Sum of (+)		N/A	9	9	15	12	9
Sum of (S)		N/A	6	9	3	0	9
Sum of (-)		N/A	9	6	6	12	6

The criteria for the decision matrix is derived based on the QFD. The current concept (Concept A) is used as a datum because our thermal management structure need to be better than the current solution that has been implemented. Moreover, our design aims to reduce the space and make a compact structure in order to control the heat transfer. With the compact structure, the would be less heat loss via natural convection to the surrounding air. The decision matrix shows that Concept D has the highest score compared to the datum. Concept D’s only disadvantage compared to the datum is the manufacturability. This is because the structure of Concept D needs manufacturing a separate structure whereas the datum concept uses the structure of the vehicle as the thermal management structure. Concept D also offers opportunities to install some kind of active or passive venting if the engine temperature rises above the target.

Insulation Material Evaluation

With the geometry of the thermal management enclosure determined, the next step is to choose a material or materials that will provide optimal heat retention during operation. When examining the Otto cycle, higher temperatures are the driving factor for efficiency, with the upper temperature limit being the working temperatures of the materials contained within the engine enclosure. Of these materials, the limiting factors are most likely the wires and sensors routed to monitor temperature, as well as the valve seals and bearings. Because the engine is required to operate at full throttle for short intervals with relatively long periods of inactivity, the insulation material is critical to not only retain heat but allow the internal temperature of the enclosure to increase very quickly. Therefore the specific heat of the material should be relatively low to allow a rapid temperature increase within the box, yet not allow for heat transfer to the surrounding environment during the long periods of inactivity nor overheat in the event of extended operation when traversing a grade or other obstacle. The following decision matrix was developed to weigh the options and aid in the enclosure/insulation material selection.

Table 3: Decision Matrix for Thermal Insulation Material Selection

Material	Cost	Conductive resistance	Overtemp Risk (1 = High)	Radiative resistance	Durability	Ease of manufacture
Vacuum	2	5	1	1	3	2
Aerogel	1	5	4	1	1	2
Space Blanket (Mylar)	5	3	2	5	4	4
Thermal Wrap (Fibreglass)	4	4	5	1	5	4
Aluminum Foil	5	1	5	5	4	4

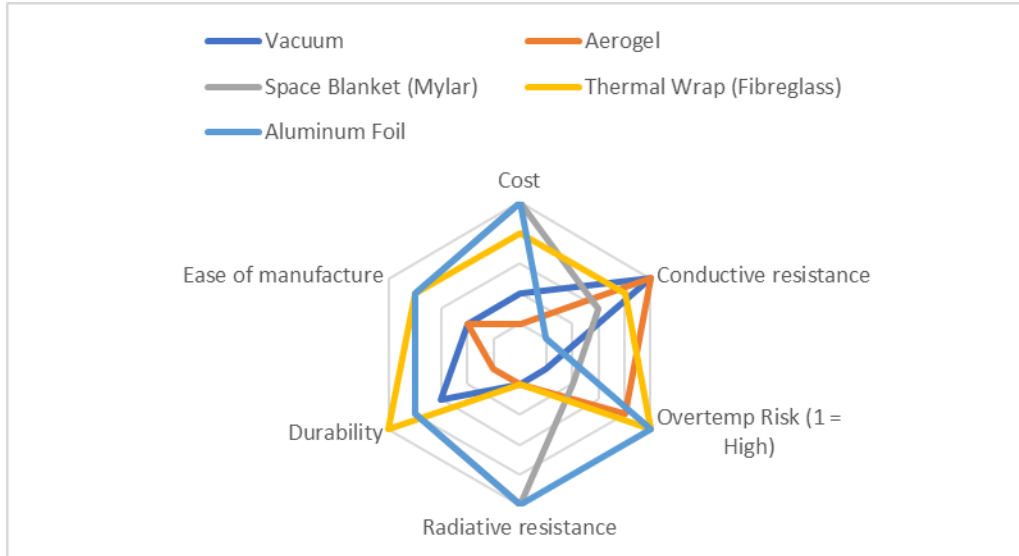


Figure 12: Radar plot associated with material selection decision matrix

In terms of the radar plots, there are clear winners on the material selection when designing around all factors. For example, aluminum foil offers low cost, high durability, and excellent radiative resistance in an easy to manufacture format. The radar plots also suggested some possible combinations of materials. For example, perhaps the aluminum foil's lack of conductive resistance could be mitigated by including some fibreglass in the design.

However, because the actual peak efficient temperature and heat retention is unknown for this engine, a determination cannot be made without further testing and analysis. The analysis done to this point (presented below) is based on assumptions that may prove inaccurate. While the above decision matrix may outline the benefits of each material in question, it is still unclear which of the requirements will be the driving factor. Therefore, a testing plan was developed to determine the effectiveness of each material. A sample of the testing plan is included in [Appendix 5](#) for determining the effectiveness of a given option. First, material combinations which appear to be effective will be simulated in Ansys with our calibrated heat transfer model. Then, the best results from these simulations will undergo the same testing procedures. The results will be compared via a decision matrix for thermal density with respect to cost, thermal efficiency boost, and weight. Of the options, a final choice will be chosen based on trends in this empirical data

Because we are not yet sure what level of thermal resistance is required, we performed some preliminary heat transfer analysis. First, we wanted to determine the primary mode of heat transfer. We plotted the heat

transfer by convection and radiation from a unit area over a range of engine temperatures. As shown in Figure 12 radiative heat transfer accounts for at least 30% of the heat transfer starting at around 325°K. An initial estimate of the heat transfer rate from the engine was calculated based on percent of fuel energy lost due through various pathways (friction, heat losses, etc), the engine displacement, and the energy content of 87 octane gasoline. This estimate was then input into the Ansys model to provide an initial estimate for later calibration.

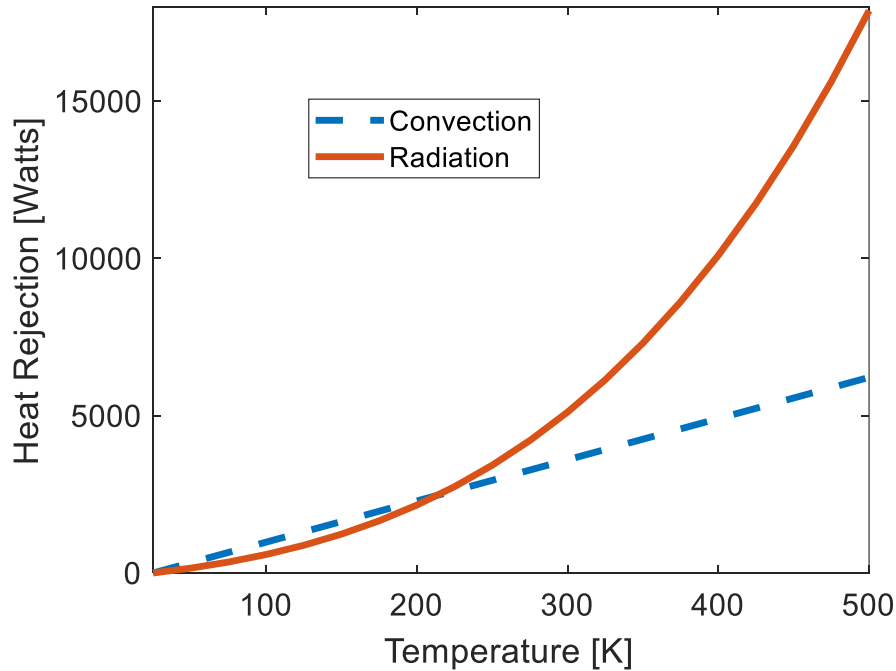


Figure 13: Heat Rejection by Convection and Conduction from Equivalent Surface Areas Using Reported Aluminum Material Properties and a Horizontal Fin Convection Coefficient.

Post-PDR feedback from Mr. Fabijanac suggested that ICE examine products such as HeatShieldProducts InfernoShield. This product is flexible, but holds its shape when deformed, and acts as a barrier to radiation and conduction. It can also be in direct contact with the heat source. There are many similar products such as header wrap, or other reflective barriers, however products like InfernoShield are both moldable and can withstand direct contact, whereas many other products can do or the other. However, we think that header wrap and an high temperature epoxy might be an affordable stand in.

Intake/Exhaust Evaluation

The intake system was analyzed by the RPM range as different ranges produce different volumetric efficiencies. Since organ pipe design and helmholtz design both have the same function, the design of the resonator for the intake was settled based on the helmholtz resonance theory due to the fact that the analysis of the helmholtz resonator began with a design analogous to the organ pipe but modified to a helmholtz design, which yielded better results. Since the vehicles enter the competition with the coast and burn cycle and the engine ranges from 1000-7000 RPM, we put our focus on the mid to higher ranges of 5000-6000. This range was chosen as we assumed it will be the most fuel efficient range based on BSFC plots, which is a function of RPM and torque. A BSFC plot is not available for the GX35 and although the graphs are different pertaining to different engines, we came to find a general trend that the least fuel consumption

occurs near the max torque around the mid to higher RPMs. With the helmholtz theory, the volumetric efficiency was based on the size of the resonator (V_2) relative to the combustion chamber (V_1), as shown in Figure 13.

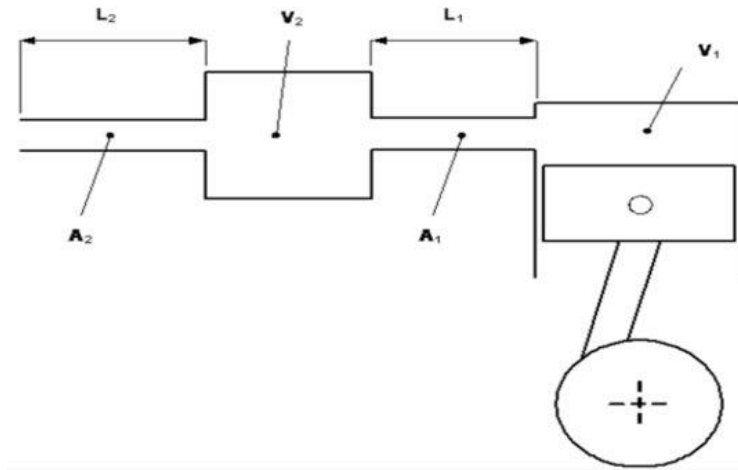


Figure 14: Intake with In-Series Helmholtz Resonator

With the helmholtz theory, a volume ratio of 10 between the resonator and cylinder yielded the highest volumetric efficiency in our interested range as shown below in Figure 14.

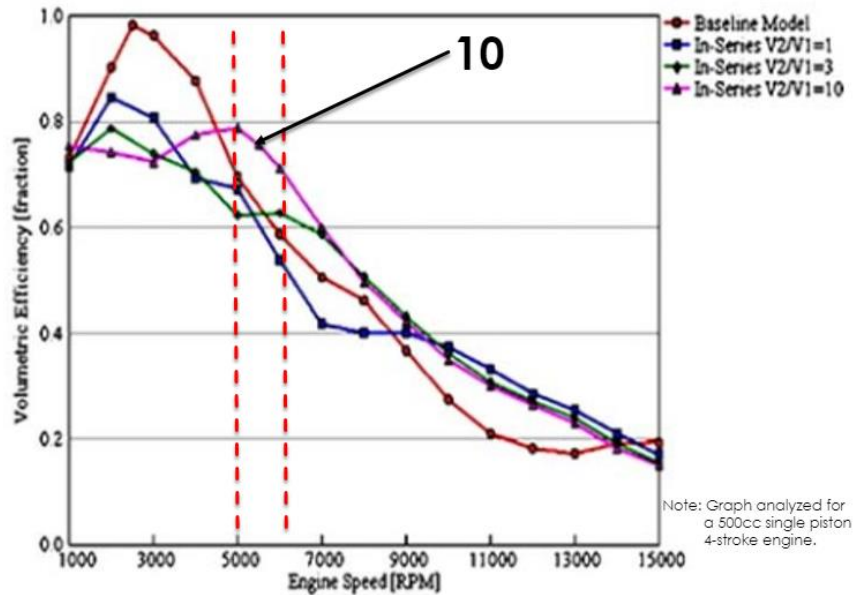


Figure 15: Volumetric Efficiency Curves for Different Volume Ratios

It is important to note that the plot is from a 500cc single piston 4-cylinder stroke. Given that there is only a change of displacement between this engine and our engine and the plot is based on a ratio, we used it to help give us an initial understanding of the RPM range we should be working at. These trends will later be validated on the engine dyno. The RPM range shown in Figure 15 correlates with the RPM range we assumed based on BSFC plots.

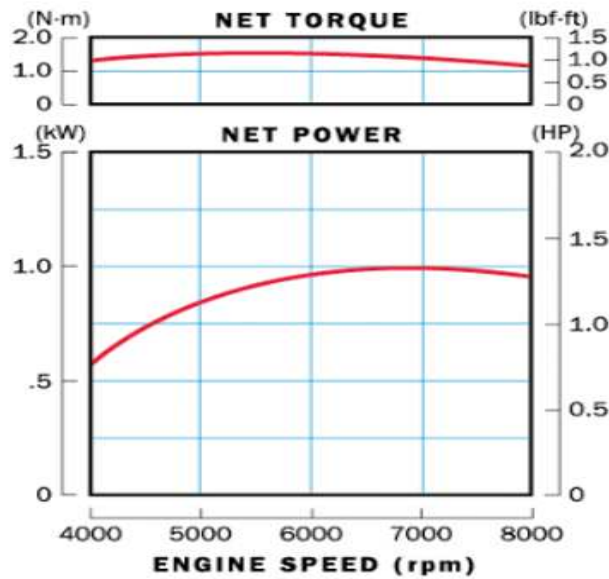


Figure 16: Plot of Torque and Horsepower vs. RPM

Table 4: Intake and Exhaust decision matrix

Intake and Exhaust Ideation					
Criteria	Base Model Intake	Resonator Intake (Helmholtz)	Organ Pipe Intake	Straight Pipe Exhaust	Resonator Exhaust
Packaging	5	5	5	5	3
Manufacture	5	3	3	5	3
Tuning	3	5	1	1	1
Material Options	3	3	3	5	3
Cost	3	3	1	5	3
Efficiency	1	5	1	3	3
Weighting	20	24	14	24	16

To further evaluate the Helmholtz model, the torque output of the GX35 maxes at 5000 RPM and is steady up to 6000RPM. Although the BSFC plots, volumetric efficiency for different volume ratios plot, and torque output all correlate with each other, the first two are based on assumptions and the third is factual for the GX35. These plots allow us to start testing with a specific scope and actual data of the engine will not be obtained until the engine is tested on the dynamometer. The decision matrix used to evaluate the different intake and exhaust designs is presented in Table 4.

Electric Starting System

The design of the electric starting system has seen substantial changes since the PDR report. Like many of the other concepts, the concept starting systems were evaluated using a decision matrix. In addition to selecting the type of clutch mechanism, we realized that small, 12VDC motors do not produce very much torque, and spin at rpms similar to the redline of the Honda GX35. Therefore, a reduction system of some kind will probably need to be employed.

The decision matrix for the engagement mechanism is presented in Table 5. A weighted decision matrix was used to place emphasis on the primary goal of efficiency. Reliability and repairability are grouped together because a very reliable design is less likely to need repair. However, some reliability issues might be acceptable if: the design is easily repairable, it's failure is easily predictable, and it offers some advantage over a more reliable system. Clear disengagement was considered as a result of conversations with Will Sirksi, while design and fabrication efforts were considered due to the expanding project scope. Of the options considered, the Honda OE mechanism scores far ahead of the alternatives.

However, not all factors were considered in this decision matrix. The Honda OE clutch must rotate backwards a few degrees in order to disengage. Originally, this is accomplished with a clock spring which is separated from the power transfer. However, this would not be possible with an electric starting motor. During final design, significant difficulties were encountered when attempting to design a robust mechanism to perform this counter-rotation. Therefore, the second-place engagement mechanism (a one-way bearing) was selected for continued development. In order to comply with Shell Eco-Marathon rules, this will require that the clutch engagement RPM is above the maximum RPM of the starter motor.

Table 5: Starter Engagement Decision Matrix

	Cost	Clear Dis-engagement	Frictional Losses	Design & Fabrication Effort	Reliability & Repairability	Weight	Sum
Weight	3	3	5	1	4	5	-
Honda OE	5	5	5	4	4	5	96
One-way bearing	4	1	4	3	5	5	78
Bendix	2	3	5	2	3	5	73
Solenoid	2	5	5	2	3	4	77
Centrifugal	2	3	3	1	3	3	55
Bicycle Cassette Sprag	5	1	4	2	4	5	77

The reduction mechanism selection is shown in Table 6. A weighted matrix was again used to emphasize the most important categories. Mounting flexibility was added due to packaging concerns inside the vehicle fairing, and clear disengagement is not a function of the type of reduction system.

Table 6: Starter Reduction Type Decision Matrix

	Cost	Efficiency	Mounting Flexibility	Design & Fabrication Effort	Reliability & Repairability	Weight	Sum
Weight	3	5	2	1	4	5	-
Belt	4	3	5	3	5	4	80
Gear	3	4	2	4	4	4	64
Chain	4	3	5	3	5	4	85

From the decision matrix, the chain drive was initially selected due to excellent scores across the board. However, packaging issues meant that a sufficient reduction ratio was not possible with belt or chain drives without using a multi-stage system or a very large and complicated bracket. Therefore, a gear reduction system has been selected by team ICE.

Preliminary Concept Design

Our preliminary concept (less the starting system) is shown in Figure 17. The intake and exhaust systems can be seen in green, and the thermal management system is made translucent to show the engine inside. Each of these systems will be discussed in detail in the following section.

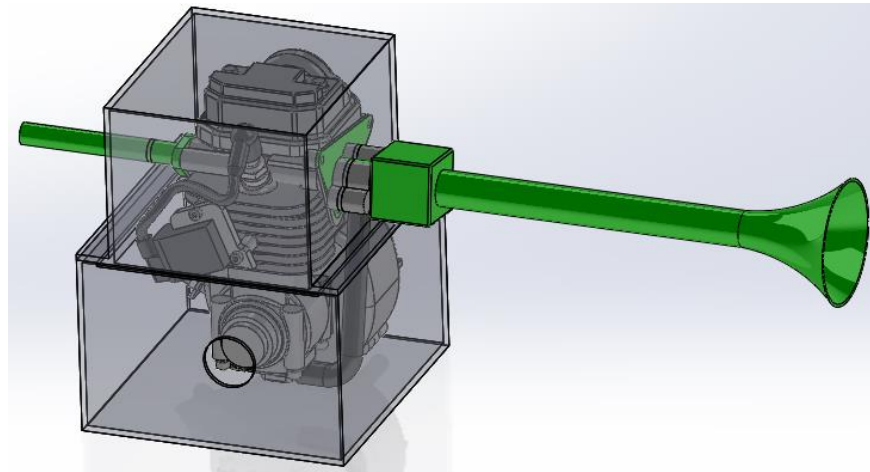


Figure 17: Assembly of the Concept Design Model

Thermal Management

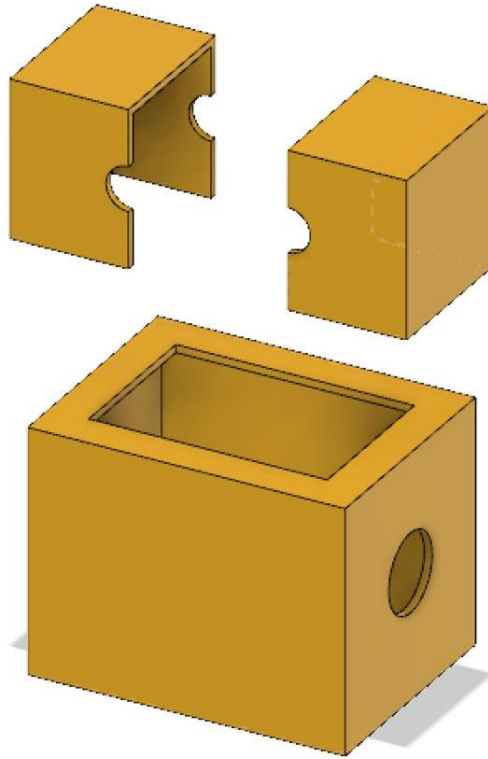


Figure 18: Preliminary concept model for the ICE thermal management system

The preliminary concept for the thermal management system is designed for maximum heat retention within an isolated area and is presented in Figure 18. This system combines the best of both worlds of two of the previous concepts: The insulated engine bay maintained a constant temperature along the entirety of the engine, but was too large of a volume of air to be efficient during the “burn-and-coast” cycle. The insulative wrap retained the heat well on the portions of the engine covered by the wrap, but allowed heat to escape from the numerous gaps in the insulation.

The model ICE has designed allows the heat rejection from the engine surfaces to the environment to heat up a very small volume of air. Effectively, the enclosure minimizes the “environment” making the net heat transfer required to increase the internal temperature low. This design also features semi-sealed ports, allowing the intake and exhaust piping to break the thermal barrier with minimal heat loss.

The concept also focuses on maintaining a system that is easily mounted and maintained in both the shop and track-side. This design features a two-step disassembly for rapid access to the critical components of the engine. The upper clamshells (Figure 20) are individually removable to allow access to the sparkplug, flywheel, intake/exhaust piping, and any sensors on the upper half of the engine for trackside maintenance and troubleshooting. The lower clamshell (Figure 19) provides the mounting surface to the vehicle, and can be easily removed for access to the engine oil, lower flywheel, and crankcase for more involved maintenance, repair, and future modification.

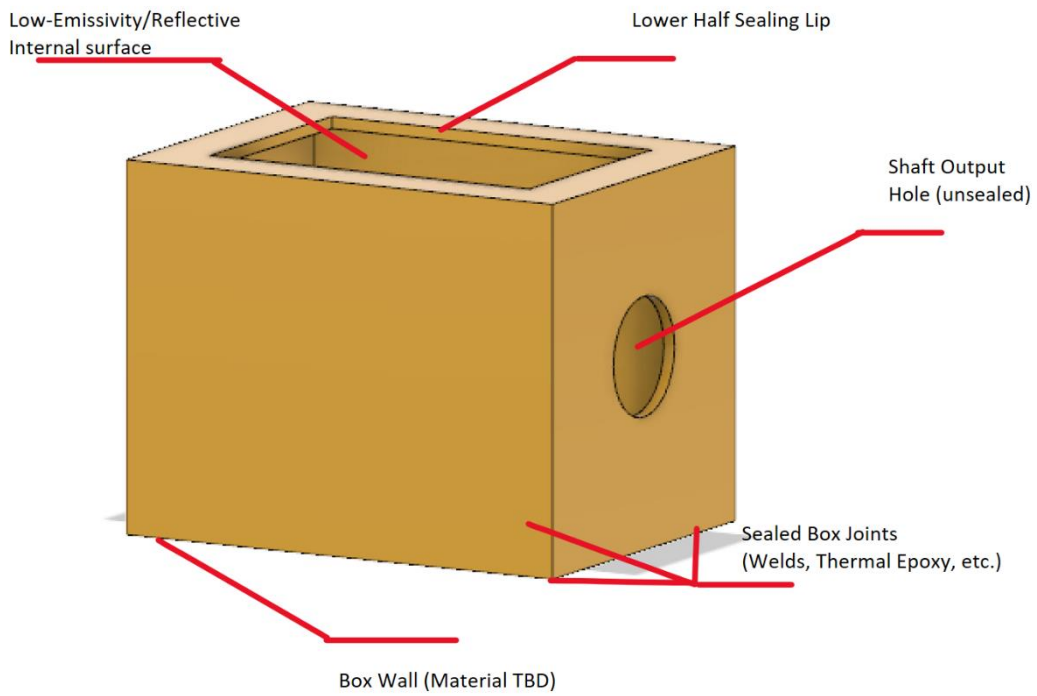


Figure 19: The lower thermal management box features a thermal insulation to retain monoblock heat, unimpeded output shaft, a retaining/sealing lip for the upper half, and a low emissivity coated surface

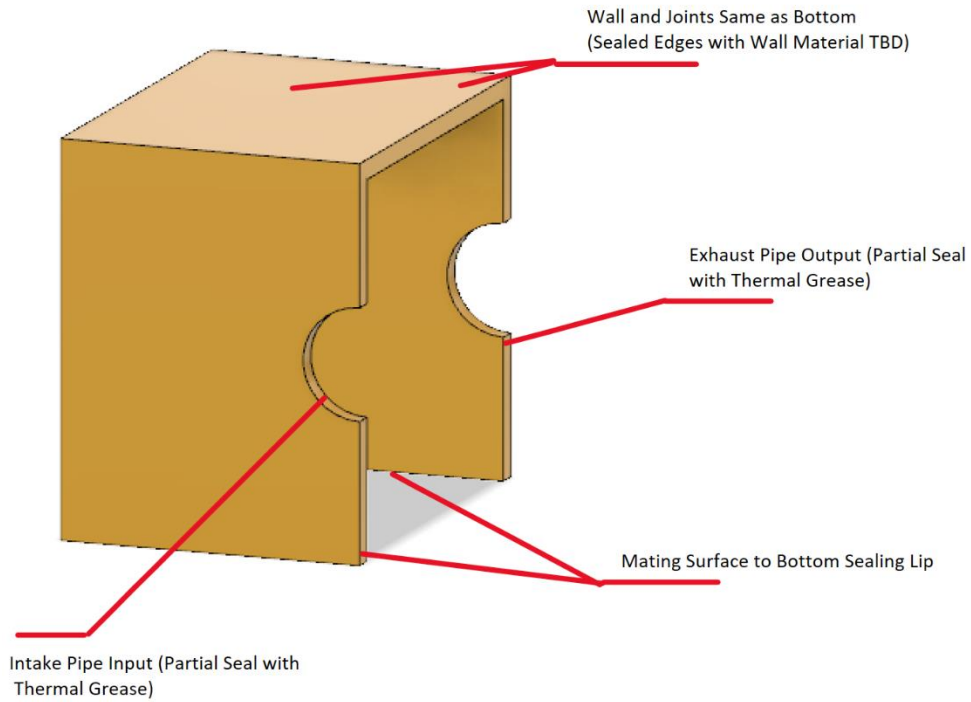


Figure 20: The upper thermal management box features a thermal insulation to retain monoblock heat, semi-sealed intake and exhaust ports and a low emissivity coated internal surface.

This model also allows for variation in the insulation medium. The close-formed clamshell will (without additional insulation) retain more heat in a closer proximity to the engine than the current aerogel-lined hood and will weigh substantially less. Based on testing and analysis, if more heat retention is required for a more optimal thermal efficiency range, different insulation mediums can be applied, tested, and subsequently removed without difficulty.

Intake and Exhaust

To test our theory, our intake system is designed in the shape of cube so the bottom plate of the cavity is able to move up or down so the volume can be adjusted and test the volume ratio accordingly. From Figure 14 it can be seen that a volume ratio of 10 would be best suited for our RPM range, but with our current design we will be able to test more volume ratios. Our prototype will be made of Polyactide (PLA) for rapid prototyping since we have easy access in campus and we can 3-D print it next quarter and start testing. The other option is ABS, but we do not have access to print ABS in campus and it will be more expensive if we have to do it outside of campus. Note, PLA does not have the best surface finish and it could a lot of losses due to friction. Our solution to this was to dip the intake into resin to have a softer finish that would be ideal to less frictional losses. For thermal management, the intake will be wrapped with header wrap to keep the air in the chamber cool from the cabin temperature. Colder air is more dense which means more oxygen for combustion as opposed to warm air from the cabin.

For the exhaust prototype we will be using stainless steel since it is easy to get and easy to adjust length for tuning. The only concern is that models investigated, the exhaust length was only slightly less than a meter long which would be a lot of material and will contribute to more weight. Once we know the operating temperature of the exhaust, we will be able to select from more materials to account for the length to weight ratio. We know that exhaust is highly dependant on temperature and that higher temperature leads to lower exhaust length. In order to keep the exhaust length shorter, after we know the operating temperature and the length comes out to be long, the exhaust will also be wrapped in order to keep temperature high

Figure 21 shows the preliminary design of the intake system with the Helmholtz resonator. As explained earlier, the design of the resonator was model as a box so we are able to adjust different volume ratio of the resonator to the cylinder. The bottom part of the resonator will consist of an adjustable plate that will be able to move up or down in order to test the different volume ratios.

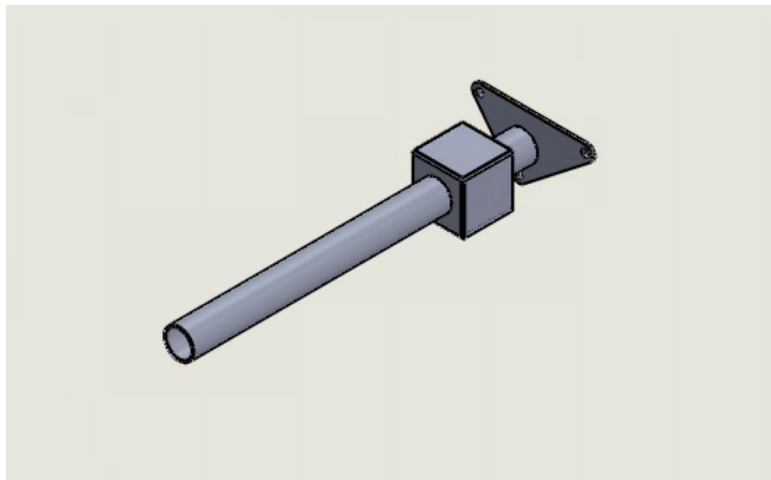


Figure 21: Preliminary design of the intake system with a Helmholtz resonator

Figure 22 shows the preliminary design of the exhaust pipe. Since the exhaust is highly dependant on temperature we decided to model the exhaust as a straight pipe and tune the exhaust to the correct length. A straight pipe sounded more resonable because the length of the pipe can be easily modified to investiage different lengths, avoid a negative change in efficiency. The overall theoretical efficiency increase was of only 5% compare to 12% of the intake so we aim to make the exhaust simpler and focus on the intake.

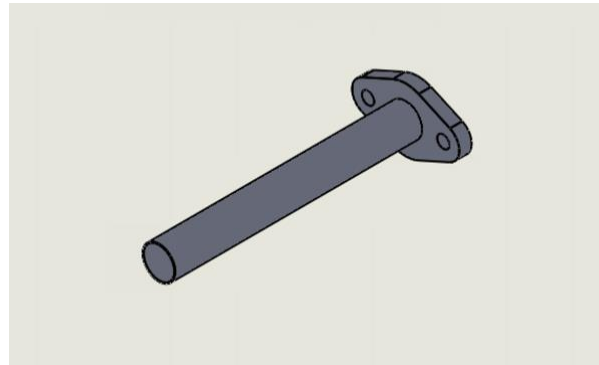


Figure 22: Preliminary design of exhaust pipe

Compression Ratio

Our team wanted to take advantage of the theoretical improvements offered by increasing the compression ratio. However, we can't find any information on the knock limit of the 87 octane fuel. We first considered testing a series of pistons with increasing compression ratios, but decided that the testing involved would be to time consuming. Additionally, from our conversations with Dr. Lemieux, and our team's experience with the manufacturing capability on campus, we felt that making a large number of custom pistons would put us in danger of falling behind schedule.

Instead, team ICE has decided to utilize off the shelf parts in order to investigate the compression limit and then follow up by purchasing or manufacturing a small number of pistons. We plan to do this by first installing a piston which will result in a very high compression ratio. Then, we will adjust the dynamic compression ratio (the realized compression ratio when the engine is running- e.g. not determined solely by volume ratio) until we reach the knock limit for an engine on a tune designed to maximize efficiency.

The parts we plan to use include a Honda GX31 piston and the Honda GX35's exhaust decompression system. The Honda GX31 piston has been reported by hobbyists to fit in the Honda GX35 engine using the GX35 connecting rod and crankshaft. The GX31 piston is reported to be taller from the wrist pin to the piston crown, meaning that there will be less clearance volume, and therefore a higher compression ratio. There are no drawings or specifications available to corroborate these claims, but the GX31 has the same bore as the GX35 (39mm) and the same wrist pin part number (13111-ZM5-000). Unfortunately, there is conflicting information about piston-valve/cylinder head clearance. Some people claim that approximately 20 thousands need to be removed from the piston crown, others say that no material needs to be removed. In any case, a piston kit including rings and wrist pin is ~\$30 online. We think the potential advantages and low cost make it worth trying.

The GX35's exhaust decompression system is a flyweight actuated secondary cam lobe which opens the exhaust valve for up to approximately 60° during the compression stroke. The secondary cam lobe can be seen in Figure 23. We plan to modify or shim the flyweight system so that we can lock it in a certain position

for testing. This will allow us to adjust the dynamic compression ratio down from the geometric ratio (reported by hobbyists as 12.5:1). Note that this system may not work well for an Atkinson type cycle. Because the exhaust valve opens on the compression stroke, fuel will be pumped out of the combustion chamber without being combusted. We anticipate that this will lead to a large increase in BSFC, and may also represent a safety hazard (which we have accounted for).

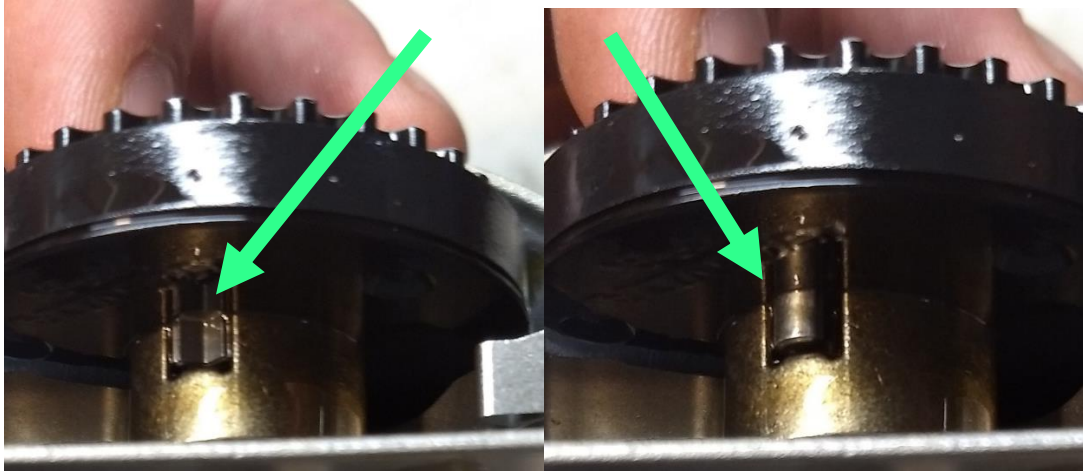


Figure 23: Secondary Exhaust Cam Lobe in the Fully Deactivated (Left) and Activated (Right) Positions

The approach outlined above will allow team ICE to quickly evaluate a series of compression ratios through easily made adjustments which are accessible from within the valve cover. Compared to an approach requiring several tests with different pistons, we anticipate a significant decrease in manufacturing, setup, and testing time.

Electric Starting System

Initially, design work was started with the goal of integrated with the Honda clutch. It essentially acts as an out-of-plane one way pawl clutch. The clutch is engaged by rotating the clutch drum faster than the crankshaft of the engine. To disengage the clutch, it must be rotated backwards roughly 45°.

A new clutch drum (Figure 24) and bracket (Figure 25) were modeled, and AGMA calculations were done on a proposed gear reduction.

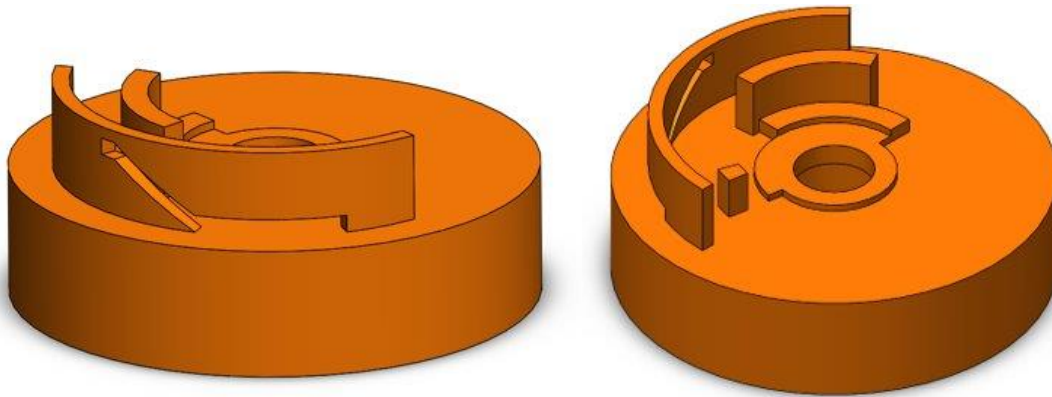


Figure 24: ICE Honda Clutch Drum

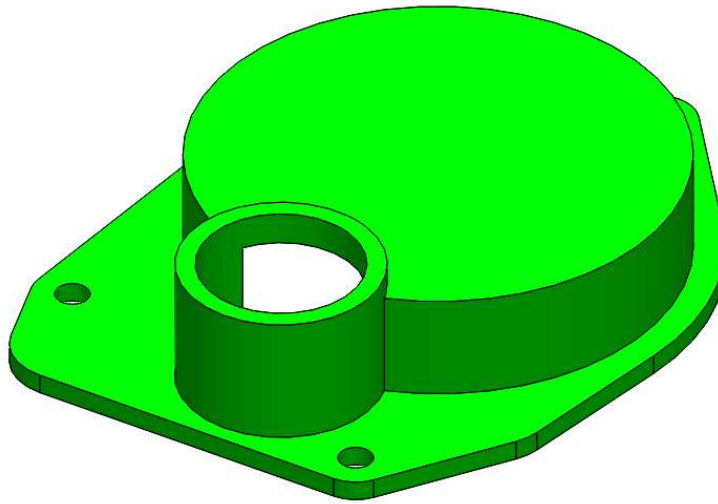


Figure 25: Early Starter Bracket Prototype

It was expected that machining the features on the top surface of the clutch drum would be difficult, so initial prototyping was to be done in ABS plastic. The lifetime of these parts was going to be evaluated through use on the dyno. If the lifetime was insufficient, some preliminary plans to produce all metal, or plastic/metal hybrid, clutch drums were drawn up.

However, achieving the 45° counter rotation proved to be more complicated than expected. Driver workload is already reported to be high by the SMV team, therefore we could not implement a two-button solution (push to start, push to disengage). Ideally, a circuit or mechanical device would implement this counter rotation. Coil, clock, or leaf springs could be inserted into the clutch mechanism, but some sort of detent or stop mechanism would be required to carry the starting torque. It would also create a delay between pressing the starting button and the begin of power transfer from the starter motor to the combustion engine. A 555 timer circuit was also investigated, but ICE has insufficient experience designing these circuits, and did not have confidence in their design. Finally, a small microcontroller could be used – but this was judged to be a bit excessive.

The combination of the unknown lifetime of the plastic part, complex manufacturing, and difficult disengagement mechanism lead ICE to design a new starting system from the ground up. We still consider the Honda clutch to be a very advantageous design. It is lightweight, robust, and introduces zero frictional losses to the engine once disengaged. Therefore, we recommend that SMV further explore this solution once more information is known about starting loads and speeds.

In the meantime, a design using a one-way bearing and gear reduction is presented in the Final Design section: Electric Starting System.

Final Design

The final design consists of four subsystems designed around an initial target of 5000RPM and 170°F. The intake and exhaust systems are selected to increase the volumetric efficiency of the engine, and the thermal management system is intended to increase the thermal efficiency. The electric fuel injection system will allow the SMV team to adjust the engine tune in order to achieve maximum fuel efficiency. Finally, a

dynamometer fixture has been designed to attach the GX35 so that ICE and SMV can test the engine in the lab at Cal Poly.

Post-CDR Change Summary

Thermal Management System

The thermal management system saw no changes between CDR and FDR.

Intake and Exhaust

Changes to the intake system and resonator were made since the Critical Design Review due to the confirmation of using the electronic fuel injection kit and packaging changes, in addition to more simulation analysis ran on Lotus.

- The resonator was sized shorter in length but wider to keep the same volume ratio of 10 due to packaging constraints.
- The runner length connecting the resonator to the intake port is tapered throughout rather than a constant cross-section for better efficiency.
- The runner length was modified to have a 30-degree bend due to packaging constraints.
- An adapter was designed to attach the resonator to the fuel injector.
- The scope of the exhaust was paused due to unforeseen circumstances after Critical Design Review.

Dynamometer Fixture

Based on the CDR feedback, the dynamometer fixture designed was edited to be more reliable and easier for assembly. The main changes in this subsystem are as follow:

- The v-belt system was changed to a tooth belt system to prevent belt slippage.
- The bearing plates are redesigned so that it is easier to assemble.
- A bearing plates now have a bar at the base so that the adjustments can be made while aligning the reduction to the dynamometer.
- Countersinks are added to the coupler so that it can be located using the M8 countersink screws.
- Instead of keyways, set screws and flat notches on the shafts are used to secure the shafts to the couplers or sprockets.
- Slots are used in engine mounts instead of counterbores to improve the ease of assembly and alignment.
- Tensioner is designed for belt tension with an idler pulley.

Electric Starting System

Some minor changes were made to the starting system since the Critical Design Review.

- Orientation of the gear was reversed and the bracket modified to further simplify manufacturing.
- Mounting holes changed to slots so that the gear meshing could be adjusted.

- Center shaft through hole was changed to a blind hole because the full depth was not needed.
- 22mm retaining ring in the bore of the gear was also removed because suitable tools to manufacture the groove were not available. Instead the setscrew hole included on the gear by KHK was used to retain the bearing.
- Bracket was threaded for starter fasteners.

The new design is shown in Figure 26.

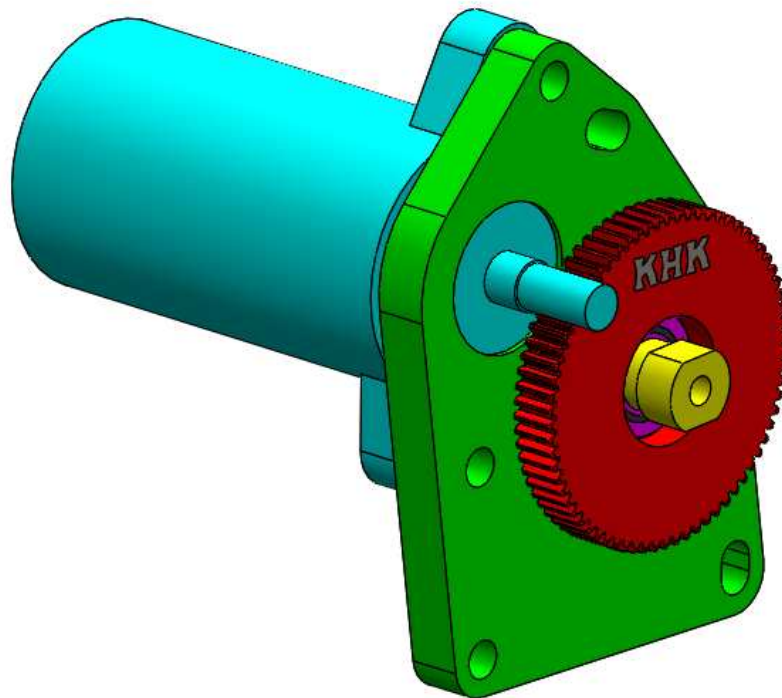


Figure 26: Revised Electric Starting System

Electronic Fuel Injection

Thermal Management System

The thermal management system consists of an insulating box and a thermally insulating wrap. The insulating box contains the majority of the fins on the Honda GX35 to restrict airflow. By minimizing airflow, the local air will increase in temperature due to convection but will not be moved out of the fin location. During testing, if overheating becomes an issue a small amount of airflow can be introduced back over the fins to allow the engine to cool slightly. To stay customizable during testing, the insulating wrap is attached to the engine valve cover, oil pan, and crankcase with a high temperature RTV silicone. The wrap has parting lines so that the various components can be removed from the engine, but the wrap is not designed to be removed from the engine. The geometry of the insulative material is selected such that all

foreseeable maintenance to the engine can be performed without removing any material. Should more airflow over the engine be required, the insulative material can be removed and replaced.

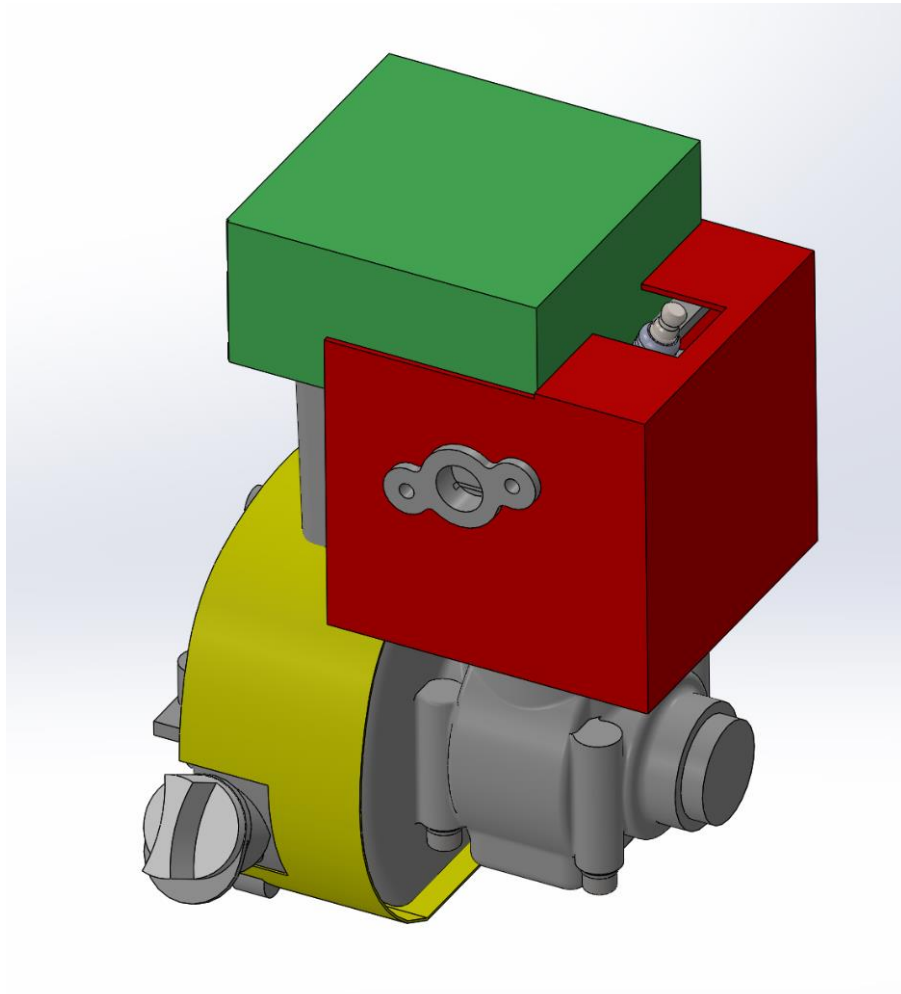


Figure 27: Engine covered in thermal shroud

The insulating wrap is made from Heatshield Products HP Heatshield Mat. This product is typically used for racing engine application, and is designed to insulate temperatures up to 1100 degrees Fahrenheit. It is designed with a self-adhering surface that will conform to the engine. To optimize material used and allow easy access to components that require maintenance, the geometry in Figure 27 will be cut and molded from the Heatshield and attached to the engine. In addition to maintenance, the intake and exhaust systems have been taken into account. Cutouts are provided for each of these systems, and the assembly plan takes into account the thermal management application.

Evaluation of the thermal management system will be conducted on the engine while on the dynamometer. Testing will follow the testing plan called out in Appendix 11:. The focus of this testing plan is to evaluate the feasibility of this material and determine the appropriate temperature to target for peak engine efficiency. Should the engine overheat during this testing, further thermal management geometries/designs will be considered and tested to the same parameters.

Intake and Exhaust

The intake and exhaust will be tuned together to achieve the highest efficiency from the engine. Due to the scope of the exhaust being paused after Critical Design Review, the intake will be tuned to achieve the highest efficiency from the engine, while prioritizing fitment and placement constraints inside of the chassis. While a straight length for the intake was analyzed to achieve the highest efficiency, this is not feasible so the design considers placement of the engine, fitment of the fuel injector, and chassis constraints that will produce the most linear piping for the intake.

Resonator

The resonator is a cylinder with a tapered inlet to help better guide the pressure flow. From the Helmholtz analysis, the geometry of the resonator is not as important more as the volume ratio (of 1, 3, and 10) between the resonator and the cylinder. Although the geometry helps with guiding the pressure flow, the volume of the resonator plays a much bigger role in allowing air expansion to increase the pressure of the incoming air, in addition to making the air denser. More analysis was conducted on Lotus and it was found that tapering the runner length would result in higher efficiency than a length was a constant cross section. Figures 28 and 29 below show the changes of the resonator before and after Critical Design Review.

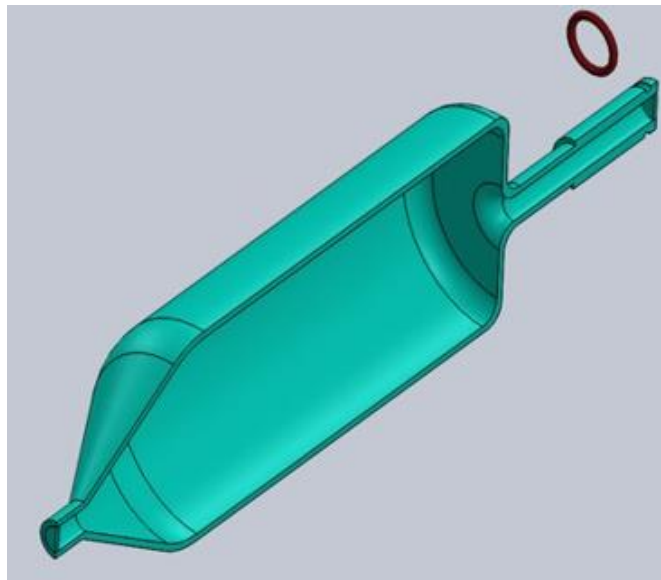


Figure 28: Isometric Section View of Initial Design of Resonator

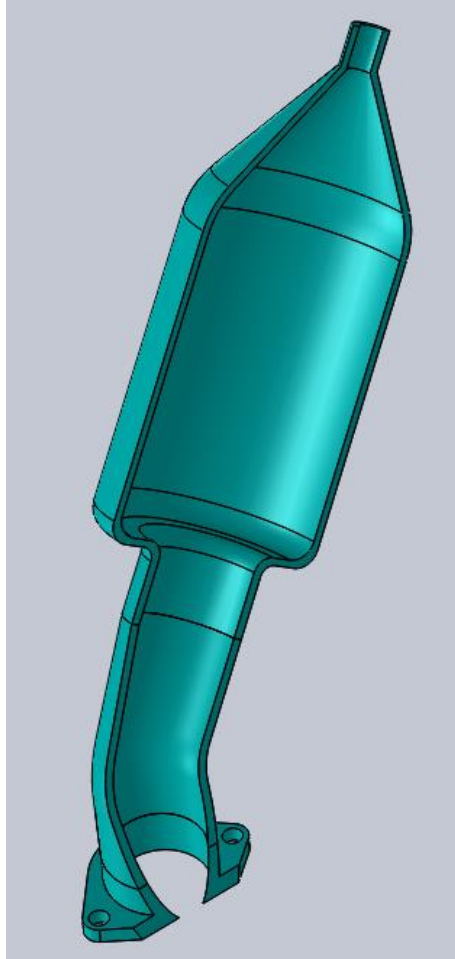


Figure 29: Isometric Section View of Final Design of Resonator

With the installment of the electronic fuel injector, the runner length needed to have a bend of 30-degrees from the vertical to not come in contact with the rear wheel. Since the throttle body from the electronic fuel injector kit was not to be used, a custom adapter had to be designed to fit flush with the port of the fuel injector. Because the material for the piping was already ordered before the final changes occurred, the diameter of the inlet to the resonator was kept the same.

The placement of the engine prioritizes the routing of the intake from the atmosphere to the resonator. After Critical Design Review, it was realized there were more packaging concerns so the routing of the piping needed to be configured. Because placements of all the components were not yet complete, the routing of the piping could not be finalized.

Exhaust

Unlike the intake, the length of the exhaust is very sensitive to RPM changes. Even though bends in the exhaust are not favored for performance, the length of the exhaust has a bigger effect on efficiency so the routing of the exhaust contains bends that achieves the desired length (approximately 3 feet from exhaust port to atmosphere) at the targeted working RPM range of 5000.

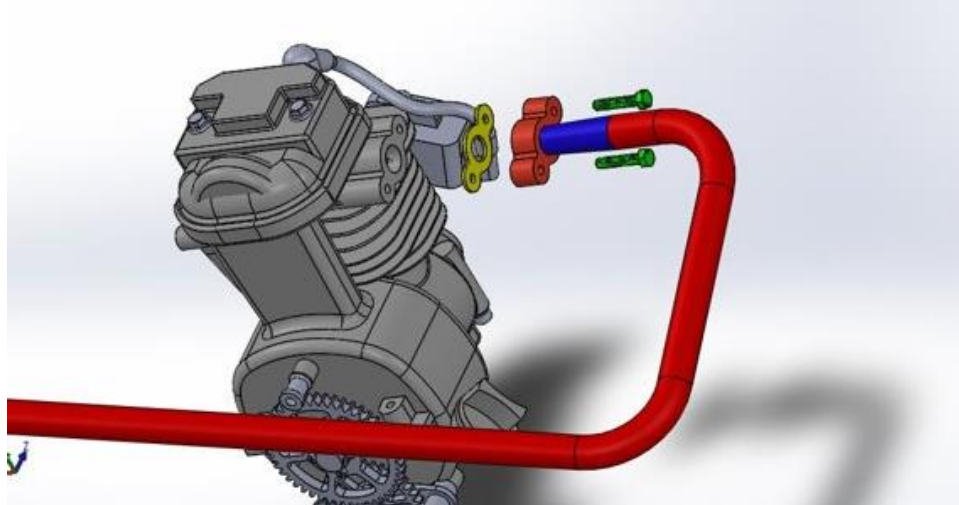


Figure 29: Schematic of Exhaust with Components

Lotus Engine Simulation

The initial analysis for the volumetric efficiency of the Honda GX35 was based on a 500cc four stroke single cylinder engine, but we proceeded with that analysis for the GX35 due to the only difference between the two engines were cylinder sizes. With the use of Lotus Engine Simulation, we were able to test our initial analysis to see if the volume ratios of 1, 3, and 10 would produce similar volumetric efficiency curves as the bigger engine that was analyzed in the Helmholtz analysis. Table 7 lists the parameters that were used to simulate the response of the GX35 in Lotus. It is to note stock configurations of the GX35 were used for the valve timing, so it was not configured throughout the simulation. The first simulation consisted of the engine fully stock with no intake or exhaust. This data from the stock simulation will allow us to see if the data being outputted by Lotus is calibrated correctly in relation to the data that will be outputted by the dyno.

Additional simulations with intake and exhaust configurations were ran to test our analysis that came from the bigger engine. 4 simulations of the engine were tested in the order of:

1. With exhaust and no intake
2. With exhaust and volume 1 resonator
3. With exhaust and volume 3 resonator
4. With exhaust and volume 10 resonator

Since the scope of the exhaust was paused, more simulations were conducted on Lotus with just the resonator and the runner length. The volume ratio of 10 still yielded the highest efficiency of the three ratios at the targeted range of 5000 RPM and up. In addition, the volume 10 ratio was tested with varying diameters of runner length and it was found that having a tapered length yielded in even a higher efficiency than a constant cross section length. Since the simulations were conducted before the electronic fuel injector kit was included, the ratio of the diameters of the tapered runner length from the resonator port to the intake port was used to modify the diameters of the runner length that was to be connected on the electronic fuel injector. Even though the simulation showed a higher efficiency with a tapered runner length, the final design of the runner length could not be simulated on Lotus because the software could not account for the 30-degree bend or the inclusion of the electronic fuel injector. The diameter of the piping of the inlet to the resonator was kept the same due to the materials arriving before the final changes to the resonator occurred.

Though it is kept the same, simulations ran on Lotus showed that opening the restriction of that diameter increased the volumetric efficiency as it allowed higher air pressure into the resonator. With this data moving forward, SMV can decide what size piping to use as the chassis is compact and bigger diameters of the piping would need to be sufficed with the placement of other components.

Figure 30 below shows the volumetric efficiency curves from the Lotus simulations. Figure 31 below shows the volumetric efficiency curves for the bigger engine tested by the Helmholtz analysis. In comparison between these two graphs, we are not looking for the same curvatures, but rather confirm the volume ratios are performing correctly in specific RPM ranges. It is to note that the bigger engine was tested with straight piping for the exhaust and intake, but with our current construction of the piping of the intake and exhaust for the GX35 we are still getting the highest efficiency with the use of the volume 10 resonator for our targeted RPM range of 5000 and higher.

Table 7: Engine Configurations of the Honda GX35 for Lotus Simulation

Bore (mm)	39
Stroke (mm)	30
Conrod length (mm)	51
Compression ratio	8:1
Exhaust port diameter (in)	0.475
Intake port diameter (in)	0.375
Exhaust runner length (in)	35.78
Intake runner length (in)	2
Intake chamber volume (in ³)	21.358
Intake valve opening (deg)	10 BTDC
Intake valve closing (deg)	57 ABDC
Exhaust valve opening (deg)	48 BBDC
Exhaust valve closing (deg)	28 ATDC
Max lift (mm)	2.754

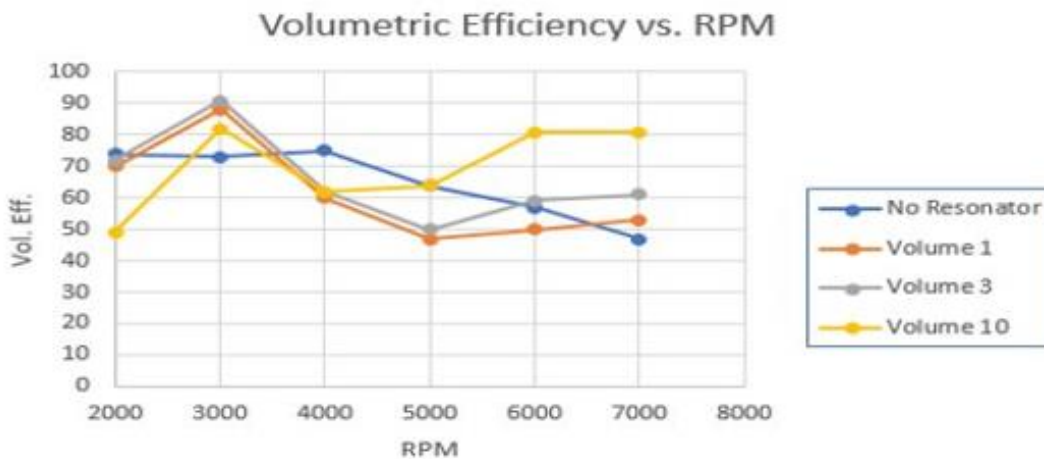


Figure 30: Volumetric Efficiency Curves of the Honda GX35 from Lotus Simulation

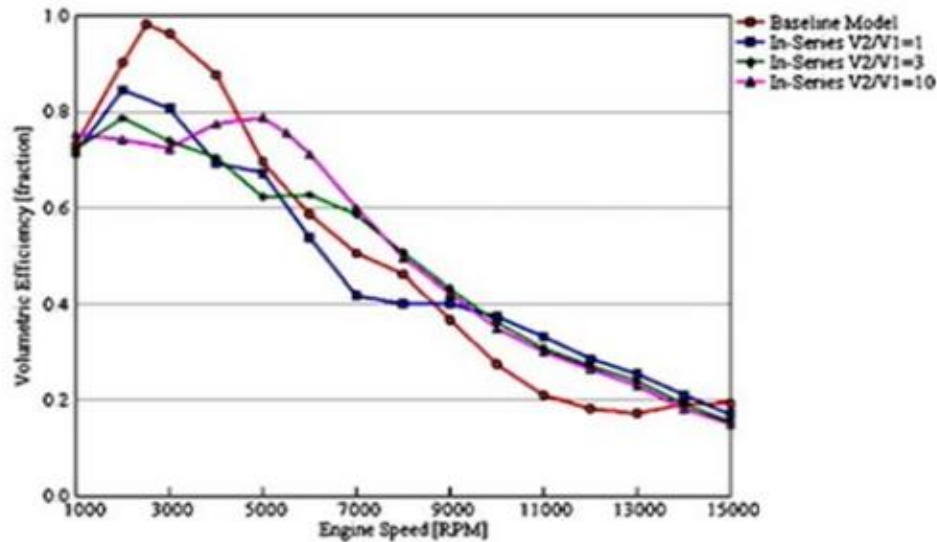


Figure 31: Volumetric Efficiency Curves from Helmholtz Theory

Safety and Maintenance

The major failure modes expected for the intake and exhaust are:

- Failure of mounting brackets and adapters
- Loosening of silicone sealant adhesive and rubber coupling

For the first case, failure of the mounting brackets will cause the exhaust to fully separate from the engine and chassis. If the engine is running, there is potential damage to the compartments inside the engine box as the hot exhaust gasses will not be routed to the atmosphere but contained inside the confined engine box. If the adapter of the intake fails, the resonator will disconnect from the engine. If the vehicle is moving, the detachment can cause the resonator to come in contact with the rear wheel resulting in damages to these two components.

For the second case, the resonator, runner length, and adapter are assembled together with sealant adhesive. These three components are attached flush to one another, so only the sealant is solidifying them in place. If the sealant is loosened, this failure would result in insufficient performance of the resonator due to pressure leakage. If the sealant is fully loosened, multiple problems could arise. Since the resonator is attached to the piping, loosening of the sealant between the resonator and the runner length could cause the resonator to act as a cantilever beam. Loosening of the sealant on both ends of the runner length can cause the runner length to fall apart from the assembly. To minimize pressure leakage or detachment issues caused by the sealant, sealant tape was wrapped around the areas where adhesive sealant was applied. The rubber coupling attaches the piping to the resonator. This failure would result in insufficient performance of the resonator due to pressure leakage. If full loosening of the coupler occurs, this can detach the piping from the resonator which will cause the resonator to input hotter air into the intake that comes from inside the chassis. The coupling will have additional securing at its two ends by steel zip ties that are provided with it.

The intake is designed with three separate components to allow for modification and maintenance of individual parts rather than one unit as a whole. If SMV later designs a resonator or runner length or both

that yields better efficiency than this design, they can simply attach the new components onto the already existing adapter for the electronic fuel injector.

Manufacturing Plan

To achieve the highest efficiency for the intake and exhaust, many of the parts need to be customized and cannot be bought off the shelf. Table 8 below lists the necessary customized parts. In addition, it lists the time and steps for each operation of a part.

Table 8: Summary of Manufacturing Plan for Intake and Exhaust

Order	List of Operations	Machine	Time Estimated	Qty	Time Estimated Total
Flange	Sawing: Cutting to length	Band Saw	10 min	1	2hr 15min
	Trimming/cut edges	CNC	1 hr		
	Port diameter match	CNC	20 min		
	Drilling and Tapping: M5X0.8	Mill	45 min		
Gasket	Cardboard to trace Flange model	NA	30 min	1	1hr
	Trace cardboard onto Fel-Pro gasket material	NA	30 min		
Taper Pipe	Sawing: Cutting to length	Band Saw	10 min	1	1hr 15min
	Turning: Taper 0.03in	Lathe	1.5 hr		
Exhaust Pipe	Sawing: Cutting to length	Band Saw	30 min	1	3hr 5min
	Bend	Tube Bender	45 min		
	Tig Welding: Flange/taper pipe/pipe	Weld	2 hr		
Resonator	Print: 3D print	3D Printer	24 hr	1	24 hr
Intake Pipe	Sawing: Cutting to length	Band Saw	30 min	1	1 hr
	Bend	Tube Bender	30 min		
Injector Adapter	Print: 3D print	3D Printer	10 hr	1	10 hr
Runner Length	Print: 3D print	3D Printer	12 r	1	10 hr

Although the parts for the exhaust are ordered, manufacturing of the exhaust is paused temporarily. For the intake system, the team was able to manufacture the resonator. Due to the electronic fuel injector being a custom component and not having a standardized diameter, the runner length also had to be 3D printed in addition to the injector adapter. Unfortunately, manufacturing of the piping layout could not be started as it was dependent on the placement of other systems in the chassis, which was not concluded yet.

Design Verification Plan

To verify our design considerations, we will be using the Lotus Engine simulation along with the dynamometer in order to verify our theory of the intake and exhaust. Once we verify the Lotus Engine simulation with the dynamometer and obtain the error between them, we will proceed to place pressure transducers along with thermocouples on the engine to record pressures and temperatures, respectively. The pressure transducer should be placed as close as possible to the intake and exhaust valves. The Lotus Engine simulation can record data along the intake/exhaust ports and all the way down to the end of each of their pipes. Although our goal is to increase volumetric efficiency, there is no direct sensor that we can place in the dyno to obtain this reading. Therefore, we will look at the pressure ratio (pressure of intake/pressure exhaust) vs the crank angle. For the exhaust tuning we want to look at the overlap period which is of 38° for the Honda GX35, as seen in Figure 32 below.

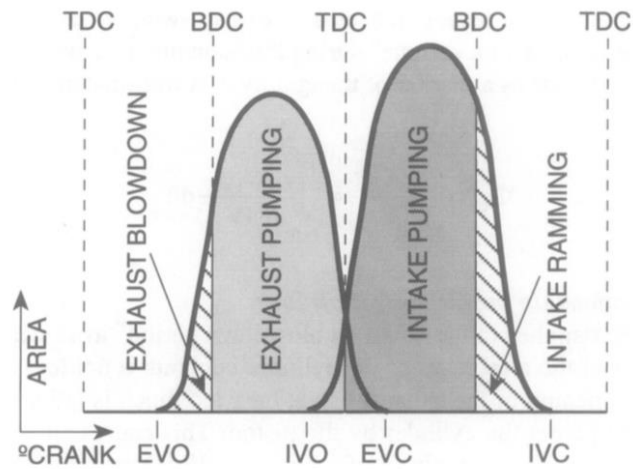


Figure 32: Intake/Exhaust Valve Operation

To verify our data for exhaust tuning, we should expect a significant decrease in pressure as soon as the intake valve opens (IVO) to when the exhaust valve closes (EVC) in the overlap period. This low pressure is sometimes referred to as the suction because it aids with exhaust scavenging. Verification of the intake will come after the EVC. Our pressure transducer on the intake port should record a significant increase in pressure, and since the pressure is significantly low during the overlap period, the pressure during the intake ramming should peak since the pressure coming from the intake is coming in at a higher rate compared to the cylinder pressure so the pressure would want to flow in that direction more efficiently. If both the intake and the exhaust are of correct length and size, we should be able to see the trend discussed earlier in the pressure vs crank angle data that we get from the dyno.

Bill of Materials

The table below shows the complete bill of materials for the intake and exhaust. Although most of the total came from the 3D printed parts, that portion of the cost was not spent as the team was able to 3D print the parts.

Table 9: Intake and Exhaust Bill of Materials

Description	Supplier	Part Number	Part Cost	Shipping Cost	Quantity	
3ft Pipe	Macmaster	44635K242	\$15.40	\$13.42	1	\$28.82
Flange	Macmaster	6620K176	\$ 17.89	\$ 0	1	\$17.89
Flange Gasket	O'Reillys	3009	\$ 8.99	\$ 0	1	\$8.99
Bolts (25 Pack)	Macmaster	91310A125	\$ 9.76	\$ 0	2	\$19.52
Flange to Pipe Connector (6 in.)	Macmaster	9210K12	\$ 7.27	\$ 0	1	\$7.27
Header Wrap	Amazon	-	\$ 22.10	\$ 0	1	\$22.10
0.5" x 0.334" x 24.0" 6061-T6 Aluminum	Online Metals	P/N: 4338	\$13.80	\$10.00	1	\$23.80
3D Printer ABS Runner Length	Protolab	-	\$200	\$20.00	1	\$220.00
3D Printer ABS Injector Adapter	Protolab	-	\$200	\$20.00	1	\$220.00
RTV Silicone Sealant	AutoZone	32329	\$7.99	\$0	1	\$7.99
Sealant Tape	Home Depot	267011	\$6.98	\$0	1	\$6.98
0.5" x 2" PVC Coupling	Lowes	792018	\$5.74	\$ 0	1	\$ 5.74
3D Printed ABS Resonator	Protolab	-	\$ 350	\$20.00	1	\$ 370.00
Subsystem Total						\$ 959.10

Dynamometer Fixture

This dyno fixture allows the team to test the Honda GX-35 engine on the Magnatrol HD-815 Dynamometer to get the base line performance of the stock engine as well as test the performance improvements due to design modifications.

Reduction Power Train

Based on the manufacturer's data, the accuracy of the dynamometer is $\pm 0.25\%$ at full scale. Since this dynamometer model has a maximum torque range of 28 Nm and our engine's maximum torque is 1Nm, an accuracy of approximately $\pm 3.7\%$ was expected when using this dynamometer. We expected that this 7.4% error band might mask any performance changes. Therefore, the team has decided to build a reduction power train to magnify the torque input to the dynamometer.

At first, we decided to use a 4:1 speed reduction gear train that was already manufactured for another engine in order to save time and money. A model of this initial design is shown in Figure 33.

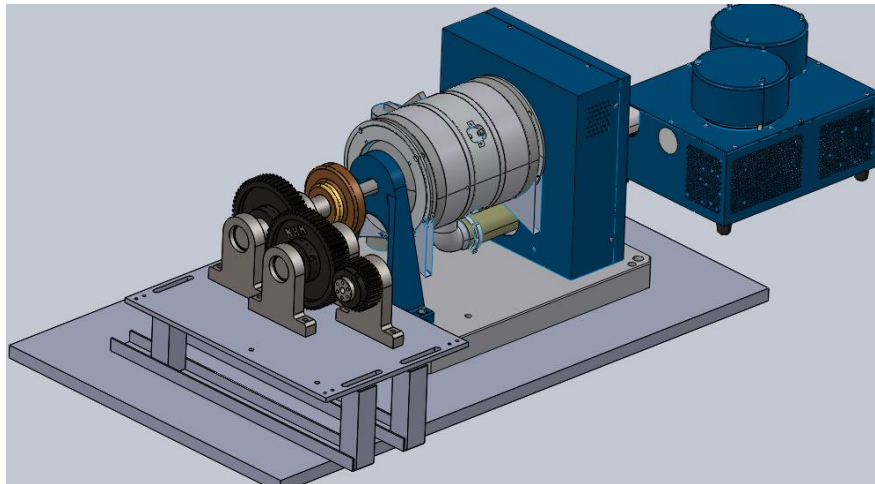


Figure 33: Gear Train Reduction and Dynamometer Concept

Since large steel gears and shafts are used in this gear train, we were concerned about the power losses due to the heavy gear train components. Moreover, there are also several exposed pinch points in this system and it raises safety concerns since the whole reduction system will be operated at 7000 RPM in the laboratory. We would need to build an enclosure around the gear train as a safety precaution. In addition, the whole gear train needs to be offset from the middle of the table because the input shaft from the dynamometer needs to connect to the gear train. Figure 34 Due to its size, we discovered that the reduction system would be off the table by approximately 3 inches. We then decided to design a new reduction system to avoid these issues. Figure 34 shows a decision matrix created to determine the type of power train that would be most suitable for the reduction setup.

Criteria	Weight	DIRECT DRIVE	GEAR TRAIN REDUCTION	PULLEY AND BELT REDUCTION	SPROCKET AND CHAIN REDUCTION
					
Easy to Couple with Dyno	3	DATUM	-	-	-
Rotational Inertia	5		-	S	S
Manufacturability	3		-	S	-
RPM Adjustability	5		S	S	S
Torque Range	5		+	+	+
Easy to Assemble	3		-	+	-
Noise	3		-	S	S
Sum of (+)			N/A	5	8
Sum of (S)		N/A	5	16	13
Sum of (-)		N/A	17	3	9

Figure 34: Decision Matrix for Reduction System Selection

In the decision matrix, each criterion is chosen so that it would reflect specific needs that would allow the team to mitigate the issues with the gear train reduction. This decision matrix shows that the alternative

way to design the reduction system with the new criteria would be a belt reduction system. This new design would also eliminate several restrictions that are imposed by the old gear train reduction system such as the coupling difficulties due to different shaft sizes. The design of the new belt drive reduction system can be seen in Figure 35.

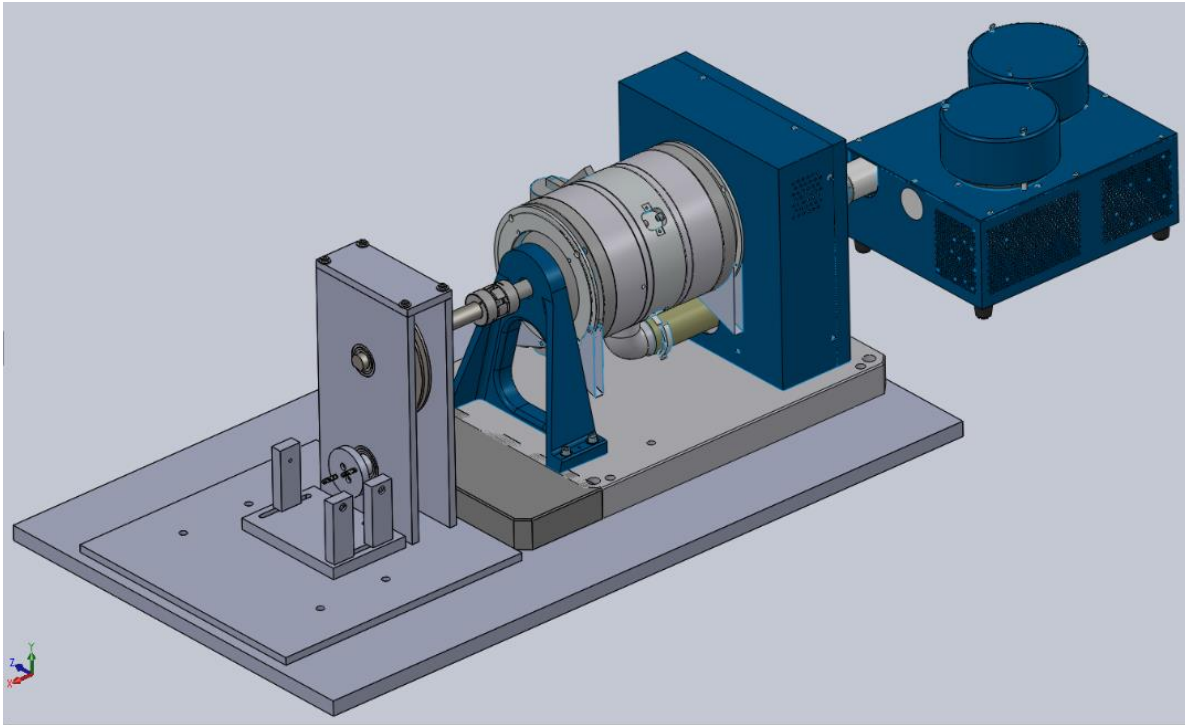


Figure 35: Set up of the Pre-CDR Belt Drive Reduction System

Initially, the team was considering using a v-belt for the reduction. However, based on the CDR feedback, our team decided to investigate a toothed belt system since it could be operated with higher reliability and test repeatability. This is because toothed belt system will prevent the belt slippage. Using the manufacturer's belt section selection chart, we chose the 5MGT cross section for 1kW power and 7000 rpm at the driving pulley. The pulleys are then sized to have the highest speed ratio. The manufacturer recommended a speed ratio of 4: 1 using timing pulleys with 20 teeth and 80 teeth. The updated reduction assembly can be seen in Figure 36.

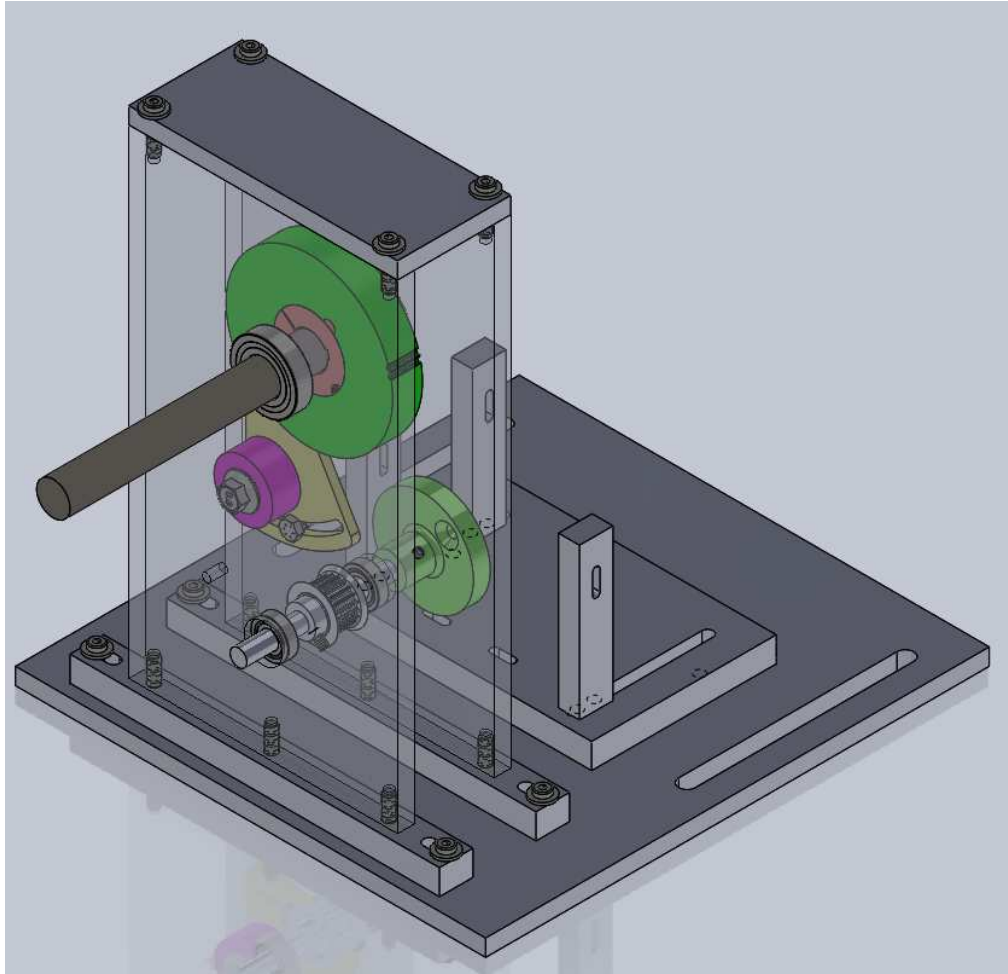


Figure 36: Assembled View of the Dynamometer Fixture (Post CDR)

The calculation attached in the Appendix 12: shows that the shaft experiences approximately a load of 60 lbf. For the shaft of the large pulley, we are planning to use a shaft with an outer diameter value of 1 inch. The bearing catalog rating is calculated as shown in Figure 37. The C_{10} value from the calculator is at 3.8 kN and the C_{10} value of the bearing with 25 mm bore that we plan to use is rated at 14 kN. This means that the bearing has a safety factor of approximately 3.7. Similarly, the C_{10} value for the bearing with 12 mm bore is rated at 6.89 which gives a safety factor of 1.8.

Symbol	Value	Name	Unit	
F_D	0.3	Force Desired	kN	
L_D	5000	Life Hour Desired	hr	
n_D	7000	RPM Desired	rev/min	
L_R	5000	1000000	Life Required (CHECK COMMENT)	CHECK
n_R	1	RPM Required	rev/min	
a	3		N/A	
C_10	5.73879355	3.84173749	kN	

$$C_{10} = F_R = F_D \left(\frac{L_D n_D 60}{L_R n_R 60} \right)^{\frac{1}{a}}$$

Figure 37: Bearing Rating Calculator

The shaft loads using the Marin equation and the safety factor is determined for the shafts of both pulleys. For the large pulley, the shaft has a safety factor of 12. This shaft size is constrained because we are planning to make the size of the output shaft from the reduction be the same as the dynamometer's shaft size for easy coupling. The shaft is secured onto the pulley with a 1610 SDS tapered bearing. Figure 38 shows the subassembly of the large pulley to the shaft.

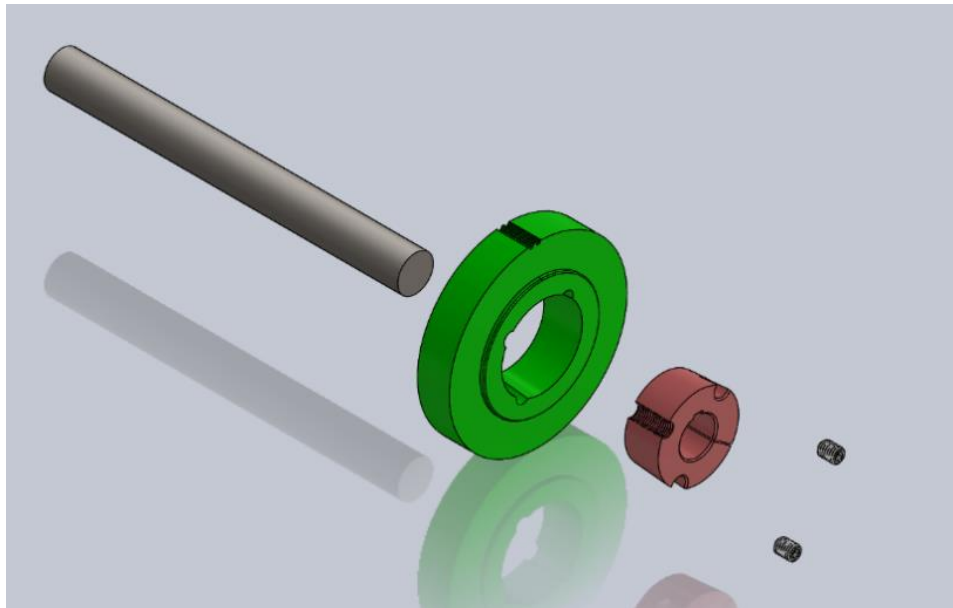


Figure 38: Large Pulley Subassembly

The 1" shaft is the output shaft of the reduction fixture and it connects to the input shaft of the dynamometer using an existing flexible coupler. The alignment of the shaft is verified by measuring the total run-out of the shaft of the reduction relative to the dynamometer shaft. Based on the coupler's manufacturer's recommendation, .015" total indicator reading is required for smooth operation with the coupler. The verification procedure is attached as Appendix 16: at the end of the report as part of the dynamometer fixture user manual.

For the small shaft, the safety factor is calculated to be at 1.5. The shaft design takes into account of the

coupling with the engine at the flywheel. The shaft is designed intentionally with a lower safety factor compared to other components. This acts as a safety mechanism since the shaft will fail before damaging other expensive components. Moreover, the small pulley assembly is not massive and is located between two thick aluminum plates. These plates will act as safeguards and prevent injuries in case of any failures. Figure 39 shows the assembly of the small pulley and the engine flywheel. The engine to reduction coupler is located onto the flywheel with the two countersink screws to ensure the alignment between the engine and the reduction fixture. Set screws are then used to secure the shaft to the coupler as well as the pulley.

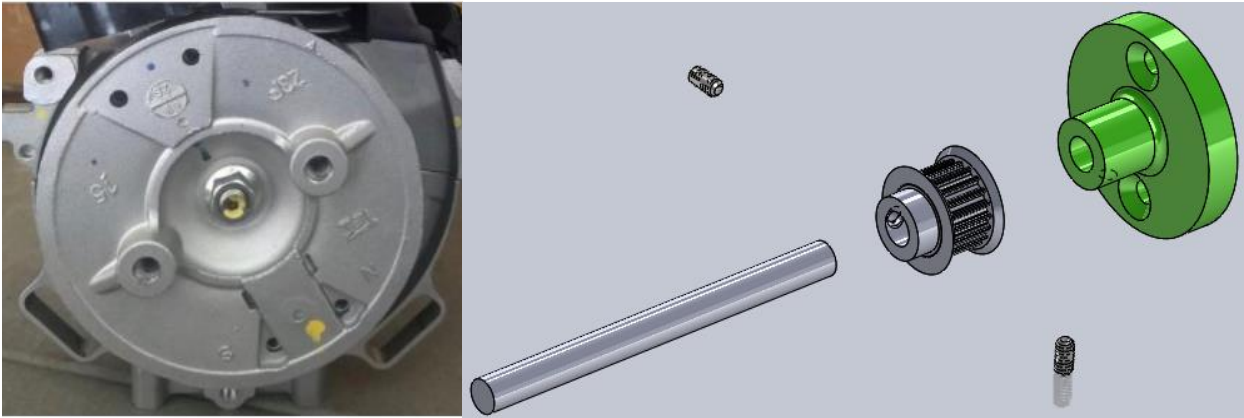


Figure 39: Engine Flywheel and Small Pulley Assembly

In addition, the design of the bearing plates is edited so that the bolts can be easily accessed while aligning the two plates. Figure 40 shows the bearing plate subassembly. Instead of installing the bearing plates directly onto the base plate, a bar is added as the bearing plate base. This allows the team to install the screws from the top side without any interference during the alignment process. Moreover, the thickness of those bars can be changed as needed to get the shaft alignment desired.

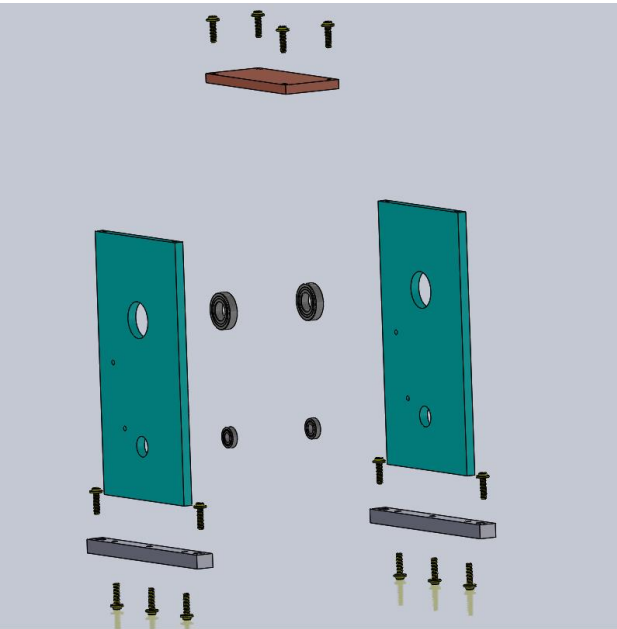


Figure 40: Bearing Plate Subassembly

A tensioner is also included to tension the belt properly. Figure 41 shows the tensioner subassembly. An idler is used to tension the belt from the back side. The hole and slot on the tensioner base allow the tensioner subassembly to pivot about the hole and it can be tightened down after the belt has been tensioned.

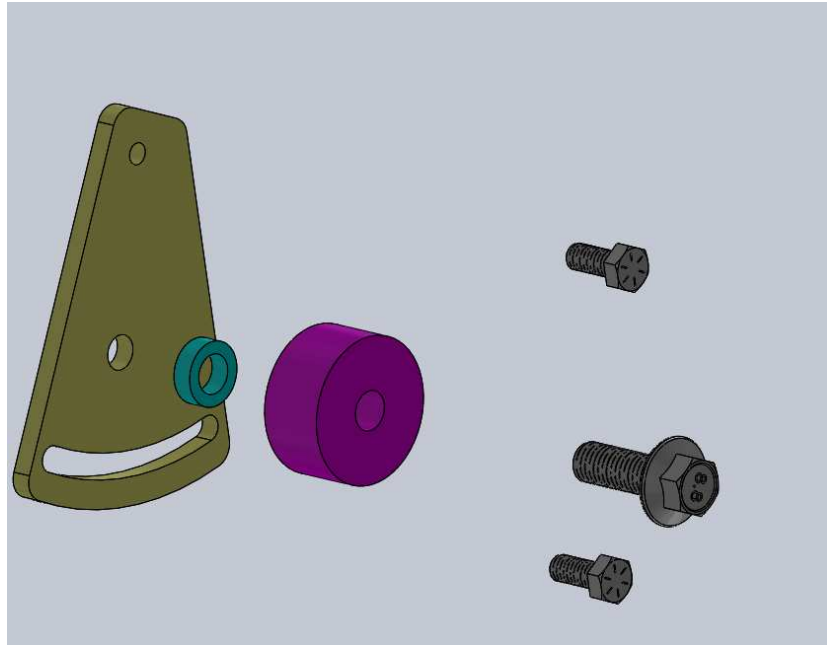


Figure 41: Tensioner Subassembly

Engine Mount

An engine mount was also designed so that the engine can be located and secured inline with the input shaft to the reduction power train. Since the engine CAD model is not available with the accurate bolt hole locations, we reverse engineered the locating holes on the engine so that an accurate mount can be designed. The exploded view of the engine mount can be seen in Figure 42.

When designing the engine mount, the team only focused on locating and securing the engine's six degree of freedom and ease of manufacturing. Other factors such as the weight of the mounts were not considered during the fixture design phase since those factors do not affect the functionality of the mount. Therefore, the risers are oversized based on the size of stock readily available for ICE. The use of slots in the risers allow the team to easily adjust the mounting as needed.

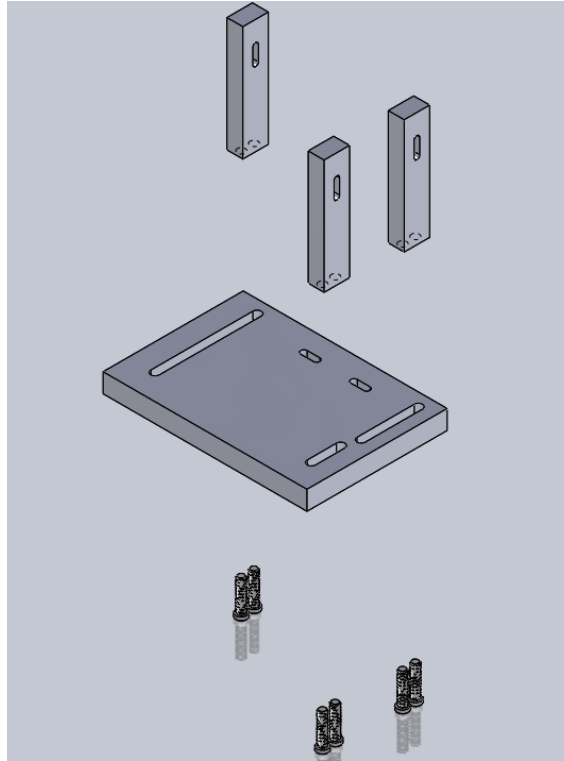


Figure 42: Exploded View of the Engine Mount

Safety and Maintenance

Although the reduction has been redesigned to have minimum pinch points and exposed parts that are rotating at high RPMs, there is still a risk of personal injury while operating the dynamometer. Team members should always wear personal protection equipment and follow the safety guidelines in the laboratory.

The major failure modes expected for this system are as follows:

- Failure at the coupling
- Excessive wear or failure of the belt
- Loosening at the fastener joints

Failure at the shaft coupling can occur due to poor alignment of the shafts. Therefore, a flexible coupler is chosen as it provides extra allowance at the connection. Based on the manufacturer's specification, the coupler allows for a maximum .015" concentricity between the shafts. We designed the riser plates so that the parts can be manufactured to meet those specifications. The flexible shaft coupler acts as a sacrificial component so that if there is significant misalignment, the coupler would break without causing injuries or damaging expensive components such as the dynamometer.

The excessive wear or failure of the belt will most likely be due to poor tensioning of the belt or pulley misalignment. To mitigate this, the team follow belt manufacturer's recommendation for tensioning and verify that the belts are tensioned to the requirement. The pulley misalignment can be reduced by taking precaution during the assembly of the fixture and qualifying the assembly via measurements before operating. Since the pulleys and belt are placed between the two plates, it would prevent parts from flying

out in the event of a failure. The team also installed a safety cover over the coupler and the exposed gap between the two plates.

Since the whole fixture assembly will experience vibration from the engine, the fasteners could become loosened over time. Before every operation, the team should check that all the fasteners are fully tightened and aligned. This failure mode can be avoided by including safety checks as a standard procedure whenever the dynamometer is going to be operated.

Components are mainly assembled in two methods: threaded fasteners and press fits. Since the four ball bearing needs to be pressed into the plate, it would be difficult to do maintenance on those components. All other components can be adjusted or swapped out easily.

Manufacturing Plan & Report

PART NAME	LIST OF OPERATIONS	MACHINE	TIME ESTIMATE (EACH)	Qty	TIME ESTIMATE (Total)
Engine Mount Riser	Sawing: Cutting to length	Band Saw	10 Min	3	30 Min
	Milling Op1: Trimming Saw Cut Ends	Manual Mill	1 Hour		3 Hours
	Drilling and Tapping Op1: 5/16-18 holes	Manual Mill	30 Min		1.5 Hours
	Slotting	Manual Mill	30 Min		1.5 Hours
Engine Mount Plate	Sawing: Cutting to length	Band Saw	10 Min	1	10 Min
	Milling Op1: Slotting and Trimming Side	Haas VF2	3 Hour		3 Hours
Large Pulley Shaft	Sawing: Cutting to length	Band Saw	10 Min	1	10 Min
	Turning Op1: Turning 1"OD	Manual Lathe	1 Hour		1 Hour
Bearing Plates	Water Jetting: Getting Stock to Size	Water Jet	30 Min	2	1 Hour
	Milling Op1: Milling Out Bores for Bearing	Haas VF2	3 Hour		4 Hours
	Drilling and Tapping Op1: 5/16-18 Holes on One End	Manual Mill	1 Hour		2 Hours
	Drilling and Tapping Op2: 5/16-18 Holes on other End	Manual Mill	1 Hour		2 Hours
Bearing Plate Base	Milling Op1: Face and Trim Side	Haas VF2	1 Hour	2	2 Hours
	Milling Op2: Face and Slot	Haas VF2	1 Hour		2 Hours
Bearing Plate End	Water Jetting	Water Jet	30 Min	1	30 Min
Engine to Reduction Coupler	Sawing: Cutting to length	Band Saw	10 Min	1	10 Min
	Turning: Turn the OD to Size	Manual Lathe	30 Min		30 Min
	Milling Op1: Milling Circular Contour and Counterbores	Haas VF2	3 Hours		3 Hours
	Drill and Tap: Drill and Tap Set Screw Hole	Manual Mill	1.5 Hours		1.5 Hours
Small Pulley	Turning Op1: Turning ID to Size	Haas TL1	3 Hours	1	3 Hours
	Drill and Tap: Drill and Tap Set Screw Hole	Manual Mill	1 Hour		1 Hour
Small Pulley Shaft	Turning: Turn the OD to Size	Manual Lathe	1 Hour	1	1 Hour
Reduction Base Plate	Water Jetting: Getting Stock to Size	Water Jet	30 Min	1	30 Min
	Drill and Tap: Drilling and Tapping Bolt Holes	Manual Drill	3 Hours		3 Hours
Tensioner Base	Water Jetting	Water Jet	30 Min	1	30 Min

Figure 44: Summary of the Manufacturing Plan for the Dynamometer Reduction

Due to the number of components needed for this reduction system, the team started manufacturing the parts as soon as possible. Figure 44 shows the routing for each component as a manufacturing plan. It lists the steps or operations required to make a specific part and time taken for each operation. This plan is used as a guide to prioritize and allocate required resources during manufacturing.

The team was able to manufacture most of the components successfully. Most of the machined components are completed and the important dimensions are verified using fixed gauges, vision systems and coordinate measuring machines (CMM) as needed. Figure 43: Engine, Engine Mount and Coupler Assembly. Figure 43 shows a completely machined assembly of engine mount with the coupler attached at the flywheel. The countersink hole was undersized by mistake and it was repaired using a manual mill.

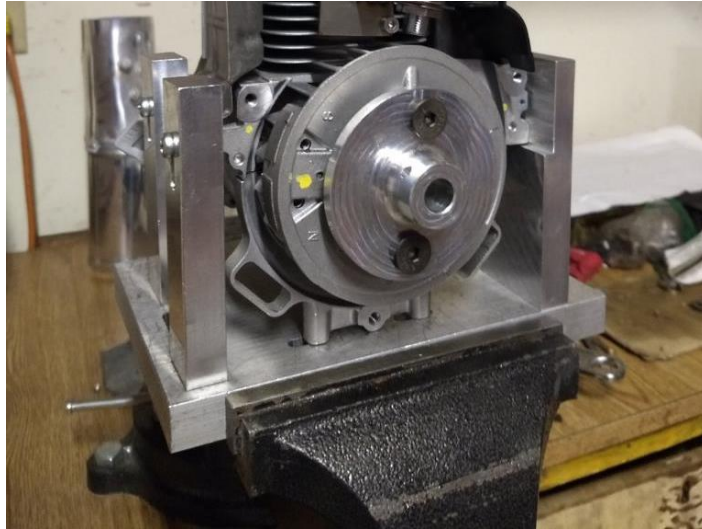


Figure 43: Engine, Engine Mount and Coupler Assembly

Moreover, Figure 44 shows the assembly of the dynamometer fixture. The bearings are press-fitted onto one plate and slip-fitted onto the other one. Both the small pulley shaft and large pulley shaft has a locational clearance fit with the bearings.



Figure 44: Dynamometer Fixture Assembly

Nevertheless, there were still some reworks required for some of the parts. Most of the reworks were needed because the team did not use the correct “.dxf” file for water jetting and we also forgot to account for the kerf width of the water jet nozzle. This led to undersized parts as shown in Figure 45. The bearing plate end was cut undersized, and it needed to be reworked.

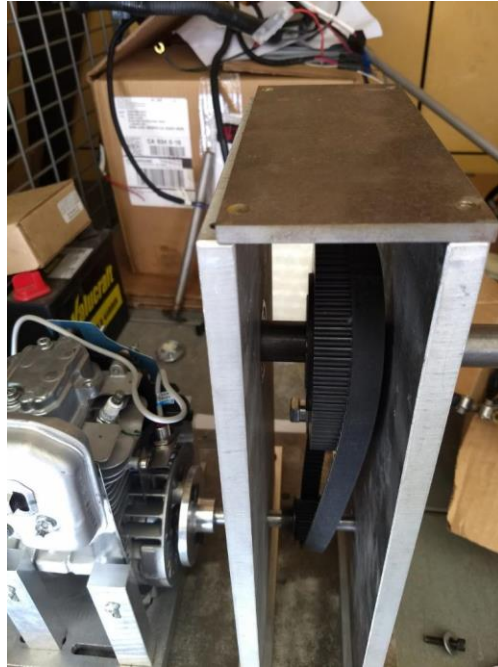


Figure 45: Undersized Bearing Plate End

One of the bearing plates was machined with oversized bores for bearing housing. The mistake was due to the cutter compensation error. Since the bores are oversized by only .001", the team decided to use the part for final assembly. Some Loctite was applied to keep the bearing in place, but the correct type was not available. Figure 46 shows that the bearing becomes out of place after a few tests on the dynamometer. As a recommendation, the next design iteration should include installing some sheet metal flanges on the bearing plates to retain the bearing outer race in the plate. Some flanges were already manufactured by the ICE team and are included in the delivered hardware. Alternatively, future teams may elect to use one or more small fasteners and washers in order to retain the outer race in the bearing plate.

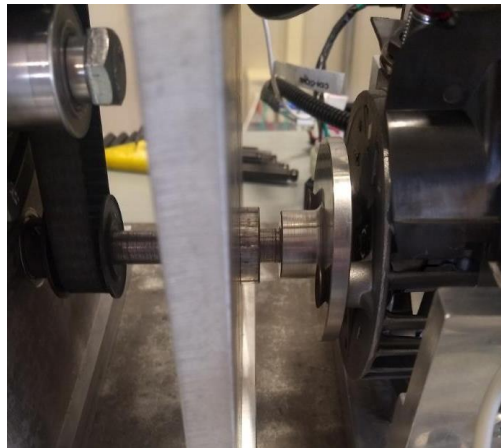


Figure 46: Oversized Bearing Bore Issue

Overall, the manufacturing was a success. All the components fit together and can be assembled as intended. Several tests are conducted on and off the dynamometer and there is no failure detected in the system.

Design Verification Plan & Report

Since there are several parts that need to be manufactured with high precision, the team used CNC mills and lathes to fabricate parts that need to have a better control on the dimensional tolerances. All the dimensions with tight tolerances are measured before and after assembly using a coordinate measuring machine to verify that the parts are manufactured to meet the design requirements.

Our team conducted the first test run without connecting the output shaft to the dynamometer to verify that there were no seized components in the system and the system functions as intended. From this attempt, we learned that an extra guard was required to shield the rotating components. This is essential for the operator safety. After some feedback from Dr. Lemieux, the team installed a sheet metal guard that not only covers the pulleys but also the coupler at the dynamometer.

The alignment with the dynamometer was tested in the engine lab. After the shafts were virtually aligned, a test indicator with a magnetic v-block was attached to the shaft at the dynamometer and the total runout was measured. The whole fixture assembly was then adjusted to get the desired shaft alignment. The team was able to achieve .012" total indicator indicating (TIR) during alignment. Figure 47 shows the final assembly of the reduction system attached to the dynamometer for testing.

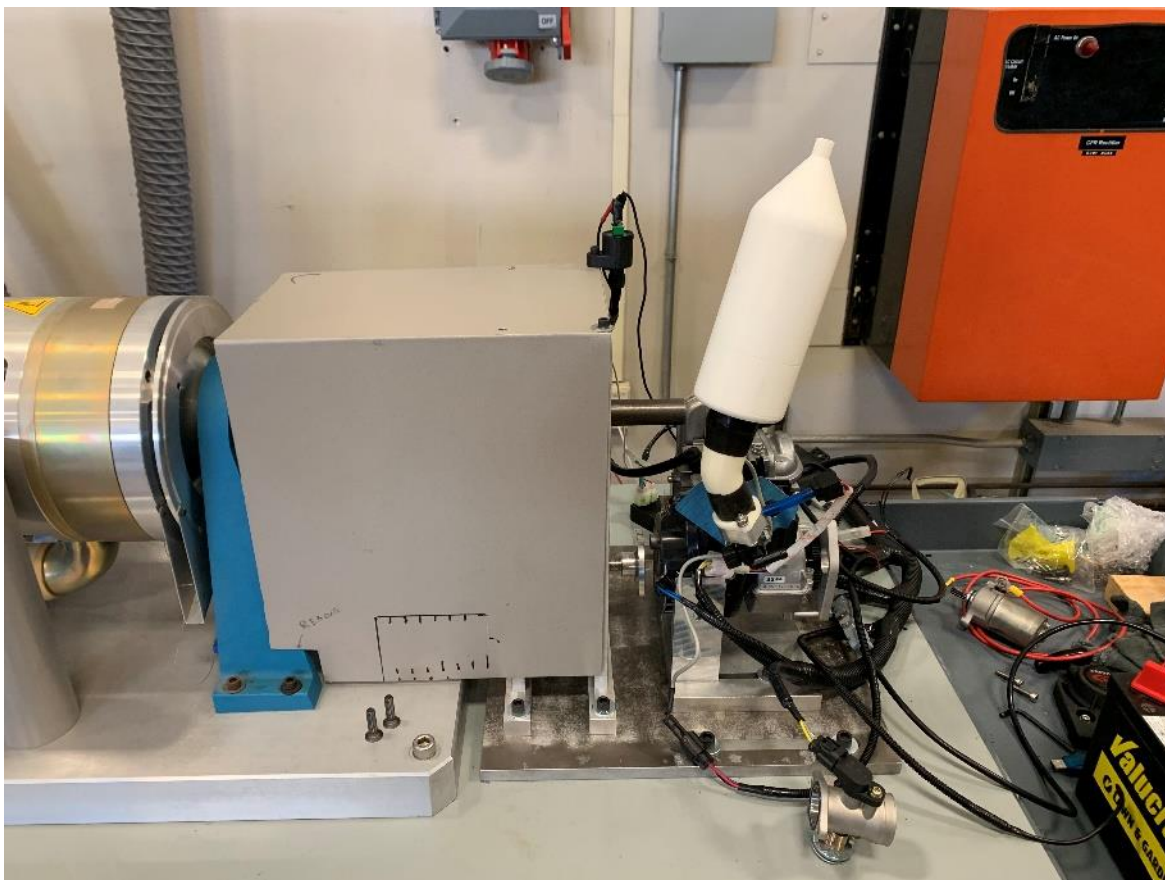


Figure 47: Dynamometer Reduction Fixture Final Assembly (During Testing)

The testing process was overall successful. Testing was conducted successfully and there were no major failures in terms of components. One bearing becomes out of place and the issue was resolved temporarily

with the use of Loctite. Some minor design changes such as installing sheet metal flanges would prevent such incidents in the future.

Bill of Materials and Cost Summary

The team created a bill of materials that specifies the components, materials and the hardware used for manufacturing the reduction system. Table 10 shows the information included in the bill of materials. This does not account for raw material used to fabricate all the machined parts. The raw materials used in machining process are all recycled from scrap plates and bars found at machine shops on campus. Although the use of the recycled material saved a large sum of money, our team has to do several pre-machining preparation to the acquired material. If the reduction system is fabricated using external vendors for machined parts, the total cost will be higher than the initial estimated cost due to the man hours required.

Table 10: Bill of Materials for the Dynamometer Fixture

Part	Supplier	P/N	Cost	Shipping	QTY	Total
Gates 7709-1080-p80-5MGT-15	MRO Supply	173041	\$ 67.83	\$ 0.00	1	\$ 67.83
Gates 7709-3020 P20-5MGT-15-MPB	MRO Supply	173046	\$ 33.50	\$ 0.00	1	\$ 33.50
Gates 9400-7125 625-5MGT-15	MRO Supply	2231916	\$ 20.27	\$ 0.00	1	\$ 20.27
1610 Bushing 1" ID	MRO Supply	249462	\$ 18.60	\$ 0.00	1	\$ 18.60
R16-2RS-ZZ Bearing (1" ID)	Big Bearing	SKU:R16	\$ 3.53	\$ 7.99	4	\$ 22.11
Sumray 5M Idler Pulley (12mm Bore)	Ali Express	58409-M	\$ 1.20	\$ 0.00	3	\$ 3.60
R8-2Z Bearing (1" ID)	McMaster	60355K601	\$ 7.08	\$ 10.00	2	\$ 24.16
Fasteners	Miner's Ace Hardware	-	\$ 0.75	-	33	\$ 24.75
Final Cost						\$ 214.82
Initial Budget						\$621.72
System Savings						\$ 406.9

Electric Starting System

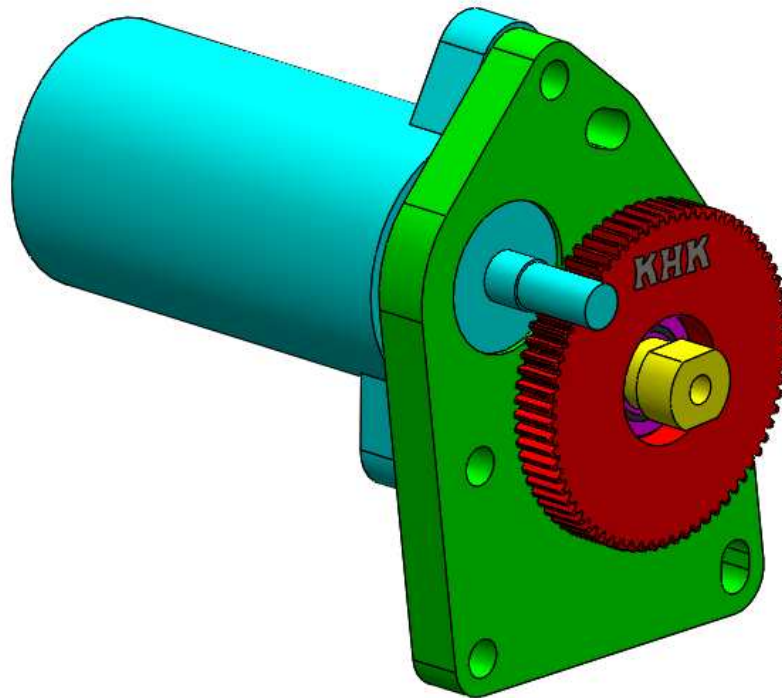


Figure 48: Electric Starting System

The electric starting system uses a one way bearing and a gear reduction system to start the engine using the starter motor previously used on the Yamaha 50cc engine. The starter motor drives a 70tooth gear which transmits torque through a one-way bearing to the engine crankshaft. An aluminum bracket with aluminum spacers supports the starter motor, and an adaption shaft is used to mate the one way bearing to the engine.

Motor

The Yamaha starter motor was selected because the GX35 starting torque and speed are not yet known. The power needed to start the Honda is expected to be less than the Yamaha because:

- The Honda has a smaller displacement
- The Honda has a lower compression ratio
- The Honda has an exhaust decompression system to reduce starting effort

The power required to start either engine is mostly dictated by the work required for compression and the starting RPM. The compression work was evaluated using a Matlab program supplied in [Ferguson], and is presented for both engines in Figure 49. The work was also estimated using the cold-air model, with results shown in Table 11.

Table 11: Cold-Air Model Estimates of Compression Work for Yamaha and Honda

Engine	Specifications	Compression Work (J)
Yamaha XF50	49cc – 12:1 compression	22.5
Honda GX35	35.8cc – 8:1 compression	13.5
Honda GX35 w/ GX31 piston	35.8cc – 12.8:1 compression	17.0

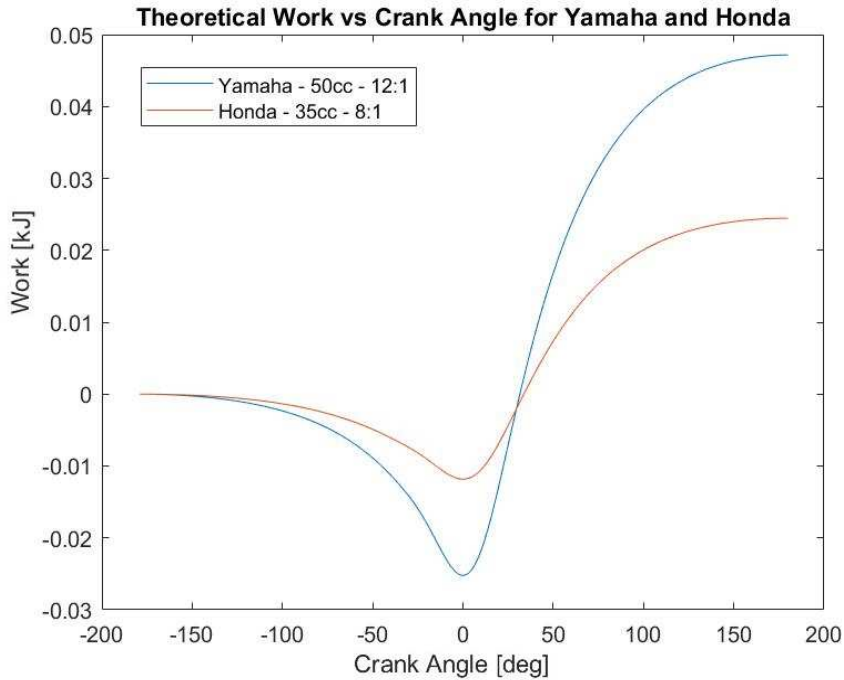


Figure 49: Comparison of Simulated Work vs. Crank Angle for the Yamaha and Honda

In Figure 49 the Yamaha is shown to theoretically require substantially more power to start. In addition, the Honda has a low speed exhaust decompression system to further reduce the cranking work requirements. Therefore team ICE believes the Yamaha starter motor will likely have sufficient power to start the Honda.

Ultimately, the power required to start the Honda will be determined by measuring the amperage draw of the Yamaha starter while starting the Honda. Assuming a certain efficiency, it will then be possible to determine the power required to start the Honda, and a different starting motor could be selected if the Yamaha is not suitable. For now, the 13.5 J of work was divided by 4π radians to get an average estimated cranking torque of 1.07 Nm. This seems incredibly high considering that peak torque output is rated as 1.6 Nm, but a better method to estimate the torque has not been found.

The cranking RPM is yet to be determined, but engine RPM datalogs were collected while using the hand starting system. Based on personal experience, an RPM in the low hundreds was expected by team ICE. More details are presented in the Design Verification Plan & Report. This data could be used to select a new motor and reduction system.

Both of these measurements are outlined in testing plan in Starter Testing & Analysis Plan.

The Yamaha starter is attached to a bracket which mounts via the same bolts as the clutch cover. A hole is

placed in this cover to allow the pinion to mesh with the gear.

Late in the manufacturing process it was discovered that the mounting holes on the starter are not perfectly in line. That is, instead of being at 180° the holes are at roughly 172° . The Mustang 60 CMM was used to determine the actual angle of the mounting holes. A representative schematic is shown in Figure 50.

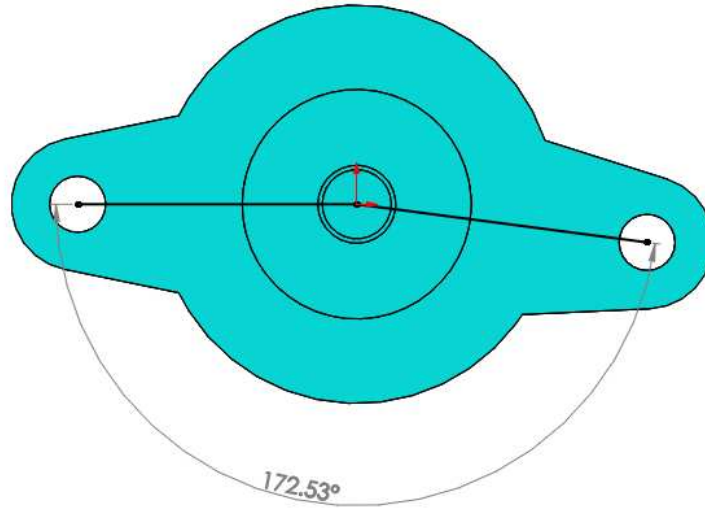


Figure 50: Starter motor mounting hole angle

Clutch & Reduction Systems

AGMA calculations presented in [Shigleys] were used to evaluate failure of the gear and pinion from bending and contact stresses. Major assumptions were required to determine the transmitted force – these are presented in the Motor selection section preceding this one. Lifetime requirements were calculated as follows:

- Simulation senior project team estimates 30 starts per competition lap
- ICE estimates four full revolutions per starting attempt
- ICE estimates a starting speed of 200RPM.

From this information, and attempting to minimize weight, we set the minimum number of starts to 120.

The bearing selection was dictated by the size required for the adaption shaft, and therefore the bearing has a safety factor of roughly 38. The CSK8 sprag roller bearing was chosen over a one-way needle bearing because it can carry axial loads as well perform clutching actions. The needle bearings found by ICE do not support axial loads created by the geartrain, and would therefore need to be combined with a second bearing. The width of this bearing combination was roughly 4 times that of the sprag roller bearing. This was not possible for packaging reasons.

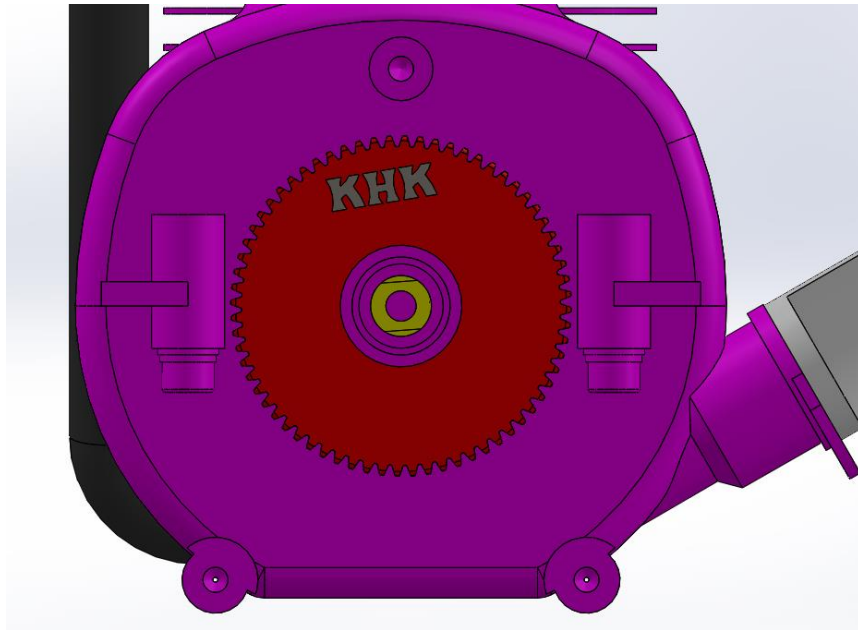


Figure 51: Clearance Requirements for Starter Gear

The gear selection was primarily driven by the module of the existing pinion on the Yamaha starter, and the space available between the mounting bosses on the GX35 (Figure 51). The largest possible reduction was chosen in order to mimic the large reduction used in the Yamaha XF50 design as closely as possible. This combination of module and diameter requirements led to the selection of a KHK 70T gear (SS0.8-70A). This is an unhardened steel gear. The Yamaha pinion has 9T and appears to be hardened. Based on the material properties of the gear, estimated loads, and other properties, AGMA calculations were performed for the system. The limiting component is the pinion in contact with a safety factor of 4.4. However, this is assuming an unhardened material. Additionally, in our experience, AGMA calculations are fairly conservative. Finally, the safety factor in bending was ~18.

ICE concludes that the reduction and clutch design is exceptionally robust, and could perhaps be lightened through machining the gear and pinion to a narrower face width. We recommend that the SMV team re-evaluate the starter design once the loads and starting RPMs are better understood.

The AGMA and bearing calculations are shown in Starter Calculations.

Mounting Bracket

During the CDR presentation, an alternative manufacturing method for the original bracket was suggested. Instead of a single piece, it would be made out of two separate pieces. This design is shown in Figure 52.

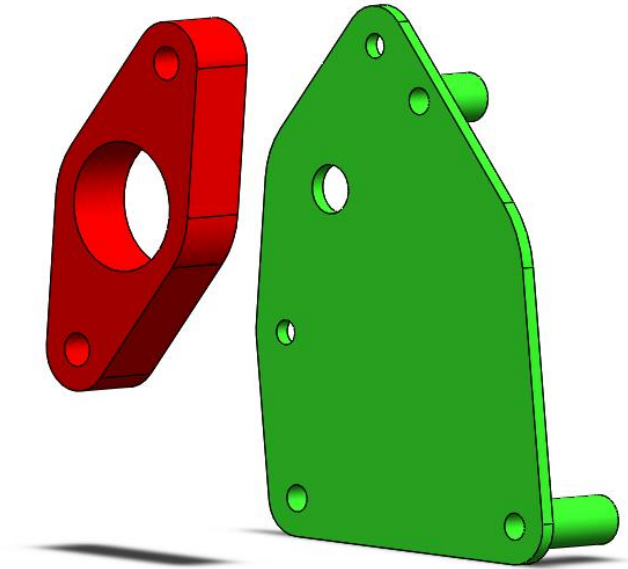


Figure 52: Proposed Alternative Manufacturing Method for the Original Starter Bracket

Following CDR the bracket design was re-evaluated. The team secured a relatively large quantity of scrap aluminum plate which was thick enough to allow for a single-piece bracket. Simultaneously, a 1:1 print of the original design was made to check fitment of the engine and starter motor. Because of this we noticed several dimensions needed to be changed. The actual dimensions were determined with the Mustang 60 Coordinate Measuring Machine (CMM), as shown in Figure 53.

Finally, some ability to adjust the meshing of the gears was desired. These changes resulted in a new bracket design, which is shown in Figure 54, and could be made on the waterjet.



Figure 53: Measuring the mounting hole and crankshaft locations of the GX35 on the Mustang 60 CMM

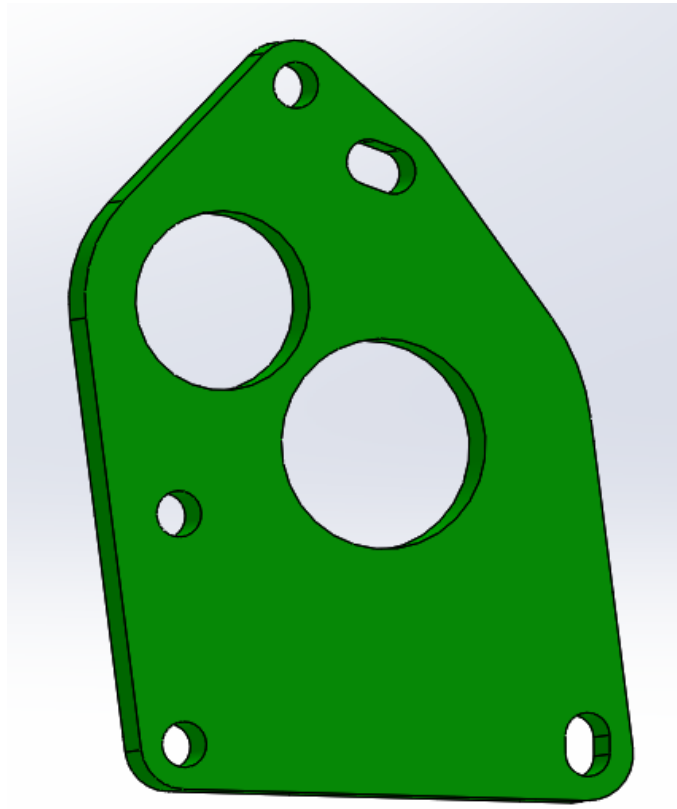


Figure 54: The new bracket design

Safety

The major failure modes expected for the starter system are:

- Failure of mounting brackets or threads
- Loosening of the adapter shaft or bearing
- Failure of gear teeth

For the first case, the starter and starter bracket housing will partially or fully separate from the engine. If the engine is running, there is potential for damage to these parts.

In the second case, the gear, and one-way bearing, plus potentially the adaption shaft, would separate from the engine. If the starting system was currently cranking, this assembly would have some rotational inertia. However, this assembly would be contained by the steel spacers and 1/16" shield (not drawn).

Similarly, in the third case, the failing starter gear teeth will be contained by a 1/16" shield (not drawn) which fully encloses the geartrain.

This same shield also prevents entanglement of clothing, hair, or appendages in the gear mechanism when the fairing is removed and the engine is running or starting.

Packaging, Repair, and Maintenance

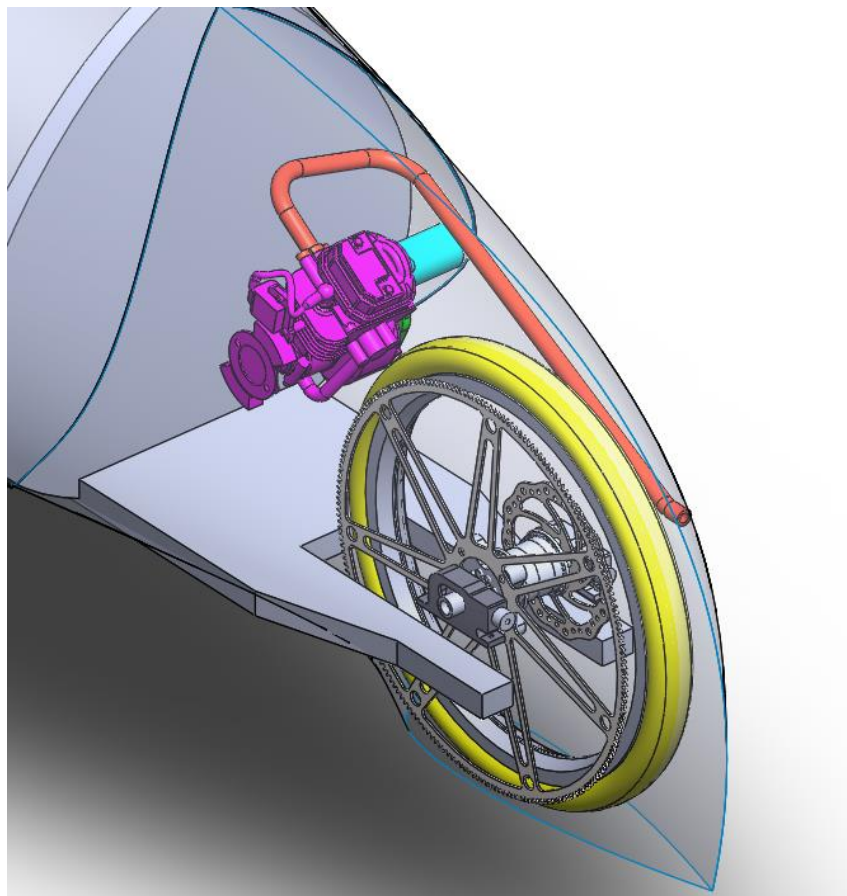


Figure 55: Packaging of Starter and Engine Assembly in SMV Chassis

Early this quarter, packaging information was finally made available to our team. Subsequent internal conversations about the intake and exhaust packaging, and conversations with SMV about clutch packaging, resulted in a well defined location for the engine package. It's location is summarized in Table 12.

Table 12: Engine Package Location

Description	Dimension
Drivetrain Center-to-Center Distance – from the center of the rear axle to the center of the engine crankshaft	16"
Engine Mounting Angle – angle between the top of the skate deck and a plane parallel to the flat portion of the valve cover	35°
Clutch Space – distance from the chain centerline plane to the mating face of the engine flywheel	2"
Engine Mounting Height – distance from the lowest point of the crankcase to the top of the skate deck	4.5"

This location leaves roughly an inch of space between the exhaust pipe and the firewall, leaves ample room between the rear brake and exhaust (if a thermal barrier is needed or for maintenance), allows the oil filler cap and spark plug to be removed with the engine in the car, and fits the starter inside the aero fairing.

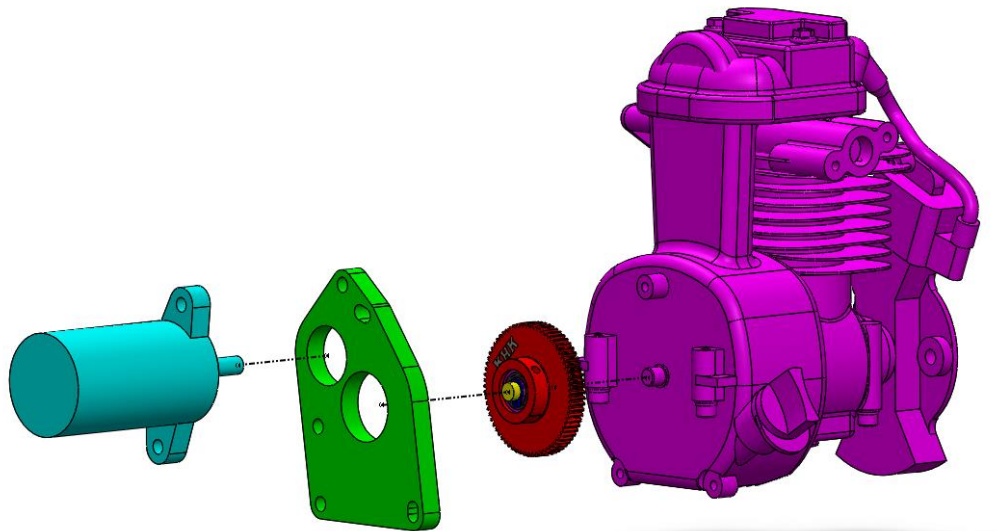


Figure 56: Starter Bracket Mounting

The gear, bearing, and adaption shaft subassembly is threaded onto the Honda crank. The one way bearing would allow for the assembly to be threaded on by gripping the gear OD. For removing the subassembly, flats are provided in the adaption shaft – otherwise the one way bearing would prevent disassembly. For

both of these operations, the crankshaft must be prevented from rotating. This has proven to be easily accomplished by gripping the flywheel OD by hand (with a glove).

The starter support bracket attaches using three allen key bolts in the same location as those used for the original Honda design. The bracket is designed so that the allen key can be used in both the high torque and long-reach orientations with the engine in the car. The starter motor is attached to the bracket using two allen key bolts, which are also oriented for access with the assembly in the car.

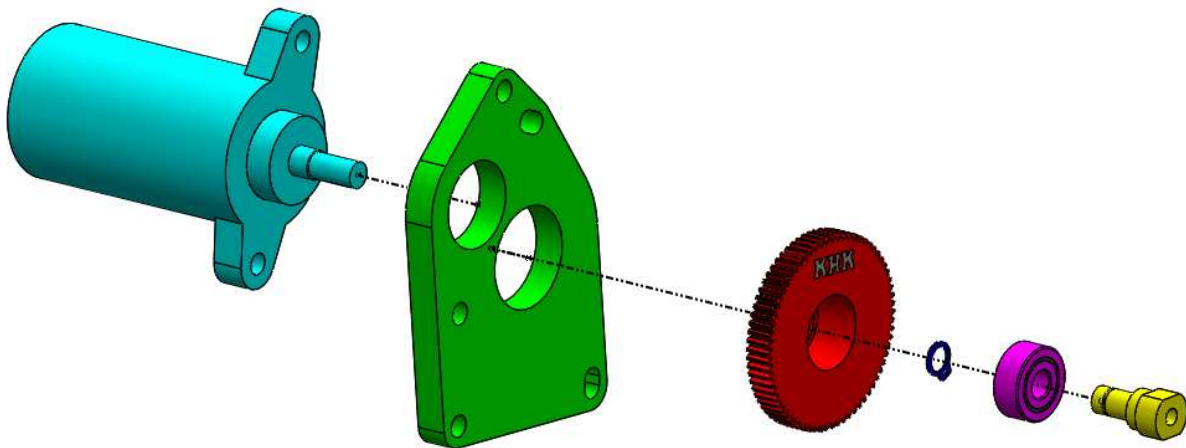


Figure 57: Exploded Diagram of Starting System

The adaption shaft, bearing, and gear must be pressed together. This assembly is held together with two lips a retaining clip, and a set screw.

Manufacturing Plan & Report

The design utilized as many off the shelf parts as is possible in order to minimize manufacturing time, operations, and cost. The needed features were designed with to simply manufacturing where possible. The major parts are as follows:

- KHK SS0.8-70A gear
- CSK08 one way bearing
- Custom adaption shaft
- Custom mounting bracket
- Hardware store steel spacers & bolts

The KHK gear required turning on the lathe in order to open up the bore for the CSK bearing. The bearing manufactures specifies a tight n6 tolerance on the gear bore. However, we found this tolerance to be very difficult to meet. On our first attempt to press the bearing into the bore the bearing seized. While attempting

to press the bearing out the required cup was not available and the bearing was destroyed. A cutoff wheel was used on a dremel to slice the remains of the outer race which was subsequently removed with a punch. The results can be seen in Figure 58. Ultimately, a 1 thou interference fit was achieved and the bearing was successfully pressed into place.



Figure 58: The gear with the remains of the outer race in the bore (left). Marring on the face of the gear was from the vise while attempting to remove the race with a drift. The pieces of the race after slicing and removal (right).



Figure 59: The custom groove cutting tool

The custom adaption shaft was turned from a steel shaft. The following features were added: reduced diameter to final dimension, external retaining clip groove, internal bore & thread, and a pair of flats. Except the flats, these featuers were all be turned on the lathe.

The retaining clip groove was cut using a custom ground high speed steel tool. The optical comparator was used to check the width of the cutting edge of the tool. The final tool is shown in Figure 59.

The bearing manufacturer specifies a N6 tolerance on the shaft diameter. Afterwords the mill was used in order to machine the wrench flats.

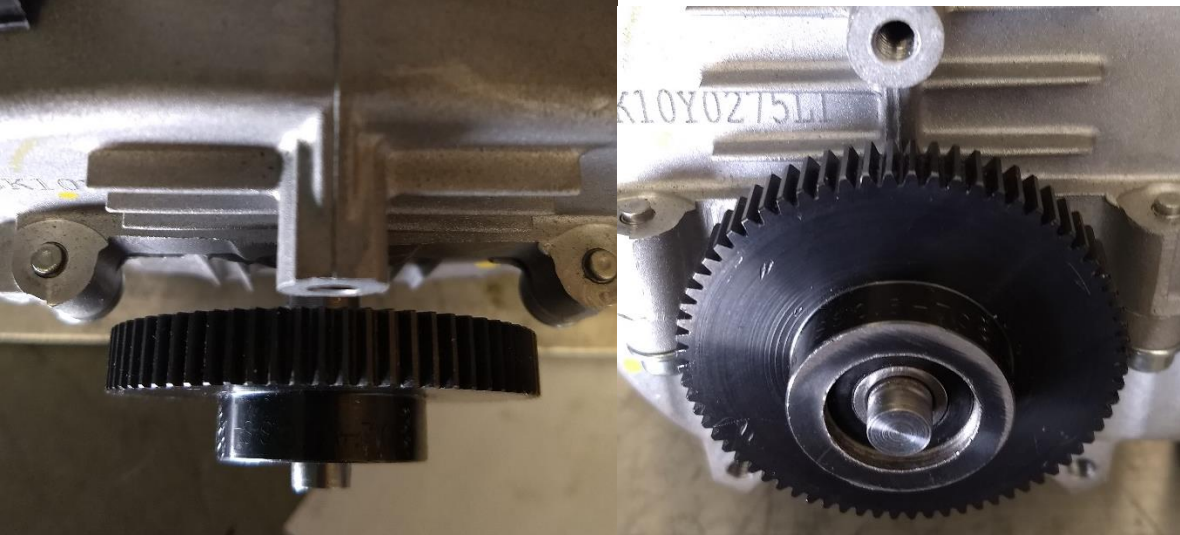


Figure 60: The finished gear and adaption shaft threaded onto the engine.



Figure 61: The gear and adaption shaft with the retaining c-clip

The mounting bracket was made with the new Mustang 60 waterjet. The material is aluminum in an attempt to reduce weight. Two sides of the bracket were made parallel to aid in fixturing if later modifications were needed. The finished bracket is shown in Figure 62.

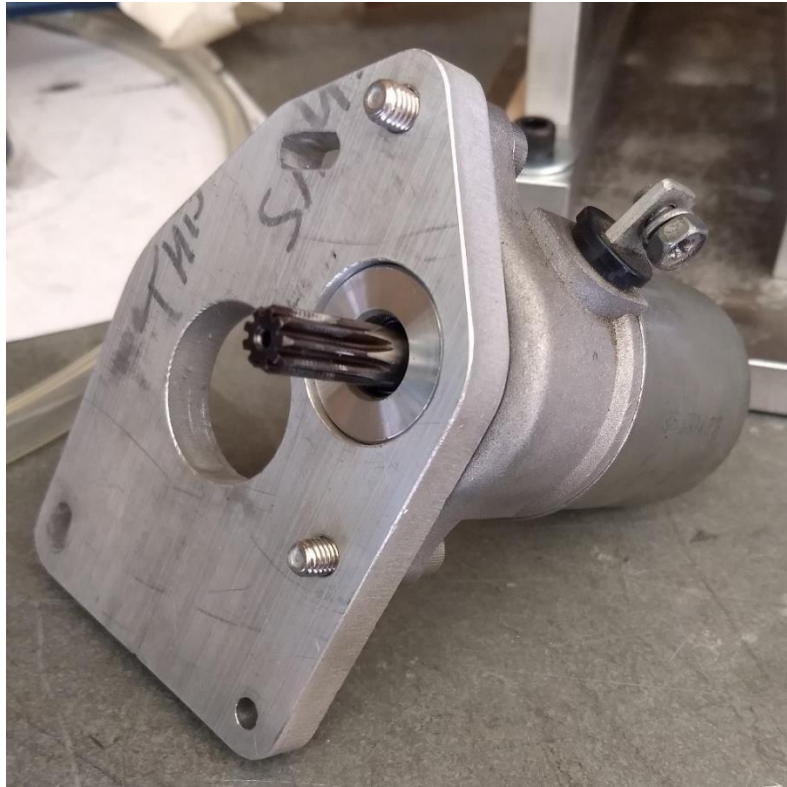


Figure 62: The finished bracket with starter motor attached before fastener trimming

Design Verification Plan & Report

The primary goal of ICE's starter system testing plan was to determine the actual starting speed and torque. These results were to be compared to the design estimates. No formal testing plan to evaluate the lifetimes of the gears or bearing was prepared at this due to the substantial safety factors.

The details of the starter testing plan are presented in Appendix 8:

Unfortunately, the amount of testing performed was limited due to a last minute complication. The current required to run the starter motor exceeds the measurement capability of the multimeters available to the team. Therefore, a shunt resistor or more powerful meter are required. This discovery was not made until late in the quarter. At that point ordering and shipping a shunt resistor or coordinating with the EE department to use higher power meters would both take too long.

However, a simple test was performed to qualitatively evaluate the effectiveness of the starter motor. The system was attached to the GX35 and reduction system, but not to the dyno itself. When powered by a 12V battery, the starter quickly brought the engine to speed and the ECU successfully took control and ran the engine. Compared to cranking times and efforts (indicated by starter motor and engine cranking noise) commonly seen in cars, the starting system was very fast and understressed. We are confident that a more

compact and lightweight system could be designed.

Additionally, we were able to determine a more accurate estimate for the cranking speed from an EFI datalog. Figure 63 shows the RPM plot used to determine the RPM range. Four RPM spikes can be seen before the engine fires on the fifth attempt.

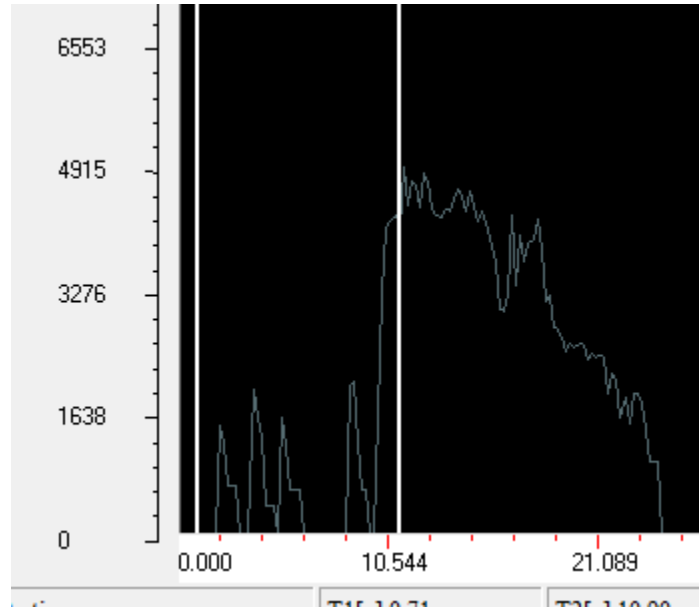


Figure 63: RPM plot used for estimating cranking speed

The first four attempts had peak speeds of 1800, 2400, 2000, and 2400 RPM. It is not possible to distinguish the end of cranking from the beginning of the engine running for attempt number five. Note that these tests were performed with the original Honda equipped pull-start system - therefore we suggest using 2000 to 2400 RPM as a target cranking speed.

Bill of Materials and Cost Summary

As anticipated, sufficient used stock material was found to manufacture all of the needed parts of the starting system. This led to a substantial savings over the anticipated budget. The retaining rings which were planned to be ordered from Zoro.com were combined with another McMaster order. The \$1.23 savings that could have been had via Zoro.com was deemed not to be worth the effort. The BOM and cost summary for the system are shown in Table 13.

Table 13: Electric Starting System Bill of Materials

Part	Supplier	P/N	Cost	Shipping	QTY	Total
Yamaha Starter Motor	N/A	-	\$ 0.00	\$ 0.00	1	\$0.00
KHK Gear	KHK	SS0.8-70A	\$ 27.02	\$ 25.00	1	\$ 53.07
CSK8 One-way Bearing	VXB Bearing	KIT8176	\$ 12.49	\$ 13.52	1	\$ 26.01
External Retaining Ring - 8mm	McMaster	90967A120	\$ 6.38	-	1	\$ 6.38
Internal Retaining Ring - 22mm	McMaster	98455A122	\$ 6.16	-	1	\$ 6.16
Aluminum Spacers – 5/16” x 1”	Miner's Ace Hardware	58409-M	\$ 1.20	\$ -	3	\$ 3.60
Final Cost						\$95.25
Initial Budget						\$169.96
System Savings						\$74.71

Electronic Fuel Injection

Design Overview

The stock Honda GX35 uses a carburetor to premix air and fuel before releasing it into the cylinder for combustion. To compete in the Shell Ecomarathon, the engine must use EFI (Electronic Fuel Injection with a fuel injector) rather than a carburetor to mix fuel and air before combustion. This fuel injector must be housed along the intake and be directly controlled by a microcontroller to regulate the fuel flow and time injection for the proper timing of the 4-stroke engine. In order to regulate this fuel flow, the microcontroller analyzes the temperature and pressure of the engine with a series of sensors.

One of the methods of increasing overall engine thermal efficiency is by “tuning” the fuel injection system. This tuning is done by altering the amount of fuel released from the injector based on the results of the temperature and pressure sensor readings. For this engine and this application, the tuning of the engine will focus on achieving the highest possible thermal efficiency while keeping the power output level above the required 1 hp at 5000 rpm.

The following components have been selected by the ICE team to remove the carburetor and incorporate an EFI system.

Table 14: EFI Bill of Materials

Quantity	Subsystem	Item	Item Description	Supplier	Estimated Ship Time
1	ECU System	ECU	Electronic Control Unit	Ecotrons	1-2 wks
1		Harness	Wiring harness for component to ECU connection (Proprietary)	Ecotrons	1-2 wks
1	Intake	Throttle Body	28mm intake throttle assembly	Ecotrons	1-2 wks
1		Intake Manifold	Adapter and injector mount	Ecotrons	1-2 wks
1		Fuel Injector	38g/min fuel injector	Ecotrons	1-2 wks
1	Fuel	Fuel Pump	31mm diameter, 2A draw, 25L/hr	Ecotrons	1-2 wks
1		Fuel Pressure Regulator	3bar regulator to increase fuel pressure	Ecotrons	1-2 wks
1		Fuel Filter/connection tubing	Fuel Filter and connection hoses/clamps	Ecotrons	1-2 wks
1	Sensors	MAP	Mass air pressure sensor (1.05bar)	Ecotrons	1-2 wks
2		Temperature sensor	Thermocouple for engine/intake temperature	Ecotrons	1-2 wks
1		CDI	ECU controlled spark advance (programmable)	Ecotrons	1-2 wks
1		O2 Sensor	Oxygen sensor and connection	Ecotrons	1-2 wks
1	Adapters	Serial Cable	ECU to computer program cable	Ecotrons	1-2 wks
1		USB Adapter	USB to RS232	Ecotrons	1-2 wks
Total Cost:			\$699.00		

In order to streamline tuning and allow the team a baseline to tune from, a kit-style system can be acquired from Ecotrons. This kit includes many of the components required to convert the GX35 engine from carburetor to EFI. The sensor and microcontroller equipment will make the conversion process straightforward and will allow the ICE team time to tune the engine to our power and efficiency goals. The critical component of this system is the fuel injector. To verify that this component will be sufficient for our application, we performed a basic fuel flow calculation across the range of our operation. The injector supplied with this EFI kit operates within our requirements.

While the EFI kit includes a throttle body and fuel pressure system, neither are required for our application. After gathering baseline data these components will be removed from the engine and replaced with the ICE team’s designs. The throttle body will be replaced with a resonator-intake system (See intake section). The fuel injector will be incorporated from the EFI kit into the new intake. The fuel pressurization system will also be removed to allow the fuel pressure system required by the Ecomarathon rules to be included.

Once this system has been incorporated on the GX35, the further optimization could result in increases in efficiency. The ECU that will drive this injector and microcontroller can be replaced and/or reprogrammed for higher efficiency based on empirical data gathered during engine tuning and testing.

Safety

The transformation from carbureted engine to EFI engine requires a few safety considerations. The largest safety concern is performing the conversion on the engine. This will require the use of basic hand tools including screwdrivers, drills, and wrenches. All Cal Poly tool safety guidelines will be followed during this procedure.

The engine EFI system runs off a 12 volt battery. This battery and all associated connections will be performed in compliance with Cal Poly safety procedures.

Repair and maintenance checklist should be performed as prescribed.

Repair and Maintenance

The EFI system must be kept clean and be easily serviceable. Additionally, several components will need to be removed and replaced with further development. The wires connecting the ECU to the sensors must

also be frequently inspected for shorts melting of the plastic shielding. To streamline maintenance, the following checklist should be confirmed every 5-10 operations of the motor.

Item	Criteria	Confirmation
Intake Sensors	Properly positioned	
	Clean and free from debris	
	Cable intact	
	Resting data accuracy	
Exhaust Sensors	Properly positioned	
	Clean and free from debris	
	Cable intact	
	Resting data accuracy	
Engine Temperature	Properly positioned	
	Clean and free from debris	
	Cable intact	
	Resting data accuracy	
Battery	Leads connected	
	Free from corrosion	
Overall System	Wires free from rotating components	
	All wires constrained near rotating components	
	Connections to DAQ/Controllers connected	

This chart can also be found in Appendix 7:.

Manufacturing Plan

The EFI kit used at the baseline for the ICE EFI development can be purchased from Ecotrons. This kit is available at 10% discount to the Cal Poly Supermileage team, and ships in 1-2 weeks. If replacement parts are required, they can be requested from Ecotrons.

Once the EFI kit is obtained, it is to be installed onto the Honda GX35 engine. This installation will be performed by the ICE team, and follow the wiring diagram provided. For tuning purposes, more data must be gathered than for normal operation. As the ICE development will include this data, a wiring diagram for the entire Dyno-Fuel-Engine system is provided as a map for assembly.

Modifications to the EFI kit and GX35 engine will also take place. Once the baseline data is gathered for the standard kit, the custom intake and exhaust can be installed on the engine. With the new intake on the engine, the fuel injector must be removed from the throttle body and installed into the custom intake.

The following wiring diagram provides the map for sensor placement and connection to DAQ or controller.

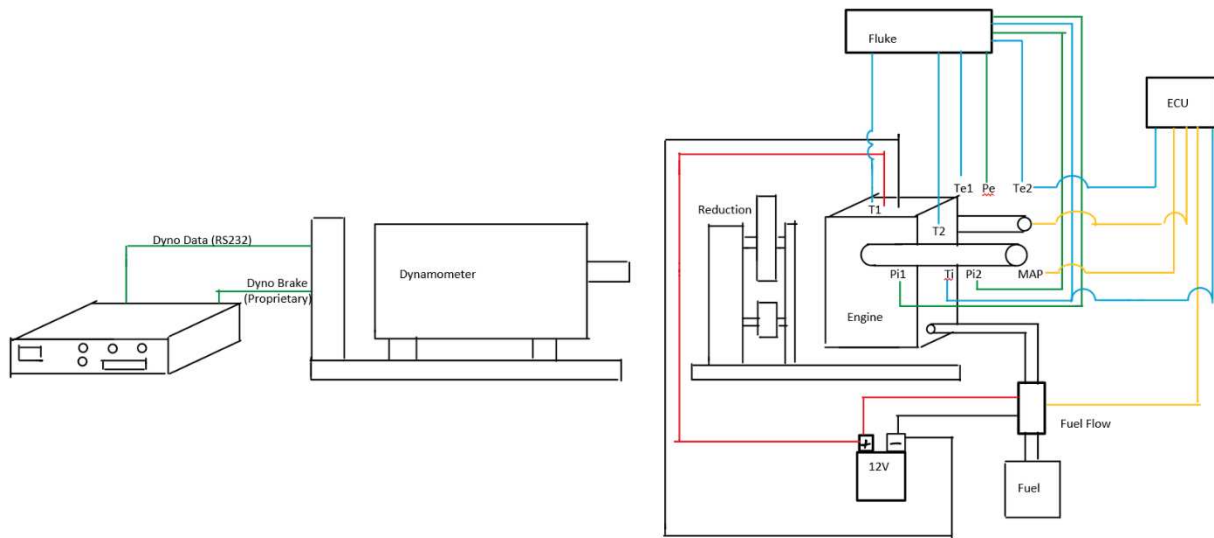


Figure 64: Wiring Diagram for EFI system

Design Verification Plan

Upon assembly, the base EFI kit will be run on the dynamometer using the testing plan provided in Appendix 11:. This test will evaluate the efficiency of EFI system. This efficiency will be compared to the carbureted engine efficiency to provide a baseline for the increase provided by an EFI.

Once testing of the base EFI kit has been completed, the throttle will be removed from the engine and the injector will be installed into the ICE custom intake. This intake will be installed on the engine, and tested to the same testing plan used for the base EFI kit. Any efficiency increase or decrease will be noted and addressed. Once the intake has been characterized, the next step is to modify the tune on the ECU (electronic control unit). Each individual tune will be tested to the same parameters called out in the testing plan found in Appendix 11:.

All testing will be performed on the Magtrol eddy current dynamometer. The engine will be mounted to the test table by a custom engine mount designed for this setup. To optimize the error on the measurements, power will be transmitted through a belt-pulley reduction. This reduction is then coupled to the dyno shaft with a sacrificial coupler.

Preliminary Testing

After successfully connecting the EFI kit to the engine, bench-tests were performed to confirm that the ECU was controlling the injector and spark timing during the engine's operation. This testing was performed with a throttle body to allow for control over air intake to help start the engine. Although the engine did run, the idle was rough and caused the engine to stall several times during testing. Given the lack of an oxygen sensor on the exhaust system, it was assumed that the ECU was unable to alter the injected fuel amount. This open loop system eventually reached an unstable state and the engine stalled out.

To analyze the performance of the engine and the EFI, the engine was then coupled to the dynamometer

fixture described in the “Dynamometer Fixture” section. At this point, the throttle body was removed and replaced by the intake resonator. The engine was then run coupled to the belt reduction system (without the engine dynamometer). Testing this configuration yielded much more stable results than open-bench testing such that the engine started quickly and maintained a more consistent and stable rpm. The success of this trial could be due to each of the two changes; the resonator could be providing the perfect amount of air to lightly constrict the intake to help start, while the added weight of the belt drive system acts as a flywheel, maintaining the rotational velocity of the engine on each compression stroke and allowing the engine rpm to remain more stable.

Once the team was satisfied with the operation of the engine and the belt reduction system, the device was coupled to the engine dynamometer. The engine was then tested at normal operation for several tests. During these tests, data was gathered to capture a baseline of the engine’s performance before modifications are made to the ECU for tuning.



Figure 65: Engine Configuration as coupled to the dynamometer

Testing Results

To complete the ICE engine project, the team has evaluated the baseline operation of the modified fuel-injected Honda GX35. Using this data the Cal Poly Supermileage team will be able to tune the engine for

performance, power, and efficiency by comparing to the baseline efficiency illustrated here.

ECU Software

The EFI ECU is equipped with a proprietary software that allows the user to tune the engine to the desired application. Comprehensive documentation of this software can be found on the manufacturer’s website. This software, when connected, provides live data monitoring for a range of variables including RPM, MAP and engine temperature (See Figure 66).

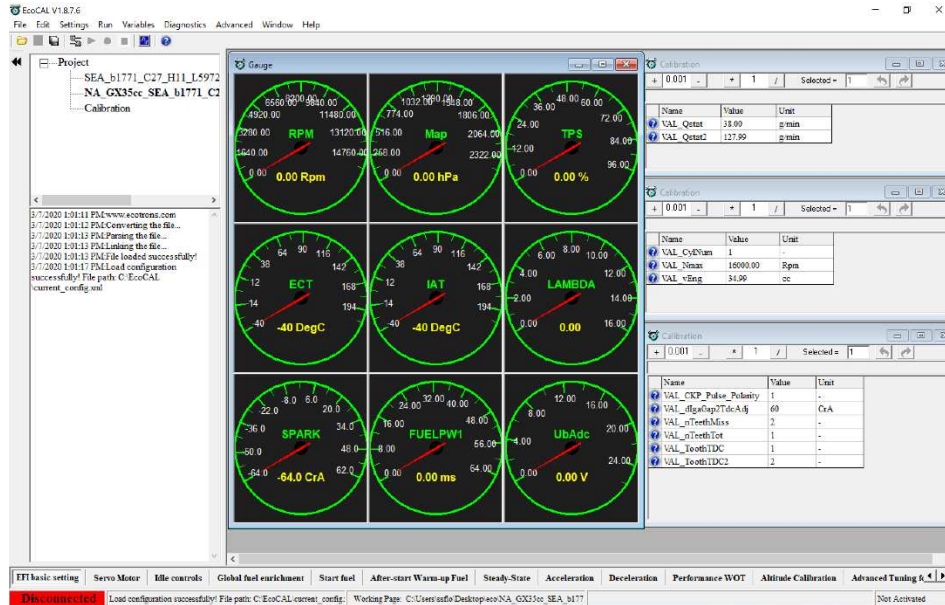


Figure 66: Ecotrons ECU software illustrating live-data variables

This live data allowed the team to confirm the readings from the dynamometer controller and validate that device’s output. The live data also helped show the issues with the engine’s performance. The team was directly able to correlate drops in RPM with variations in the spark and timing. In future tuning runs, the user will also be able to change variables like injector pulsewidth in real time and immediately evaluate the effects.

In addition to the live data tools, the data for the entire run is saved and output to a .CSV format. The Ecotrons ECU software contains a “Data Analyzer” tool that allows the user to plot and evaluate the data from each run in one place. With this tool specific events can be easily correlated to sensor or engine issues and will greatly aid in the engine tuning process. An example of this data analysis tool can be found in Figure 67. While the file is a .CSV, viewing it in spreadsheet programs is complicated by the data formatting.

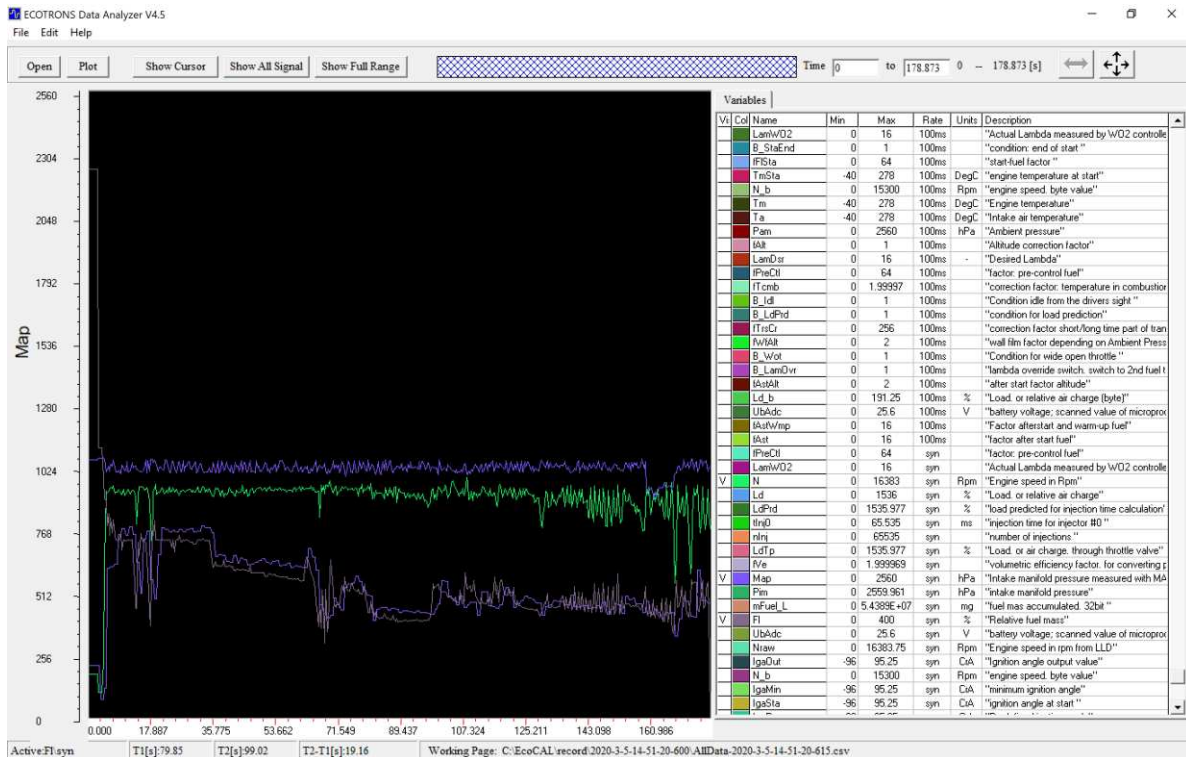


Figure 67: Engine Performance Data plotted with Ecotrons Data Analyzer for a sample dynamometer run.

The trial in Figure 67 is an example of the usefulness of the Data Analyzer. In this plot, the engine RPM can be seen in green, the manifold air pressure (MAP) in blue, the relative fuel mass in grey and the fuel flow rate in purple. For this three minute test, the engine started and ran smoothly at the beginning of the trial, but around the 160 second mark began to fluctuate. The trial ended when the engine became too unstable and the operator stopped the test. At the conclusion of the test, the operator was able to open this plot and determine that around the time the engine speed fluctuated out of control there was a severe drop in manifold air pressure. The ECU then attempted to correct the problem by increasing the fuel flow rate, which in turn caused the engine to fluctuate enough that the operator stopped the test.

The software allows the engine tune to be extremely customizable. The tabs seen at the bottom of Figure 68 each contain a different set of variables that may be altered to achieve different outputs. Once the desired ranges for tuning are determined, this software also allows for easy and rapid changes to the lookup tables used in calculating fuel addition. By modifying these tables, the power and fuel efficiency can be changed based on the requirements of the vehicle and driver. Some of these tables can be found in Figure 68.

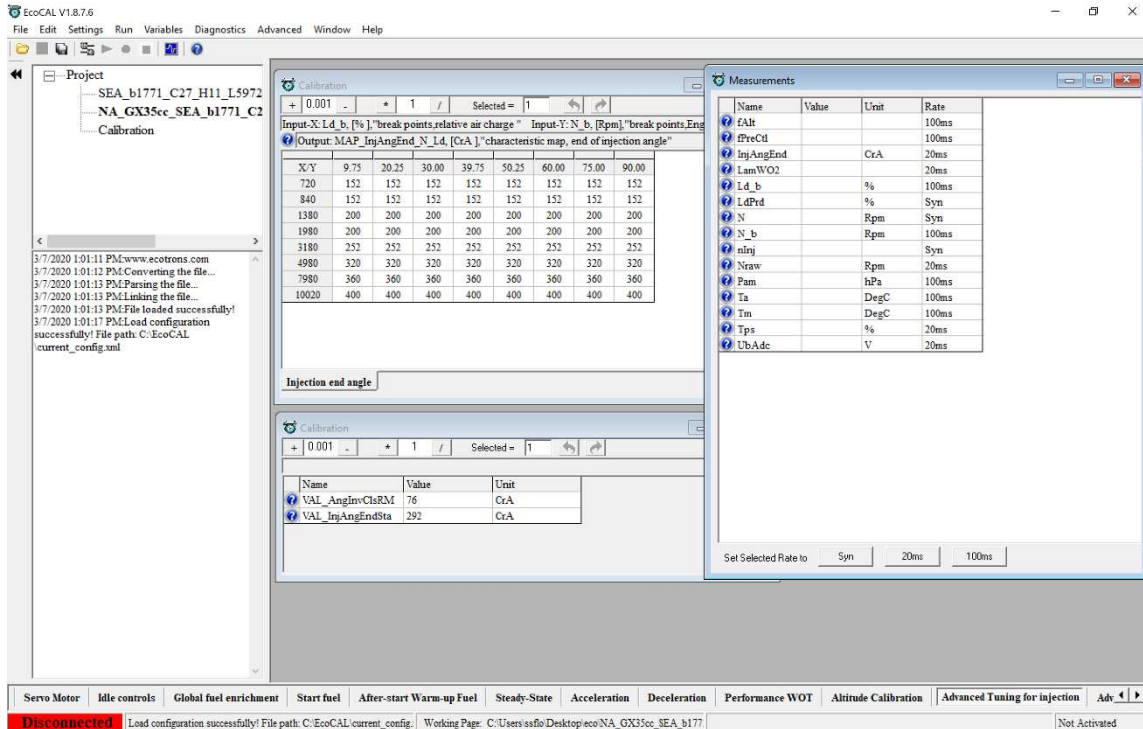


Figure 68: Lookup tables for advanced injection tuning within the Ecotrons software

Preliminary Data & Conclusions

While testing the engine-reduction-dyno configuration, the ICE team was able to collect preliminary power data. The stock Honda GX35 power curves illustrate a peak power of 1.3 horsepower at a speed of 7000 rpm, with a peak torque of 1.2 ft.lb at 5500 rpm. While the team was unable to gather data file from the dynamometer, live data was read while testing the modified GX35 with custom intake, resonator, and EFI system. The peak data from this test is was captured and illustrated below in Table 15.

Table 15: Preliminary Power & Torque Test Data

Parameter	Stock Engine (Reported from Honda)	Modified Engine
Torque	1.2 ft.lb @5500 RPM	1.63 ft.lb @5440 RPM
Power	1.3 hp @7000 RPM	1.8 hp @5980 RPM

This initial result is extremely encouraging for the viability of this engine for the Supermileage competition. Without any optimization or tuning the modified engine already produces more power and torque than the stock engine at lower speeds. Producing more power at 1000 rpm lower means that the engine will cycle 1/7th as much as the stock engine and therefore use much less fuel. Additionally, when interviewing past researchers into the supermileage requirements (see Summary of Meetings/Interviews section) developer Will Sirski estimated a required power of 1.0 hp. Because the engine is operating well above that, there is exceptional room to tune the engine, reducing fuel and power while still being within the required range for the vehicle.

However, it is the team's recommendation that the ECU be replaced with a more widely available design. While installation, tuning, and troubleshooting manuals are available, they are clearly written by someone who is still learning english. The same can be said for the Ecotrons software itself. Variables and correction tables have confusing names, which significantly complicated initial troubleshooting and data analysis. We suspect that someone with less experience with electronic fuel and spark control systems will struggle to make use of this software. Furthermore, phone and online message board support is not available. By comparison, more common aftermarket systems have large online communities, well written documentation, and a large number of people trained in their use.

Furthermore, the ECU does not have any spare inputs or outputs or any provisions for custom logic. We suspect that the SMV team may wish to collect additional data during tuning, testing, or competition. For instance, the team may wish to log the power measured by the dyno and the fuel flow from the . If these data streams must be logged by a second system, then the two logs will have to be time-synced somehow before analysis can begin. Alternatively, an ECU with additional inputs could collect all of this data into one log. Similarly, the Ecotrons ECU doesn't have any spare output pins, or any software logic, to control any additional actuators. Several different ECUs on the market today do have those capabilities.

Scope of Work

Because of the change in project goals, the scope of work for all parties has been redefined. Major changes include the change of the base engine and the removal of the new fuel system (the old Supermileage system will be used).

The I.C.E. team will be responsible for providing:

1. The modified Honda GX35 engine complete with:
 - a. Thermal management system
 - b. Intake and exhaust piping systems
 - c. An electric starting system
2. An initial ECU configuration and tune
3. A bracket to mount the GX35 to the previous Yamaha bolt pattern
4. An experimental result for the knock-limited compression ratio

The SMV club and other senior project teams will be responsible for the following interfaces with the engine system:

1. Providing the fuel tank and pressurization system
2. Final tuning of the ECU
3. Designing and manufacturing the chassis mounting bracketry.
4. Providing a clutch and transmission to transmit the engine power to the road.

For a graphical representation of each group's scope, see [Appendix 3](#).

Roles and Responsibilities

Table 16: Individual Roles and Responsibilities

Team Member	Logistical Roles	Working Groups
Ricardo Cuevas	Testing Co-Lead	Intake and Exhaust
Sam Flood	Testing Co-Lead, Co-Editor	Thermal Management, Starter
Philippe Habets	Project Planner, Co-Editor	Thermal Management, Starter
Paing Htet Lin	Manufacturing Coordinator	Thermal Management, Dyno
Jason Wu	Outside Point of Contact, Treasurer	Intake and Exhaust

In order to meet the goals we established, we created a few working groups within our team. This structure will allow us to accomplish more in less time, because we will be able to work on different projects in parallel. The groups are as follows: Intake and Exhaust, Electronic Fuel Injection (EFI), Electronic Control Unit (ECU) and initial tune, Thermal Management, Dyno, and Starting. The Dyno group will be responsible for designing the hardware which will mount the Honda GX35 to the small engine dyno. The Intake and Exhaust, Starting, and Thermal Management teams will work on the design, testing, and manufacturing of those systems. Each team member's individual roles and sub-teams are summarized in Table 6. Furthermore, we established a strict set of norms regarding methods of communication, individual responsibilities, conflict resolution procedures, and record keeping and have defined these norms in a team contract.

Project Management

In addition to specific obligations of each team member, we created a general timeline for our project using a Gantt chart. ICE's Excel based Gantt Chart is presented in Appendix 9. The intent of this plan is to provide a clear timeframe and accountability for necessary tasks and milestones. Through visual representation of our due dates, individual contributions, and milestone progress, we will be able to effectively stay on track throughout the duration of the project. Due to the nature of ICE's project, it has been decided that milestones should be broken up by quarter and completed before moving on to the next stage of development. This is to ensure that as we make progress towards increased efficiency, we are able to track the effect of each modification independently.

For the next stage of the project, the focus will be on system characterization, and model validation. Early Fall 2019 we ordered a new Honda GX35 engine, GX31 piston, and will be ordering materials needed to prototype our intake, exhaust, and starting designs. Additionally, we will perform testing to determine parameters relating to the starting, thermal management, intake, exhaust systems, and the compression ratio changes. These parameters include:

1. Starting force and speed

2. Connecting rod length
3. Efficiency vs. RPM and engine temperature
4. Efficiency vs intake and exhaust pipe length

Design Process

We began by selecting an initial set of modifications which we predicted to provide the best efficiency gains for the least risk in terms of manufacturing difficulty and race-day reliability. Once we had this list of modifications we brainstormed on potential methods of accomplishing them. This list of concepts was then reduced to a set of modifications which we believe are accomplishable and will provide measurable improvements. More details on this process can be found in the [Concept Design](#) section of this report.

Now that we have selected an initial set of concepts, we plan to test the engine in order to determine several key parameters needed to select materials, size components, and perform analysis. Of particular interest are the engine's thermal efficiency, pumping efficiency, and heat rejection over a range of temperatures and RPM ranges.

Conclusion & Recommendations

Over the last 30 weeks we made significant progress in the development of a new internal combustion engine for the Cal Poly Supermileage car of 2021. Our work included engine, intake, starting, dyno testing, and fuel injection systems. We have laid a strong foundation for the team or future senior project teams to follow up on. The engine and dyno adapter system are fully functional – paving the way for future tuning and research. And, with a small exhaust manufacturing and engine tuning effort, the engine will be ready for chassis and drivetrain integration. Alternatively, if additional time is available, we see several opportunities for development of a more fuel efficient engine.

Team ICE would like to share these suggestions for future work based on our experience over the last 30 weeks. In addition to promising or needed developments, we also have some organizational suggestions.

Engine Mechanical Design

We believe that more research into the atkinson-cycle is warranted. Compression ratio changes are also attractive, but may be made difficult by the physical construction of the Honda GX35. Piston changes are the simplest option available, but are complicated parts to design and manufacture. And skimming the head or block is not possible due to the monobloc construction.

Alternatively, a pseudo-atkinson cycle could be implemented through modifications to the valve timing. These changes would not be simple, but may be simpler than the work required to increase compression.

Some potential methods of achieving pseudo-atkinson cycle operation include:

- New cam lobe and cam-lobe followers
- Twin cam system
- Electric, hydraulic, or pneumatic actuation of the valves or cam-lobe followers

Of these options, we consider the new cam lobe and lobe followers to be most realistic. However, the other

options allow for increased control and tweaking of the system.

Finally, the Honda GX31 piston should be tested. If it really does “drop-in” without interfering with the valve-train, and the increase in compression ratio does not exceed the knock limit of the fuel, then we expect a substantial efficiency and power improvement.

Dynamometer Fixture

The dynamometer fixture was completed successfully and the engine can now be tested with an reduced error band of ~2%. Since the dynamometer has not been used for decades, it should be calibrated with the fixture attached. Due to time constraints, the team was not able to complete the calibration process. Moreover, the fixture should be tested for dynamic repeatability of the system. This ensures that future testing results are accurate and reliable.

In terms of design changes, future team should install sheet metal flanges at the bearing plate. These flanges would act as bearing retainers and prevent the bearings moving out of place during testing. Furthermore, some aspects of the bolts placement could be revised using principles of design for assembly. It would allow the operator to have abundant space for assembly tools.

Electric Starting System

The electric starting system is substantially heavier than the original Honda design. From a complete vehicle standpoint, the weight is immaterial. However, the Honda engine only employs an oil seal on the starting side. This means that the crankshaft acts as a long cantilever beam. We are concerned that the additional weight of the new system will lead to larger deflections in the crankshaft. These deflections will be worsened by the high RPM of the engine. These deflections could lead to a decreased life of the starter system, oil seal, and/or crankshaft.

Furthermore, the drivetrain clutch has not yet been integrated into the engine package. Some space was left for this system, but we suspect that it may be difficult to fit the clutch in this space.

Finally, preliminary testing by team ICE indicated that the current starting system design is overly powerful, and likely uses more space, weight, and electrical power than a smaller system.

Therefore, we suggest designing a new electric starting system with a custom toothed flywheel. This would offer the following advantages:

- Eliminate the long cantilever loading of the crankshaft
- Allow the engine to be mounted farther to the right side of the chassis
- Provide more room and flexibility for clutch integration

Data from testing of the current starting system could be used to select a motor and gear reduction ratio. A larger one-way bearing could be used to reduce starter drag, or an alternative system could be employed. It may be possible to manufacture the gear teeth using the waterjet due to the relatively low loads and cycles.

Intake System

From and research and theory, the Helmholtz adaption was to yield better results than the organ pipe adaption, so this project moved forward with the Helmholtz resonance. Even though testing of the resonator

produced resonance and the simulations showed that the resonator did increase volumetric efficiency, the simulation also showed that a tapered length yielded higher efficiencies than a constant cross section section. Because of this, we are not sure if the organ pipe analysis of just a tapered length from the intake to the open atmosphere would produce better results, so more research and testing of the organ pipe analysis is suggested.

In addition, Lotus Engine simulation is an old software. Although the program is fast and gave approximate results, it should not be used if the layout and design of the intake system is more detailed. We suggest using Abaqus to run future simulations as it can account for any geometric shape and produce better pipe flow analysis.

Although 3D printing allowed us to quickly test a complicated resonator geometry, the final product was somewhat porous. Though it produced resonance, air was able to leak in through the walls of the part when the inlet was capped. This likely had an impact on the resonators performance and therefore we recommend that follow up work is done to somehow seal the 3D printed parts.

Because exhaust and intake system work in tangent with each other, we were not able to obtain the best efficiency with both systems integrated as one due to a temporary pause on the exhaust.

Electronic Fuel Injection

We believe that any time invested in additional tuning of the EFI fuel and ignition tables would be well worth the effort. However, the Magtrol 6200 controller does not do closed-loop control. As adjustments are made to the EFI tables, power production will change, and the engine RPM will change (because the dyno load will be constant). This change in RPM will then cause the EFI system to move to a new lookup cell. This will significantly complicate tuning efforts.

Thankfully, there is a Magtrol DSP controller in the engines lab. It is compatible with the smaller Magtrol HD dynamometer for which Team ICE built a dynamometer fixture. Extended brake and control cables will need to be purchased or made to connect the two pieces of equipment. Futhermore, the M-Test software will need to be configured for the smaller dynamometer. We suggest backing up the existing configuration and creating one for the smaller dyno. Then, restoring the setup to the one needed for Lemieux's lab will be simple and quick.

Finally, it may be prudent to first move to a different ECU. The ECU included with the kit works well to simply run the engine and datalog it's sensor package. However, future work might need to add additional sensors and actuators to the system (e.g. additional temperature measurements, fuel pressure compensation, vehicle speed, variable cam timing actuation). This ECU does not have additional inputs or outputs available. Futhermore, the included documentation and the software package can be difficult to understand at best.

Should the team choose to move forward with a different ECU, the new computer can be made compatible with the current sensor package on the GX-35. The fuel injector, temperature sensors, and rpm sensors can all be easily integrated into a different ECU system. As it was also recommended by ICE to move to a MAP sensor, the chosen ECU can be selected around compatibility with this device.

Pin NO.	Component	Color(Version 2)	Color(Version 1)	Description
P1	CKP	Yellow/Black	Orange	Crank Position Sensor (connect igniting pickup sensor signal)
P2	Optional	Orange/Black	White/Black	Mil-lamp (Optional, Inj2: Blue/Red)
P3	MAP	White/Blue	White/Blue	Manifold Air Pressure Sensor Input
P4	IAT	White	White/Yellow	Intake Air Temperature Sensor
P5	RXD	White/Red	White/Red	Sent Data to RS232
P6	TXD	Blue/Red	White/Pink	Receive data from RS232
P7	ROUT	Light/Blue	White	Power relay LS Driver output
P8	CDI-CTRL	Gray	Gray	CDI control signal
P9	INJ1	Purple/White	Blue/Black	Injector #1 LS Driver Output
P10	GND	Black	Black	Power Ground
P11	O2HOUT1	Blue/Yellow	Blue/Yellow	O2 Sensor #1 Heater LS Driver output
P12	KEYSW	Purple	Pink	Key On Switch
P13	12V+	Red	Red	Reverse Battery Protected Supply
P14	GND	Black	Black	Power Ground
P15	VCC	Yellow	Yellow	+5V Volt Supply Output
P16	ECT	Blue	White/Brown	Engine (coolant) Temperature sensor
P17	TPS	White/Green	White/Green	Throttle Position Sensor input
P18	O2in	White/Black	Gray/Black	Oxygen Sensor signal input
P19	Per-SW	Orange	Gray/White	Performance Switch
P20	GND-A	Green	Green	Analog Ground

Figure 69: Wiring Pinout for Stock EFI ECU

To make wiring the new ECU simpler, the pinout for the ECU included with the ICE team's GX35 engine deliverable has been included above.

Closing Statements

We would like to personally thank Dr. Fabijanac, Dr. Mello, and the Supermileage team for their support, guidance, and confidence throughout this project. We hope that we have set a good baseline for the team to work from, and are excited to see what they can accomplish with the engine and car next year.

References

- [2] *Shell Eco-marathon 2019 Official Rules Chapter 1* Shell Eco-marathon, 2018. p 14-38 [Online]. Available: https://www.shell.com/make-the-future/shell-ecomarathon/americas/for-americas-participants/_jcr_content/par/textimage.stream/1535931413222/9d2f1507af6de1ab7745cf6a94c68aa9e631a89b/shell-eco-marathon-2019-global-rules-chapter-1.pdf
- [3] Toyota ‘Intake Manifold for Internal Combustion Engine’, 9995252, 2015.
- [4] N. Mulye, S. Sane, O. L. Neto . ‘Internally Cooled Exhaust Gas Recirculation System for Internal Combustion Engine and Method Thereof’, 0300296 A1, 2015
- [5] C.R. Ferguson, A. T. Kirkpatrick, *Internal Combustion Engines – Applied Thermosciences – 3rd Edition*, Colorado State University. 2016. p 42, 383
- [6] M. K. Khair, H. Jääskeläinen. “Exhaust Gas Recirculation .” *www.dieselnet.com*, Feb. 2019, www.dieselnet.com/tech/engine_egr.php.
- [7] Yoshihara, Yasush, et al. “Development of High Tumble Intake-Port for High Thermal Efficiency Engines.” *Development of High Tumble Intake-Port for High Thermal Efficiency Engines (2016-01-0692 Technical Paper)- SAE Mobilus*, 5 Apr. 2106, saemobilus.sae.org/content/2016-01-0692.
- [8] Pavan Prakash, D, et al. “The DCE Supermileage Engine .” *The DCE Supermileage Engine*, 5 May 2010, saemobilus.sae.org/content/2010-01-1549/.
- [9] Mckelvie, Steve. “A Critique of the ‘Flathead’ or Side-Valve Engine Design.” *Stevemckelvie.wordpress.com*, 13 July 2012, stevemckelvie.wordpress.com/2012/07/12/a-critique-of-the-flathead-or-side-valve-engine-design/.
- [10] T. Kaori, K. Yukio, T. Chikara, ‘Variable Valve Actuation Device for Internal Combustion Engine’ 10267189, 2019.
- [11] J.C. Riegger, T. Beyer, J. D. Fluharty, ‘Cylinder Head with valve Deactivators’ 10267259, 2019
- [12] “Student Success Guide,” Department of Mechanical Engineering California Polytechnic State University – San Luis Obispo, April 2018
- [13]“Effects of Air Intake Pressure to the Fuel Economy and Exhaust Emissions on a Small SI Engine.” *Procedia Engineering*, Elsevier, 12 Apr. 2014, www.sciencedirect.com/science/article/pii/S1877705813020341.
- [14] J.B. Heywood, *Internal Combustion Engine Fundamentals*, Massachusetts Institute of Technology. 1988
- [15] Lee, Kristen. “Here’s What ‘Compression Ratio’ Acutally Means And Why It Matters.” *Jalopnik*, Jalopnik, 5 Apr. 2016, jalopnik.com/heres-what-compression-ratio-actually-means-and-why-it-1819723873.
- [16] Thompson, Michael paul. “Non Mechanical Supercharging of a Four Stroke Diesel Engine.” *The ohio state university*, 1968. <https://Saemobilus.sae.org>.
- [17] Selamet, A, et al. “Insertion Loss of a Helmholtz Resonator in the Intake System of Internal

Combustion Engines: an Experimental and Computational Investigation.” *Science Direct, The Ohio State University*, 1999, www.sciencedirect.com/science/article/pii/S0003682X00000426.

[18] Malkhede, D. and Khalane, H., "Maximizing Volumetric Efficiency of IC Engine through Intake Manifold Tuning," SAE Technical Paper 2015-01-1738, 2015, doi:10.4271/2015-01-1738.

[19] Kassim, Mohd nasir, et al. “COMPUTATIONAL ANALYSIS OF AIR INTAKE SYSTEM FOR INTERNAL COMBUSTION ENGINE IN PRESENCE OF ACOUSTIC RESONATOR.” *Arpn Journals, International Islamic University Malaysia*, 2015, www.arpnjournals.org/jeas/research_papers/rp_2015/jeas_1115_2897.pdf.

[20] Sammut, Gilbert, and Alex c Alkidas. “Relative Contributions of Intake and Exhaust Tuning on SI Engine Breathing - A Computational Study.” *Sae Mobilus, oakland university*, 2007, saemobilus.sae.org/content/2007-01-0492.

[21] Moster, David anthony. “Intake Manifold Design for an Air Restricted Engine.” *university of cincinnati*, 2012.

[22] Willermark, David, and Frederick Dunert. “Gt-Power Simulation Report.” 2 Apr. 2009.

Appendices

Appendix 1: List of Customer Needs

List of Customer Needs
The engine must be fuel efficient.
The engine must have high thermal efficiency.
The engine must provide sufficient power the vehicle to complete the track.
The engine must be able to operate in environmental conditions typical for race day.
The team must be able to test the engine on the dynamometer.
Cal Poly Supermileage members must be able to operate the engine.
An average person must be able to lift and transport the engine.
The engine must be compliant to compete in the Shell Eco-marathon competition.
Cal Poly Supermileage members must be able to easily assemble the engine onto the vehicle.
The engine needs to fit in the chassis without causing interference to other subsystems.
The engine parts must be manufacturable.
The engine must not vibrate excessively.
The engine must operate without excessive noise.
Basic maintenance and troubleshooting tasks should be possible with the engine installed in the vehicle.

QFD: Internal Combustion Engine

By:
 Jason Wu
 Paing Lin
 Phillipe Habets
 Ricardo Cuevas
 Sam Flood

What	Who						How									Now							
	Assembly Team	Drivetrain	Chassis/Aero	Engine Team	Driver	Mello	1	2	3	4	5	6	7	8	9	1	2	3	4	5	6	7	
Powerful	1	1	1	5	5	5				●	○	●	○		○								
Easy to install	5	3	5	1	1	1																	
Small/Compact	3	3	5	1	1	1										5	3	1					
Light	5	3	5	3	1	1																	●
Efficient	1	1	1	5	3	5	●	●		●		○	○	●	○	5	1	5	5	5	5	5	5
Quiet	1	1	1	3	5	1	○	○															
Vibrations	1	5	5	3	5	1	○	○															
Reliable	1	1	1	5	5	5			●	●	●				○								

Relationships	
Strong	●
Moderate	○
Weak	▽

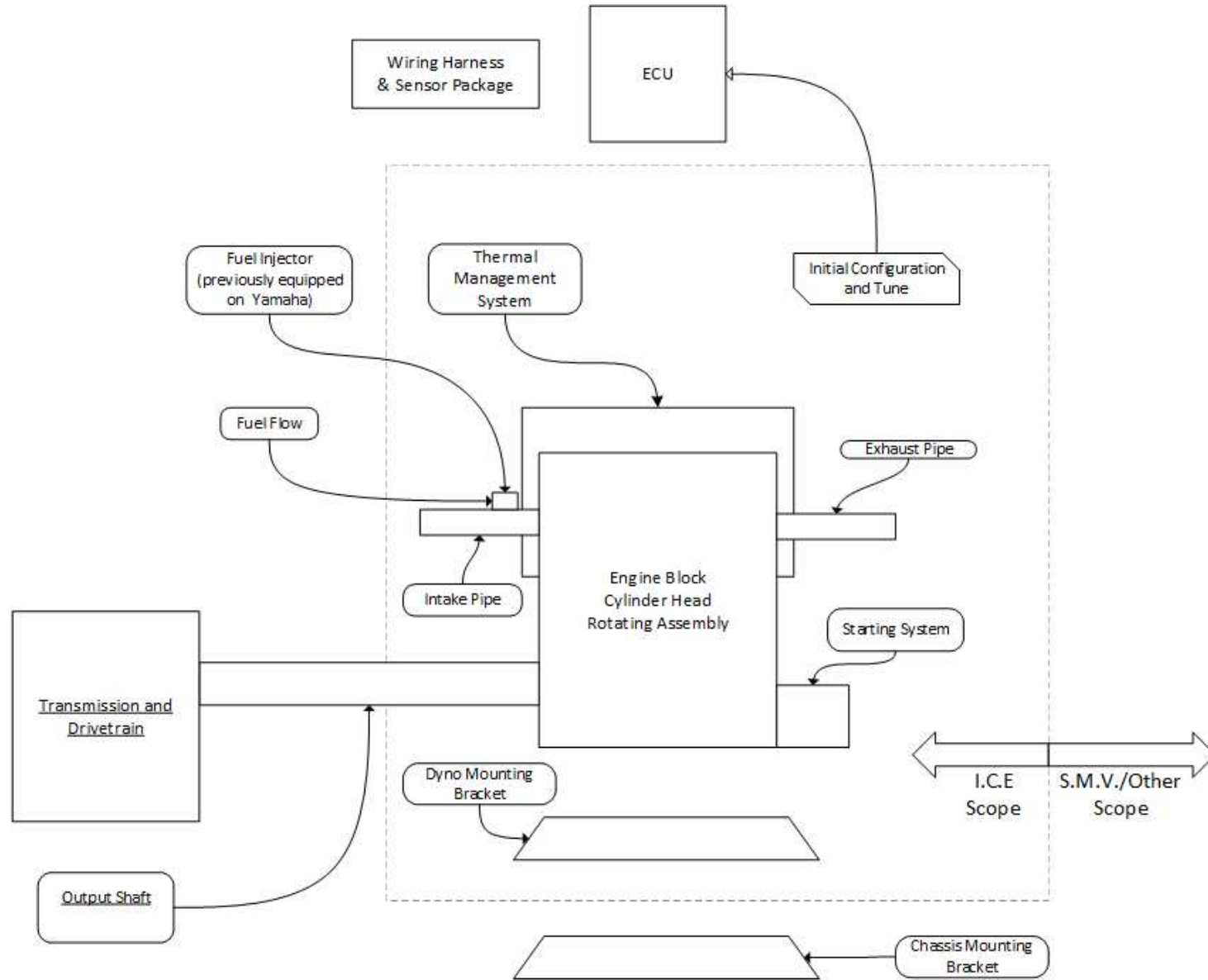
HOW MUCH											
Honda C.P		1500*									
Yamaha C.P		585	1.2:1	13:1		5k					3
BYU	134	1250		17:1							2
Illinois		1500									
Canada U.B.C		1371		12:1							
Brazil		1277									
Laval		1000	1:1.58	13:1		3100					2

120cc possi Steevd B&S, 8HP, 10ftlbs (2017)
 68cc 2017 - modified briggs

* The Honda engine was used on a different track/competition/season - numbers are not directly comparable.

Appendix 3: Boundary Diagram

!NOTE: This document is severely out of date!



Appendix 4: Engine Characterization Data Sheet

(Note – most of the data will be recorded by a DAQ system – this sheet serves to enforce safety procedures, document the engine configuration, and make notes of interest)

Test Purpose: <hr/>	
Safety Checklist <input type="checkbox"/> Hearing Protection <input type="checkbox"/> Eye Protection <input type="checkbox"/> Long Pants <input type="checkbox"/> Closed Toe Shoes <input type="checkbox"/> Fire Extinguisher <input type="checkbox"/> Dyno Guards <input type="checkbox"/> Engine & Dyno Secure	Test Engineers <ul style="list-style-type: none"> • _____ • _____ • _____ • _____ • _____
Engine Configuration <ul style="list-style-type: none"> • Intake: _____ • Exhaust: _____ • Thermal: _____ • Speed: _____ • Other: _____ 	Room Conditions Temperature: _____ <hr/> Test #: _____ Day: _____ Time: _____
Other Notes: _____ <hr/> <hr/> <hr/>	

Appendix 5: Material Testing Analysis

Insulative Material Effectiveness Analysis Test Method

Material: _____

Distance from Insulation to Engine Wall: _____

Net Thickness of Insulation: _____

Total Insulation Weight: _____

Insulation Cost Estimate: _____

Internal Temperatures

Ambient: _____

Exhaust: _____

Head: _____

Crank Case: _____

Upper Fin (Exhaust Side): _____

Lower Fin (Exhaust Side): _____

External Temperatures

Head: _____

Crank Case: _____

Exhaust Proximity: _____

Intake Proximity: _____

Appendix 6: Design Hazard Checklist

DESIGN HAZARD CHECKLIST			
Team:	ICE	Faculty Coach:	J. Fabijanac
Y	N		
<input checked="" type="checkbox"/>	<input type="checkbox"/>	1. Will any part of the design create hazardous revolving, reciprocating, running, shearing, punching, pressing, squeezing, drawing, cutting, rolling, mixing or similar action, including pinch points and sheer points?	
<input type="checkbox"/>	<input checked="" type="checkbox"/>	2. Can any part of the design undergo high accelerations/decelerations?	
<input checked="" type="checkbox"/>	<input type="checkbox"/>	3. Will the system have any large moving masses or large forces?	
<input type="checkbox"/>	<input checked="" type="checkbox"/>	4. Will the system produce a projectile?	
<input type="checkbox"/>	<input checked="" type="checkbox"/>	5. Would it be possible for the system to fall under gravity creating injury?	
<input type="checkbox"/>	<input checked="" type="checkbox"/>	6. Will a user be exposed to overhanging weights as part of the design?	
<input type="checkbox"/>	<input checked="" type="checkbox"/>	7. Will the system have any sharp edges?	
<input type="checkbox"/>	<input checked="" type="checkbox"/>	8. Will any part of the electrical systems not be grounded?	
<input type="checkbox"/>	<input checked="" type="checkbox"/>	9. Will there be any large batteries or electrical voltage in the system above 40 V?	
<input checked="" type="checkbox"/>	<input type="checkbox"/>	10. Will there be any stored energy in the system such as batteries, flywheels, hanging weights or pressurized fluids?	
<input checked="" type="checkbox"/>	<input type="checkbox"/>	11. Will there be any explosive or flammable liquids, gases, or dust fuel as part of the system?	
<input type="checkbox"/>	<input checked="" type="checkbox"/>	12. Will the user of the design be required to exert any abnormal effort or physical posture during the use of the design?	
<input checked="" type="checkbox"/>	<input type="checkbox"/>	13. Will there be any materials known to be hazardous to humans involved in either the design or the manufacturing of the design?	
<input checked="" type="checkbox"/>	<input type="checkbox"/>	14. Can the system generate high levels of noise?	
<input type="checkbox"/>	<input checked="" type="checkbox"/>	15. Will the device/system be exposed to extreme environmental conditions such as fog, humidity, cold, high temperatures, etc?	
<input checked="" type="checkbox"/>	<input type="checkbox"/>	16. Is it possible for the system to be used in an unsafe manner?	
<input type="checkbox"/>	<input checked="" type="checkbox"/>	17. Will there be any other potential hazards not listed above? If yes, please explain on reverse.	
For any “Y” responses, add (1) a complete description, (2) a list of corrective actions to be taken, and (3) date to be completed on the reverse side.			

Description of Hazard	Planned Corrective Action	Planned Date	Actual Date
<i>Spinning Output shaft</i>	<i>Spinning guard on the shaft</i>		
<i>Spinning forces</i>	<i>Train operators to avoid spinning bodies</i>		
<i>Pressurized Fluids</i>	<i>Control fluid retention</i>		
<i>Combustible Fluid</i>	<i>Standard gasoline engine procedures for engines lab will be followed</i>		
<i><u>Hazmats</u></i>	<i>Lab procedures for semi-hazardous materials will be followed</i>		
<i>High Noise Levels</i>	<i>PPE</i>		
<i><u>Possibility of unsafe use</u></i>	<i>Train all operators and limit access to equipment to faculty approved members</i>		

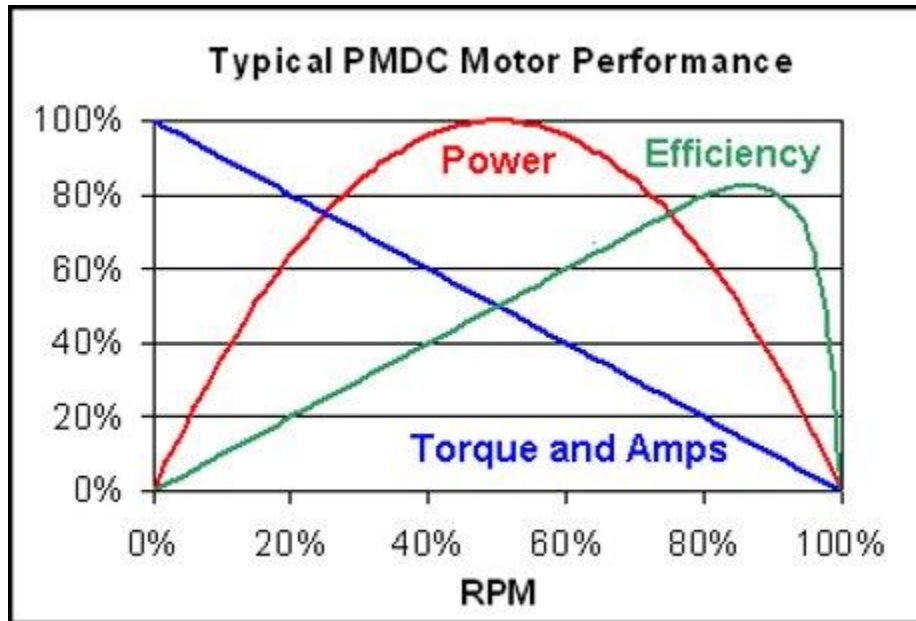
Appendix 7: EFI Safety Checklist

Item	Criteria	Confirmation
Intake Sensors	Properly positioned	
	Clean and free from debris	
	Cable intact	
	Resting data accuracy	
Exhaust Sensors	Properly positioned	
	Clean and free from debris	
	Cable intact	
	Resting data accuracy	
Engine Temperature	Properly positioned	
	Clean and free from debris	
	Cable intact	
	Resting data accuracy	
Battery	Leads connected	
	Free from corrosion	
Overall System	Wires free from rotating components	
	All wires constrained near rotating components	
	Connections to DAQ/Controllers connected	

Appendix 8: Starter Testing & Analysis Plan

This plan covers the method for estimating the starting torque and RPM for the Honda GX35 equipped with the Yamaha brushed DC starter motor with a 70:9 reduction.

The plan is to start the Honda GX35 while datalogging the current and voltage delivered to the starter motor and the RPM of the Honda. The RPM data can be used directly, but the power data must be processed somewhat. Furthermore, the starter motor is not 100% efficient. If we had a smaller dyno we could hook that motor up and build an efficiency curve, but we don't. So we'll estimate the efficiency based on this chart for a typical brushed DC motor:



Equipment needed:

- 1) IR Tachometer
- 2) 12V battery
- 3) Power or Volt/Amp datalogger
- 4) Datalogged crank position sensor for GX35

Steps:

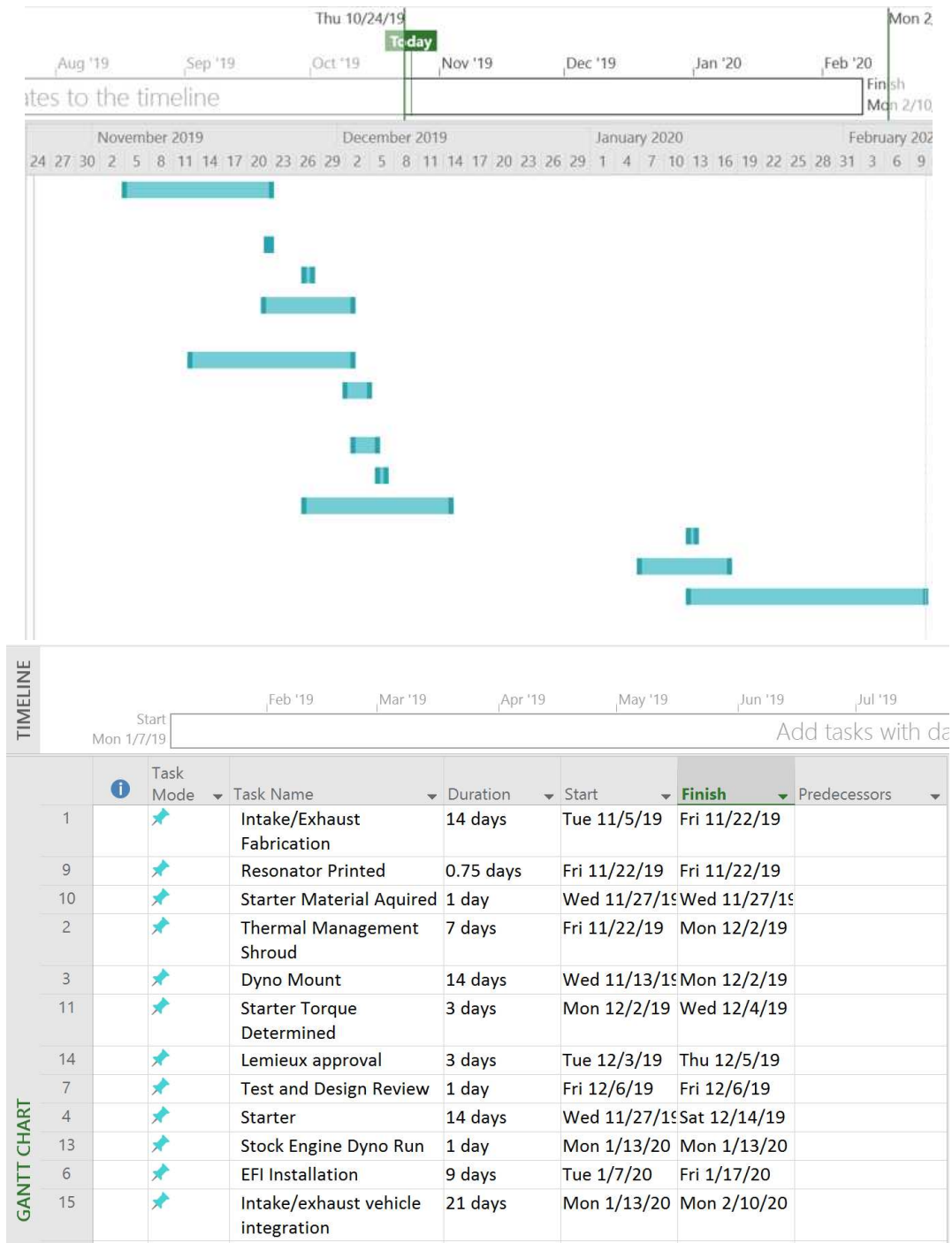
- 1) Secure the starter motor in a vise. Place a piece of IR tape on the pinion.
- 2) Connect the battery to the starter motor through a momentary switch.
- 3) Measure the starter's steady state RPM with the tachometer.
- 4) Disconnect the battery from the starter motor.
- 5) Scale the X-axis of the plot above to this RPM.
- 6) Install the starter motor in the Honda GX35.
- 7) Secure the GX35 to a suitable mount

- 8) Connect the starter motor to a 12V battery through suitable power or volt/amp datalogger and a momentary switch.

Analysis:

- 1) Synchronize the two data logs.
- 2) Calculate the power delivered to the starter motor: $Power [W] = Volts[V] * Amps [I]$
- 3) Calculate the starter motor RPM: $N_{starter} = N_{GX35} * 70/9$
- 4) Determine the efficiency at each RPM in the log by comparing it to the chart above.
- 5) Derate the starter motor by the efficiency: $Power_{starter} = Power_{logged} * \eta$
- 6) Calculate the starter torque: $Torque [Nm] = \frac{Power[W]}{RPM} \frac{2\pi Rad}{Rev} \frac{min}{60 s} \frac{W}{Nm/s}$
- 7) Calculate the motor torque: $Torque_{GX35} = Torque_{starter} * 70/9$

Appendix 9: Gantt Chart for ICE Senior Project



Appendix 10: Failure Mode Evaluation and Analysis (FMEA)

Item	System / Function	Potential Failure Mode	Potential Effects of the Failure Mode	Severity	Potential Causes of the Failure Mode	Current Prevention Activities	Occurrence	Current Detection Activities	Detection	RPN
1	Engine Bearings	Increased Friction	Reduced efficiency	4	1) Oil Starvation 2) Over Temperature 3) Wear 4) Bearing Misalignment	1) Maintain Honda specified oil levels 2) Change oil at Honda specified intervals 3) Operate the engine at safe temperatures	2	1) Listen for irregularities 2) Examine oil/have oil tested 3) Monitor engine temperatures	3	24
2		Rotating Failure/Seizure	DNF/DNS	5	1) Oil Starvation 2) Over Temperature 3) Wear 4) Increased Load 5) Bearing Misalignment	1) Maintain Honda specified oil levels 2) Change oil at Honda specified intervals 3) Operate the engine at safe temperatures	1	1) Listen for irregularities 2) Examine oil/have oil tested 3) Monitor engine temperatures	5	25
3		Locating Failure	Parts exit crankcase	5	1) Oil Starvation 2) Over Temperature 3) Wear 4) Increased Load 5) Bearing Misalignment	1) Maintain Honda specified oil levels 2) Change oil at Honda specified intervals 3) Operate the engine at safe temperatures	1	1) Listen for irregularities 2) Examine oil/have oil tested 3) Monitor engine temperatures	5	25
4	Connecting Rod	Bends	1) DNF/DNS	5	1) Increased Load 2) Piston Ring Seizure	1) Maintain Honda specified oil levels 2) Change oil at Honda specified intervals	1	1) Listen for irregularities 2) Examine oil/have oil tested	5	25
5		Breaks	1) DNF/DNS 2) Parts exit crankcase	5	1) Increased Load 2) Piston Ring Seizure	1) Maintain Honda specified oil levels 2) Change oil at Honda specified intervals	1	1) Listen for irregularities 2) Examine oil/have oil tested	5	25
6	Piston	Melts	1) DNF/DNS	5	1) Over Temperature	1) Operate the engine at safe temperatures	1	1) Monitor engine temperatures	5	25
7		Rings Seize	1) DNF/DNS	5	1) Over Temperature	1) Operate the engine at safe temperatures 2) Maintain Honda specified oil levels 3) Change oil at Honda specified intervals	1	1) Monitor engine temperatures	5	25
8	Engine - Reduction Coupler	Shear Bolts	1) Damage engine 2) Damage Dyno Plate	3	1) Excess vibration	1) Properly tighten bolts	1	1) Inspect engine mount and coupler before each run	2	6
9	Engine Mount	Shear Bolts	1) Throw Engine (Damage) 2) Damage Dyno Plate	5	1) Excess vibration 2) Misalignment	1) Properly tighten bolts 2) Confirm alignment	1	1) Inspect engine mount and coupler before each run	2	10
10	Fuel System	Seals fail	1) Gasoline release 2) Fire Hazard	4	1) Fuel over-pressure 2) Seal mis-alignment 3) Old seals	1) Do not over-pressurize tank 2) Check fuel pressure regulator 3) Install injector properly 4) Replace worn/swollen/cracked seals	1	1) Immediately respond to the smell of fuel	3	12
11	Starter	Clutch Fail	1) Starter engages during operation 2) Break Bits	4	1) Starter Fatigue 2) Over-temperature	1) Inspect Starter before use	1	1) Inspect starter before use	5	20
12	Reduction Rotating Assembly	Increased friction	1) Increased dyno inaccuracy	3	1) Bearing misalignment 2) Bearing wear	1) Maintain lubrication	2	1) Listen for bearing/gear noise 2) Check lubrication levels	1	6
13		Seizure	1) Break coupler		1) Bearing misalignment 2) Bearing wear	1) Maintain lubrication	1	1) Listen for bearing/gear noise 2) Check lubrication levels	5	5
14		Locating Failure	1) Break coupler	4	1) Extreme bearing wear	1) Maintain lubrication 2) Pre-startup checks for play	1		4	16
15	Reduction Fasteners	Bolts Break	1) Throw Mounts 2) Damage Dyno	5	1) Excess vibration 2) Misalignment	1) Properly tighten bolts 2) Confirm alignment	1	1) Listen for excess rattle	4	20
16	Gear Reduction - Dyno Coupler	Breaks	Coupler breaks	1	1) Misalignment 2) Excess load	1) Check alignment 2) Try not to increase the power too much	1		3	3
17	Exhaust	Fails to aide next exhaust discharge	1) reduce efficiency 2) reduce in power	5	length of exhaust not tune properly	Set up dyno to measure loss or gain in efficiency due to change in length of exhaust	2	1) Pressure transducers 2) Temperature sensor	1	10
18	Intake	Geometry of intake fails to increase efficiency	1) reduce efficiency 2) reduce in power	5	Geometry of intake not properly	Set up dyno to measure loss or gain in efficiency due to change in geometry	2	Pressure transducer	1	10
19	Thermal System	Engine Overheats	1) damage engine 2) lose efficiency	5	1) excessive insulation	1) Monitor engine and oil temperatures 2) Estimate engine heat rejection	2	Temperature transmitters	1	10

Appendix 11: Thermo Testing Plan

Goals:

This testing plan seeks to:

1. Determine the relationship between engine temperature and BSFC
2. Determine the engine heating and cooling time constants
3. Determine the areas of highest heat rejection

This information will be used to:

1. Select an operating temperature range
2. Estimate heating and cooling times
3. Evaluate the likelihood of overheating
4. Design an insulation system for that temperature range

Measurements:

The following measurements will be logged for each test:

1. Engine torque and RPM will be measured by the Magtrol Dynamometer
2. Fuel flow will be measured by the Max FluidPro flowmeter
3. Engine temperature by thermocouples
 - a. Heat-fin base
 - b. Crankcase
 - c. Oil pan
4. Exhaust gas temperature

Setup:

The testing will be performed on several engine and testbed configurations:

1. Unmodified engine without cowling
 - a. This test will allow the use of an IR thermometer to collect additional temperature measurements from the valve cover and
2. Unmodified engine with SMV cowling or stand-in
3. Insulated engine with SMV cowling or stand-in

Procedure:

1. Install the engine on the dyno.
2. Setup the sensor package.
3. Assemble the cowl or cowl stand-in on the test stand (if required).
4. Startup the sensor and dyno datalogging systems.
5. Start the engine and hold it at the RPM for minimum BSFC (final RPM TBD, initial guess 5000RPM)
6. Run the engine until its temperature has reached a steady state.
7. Shut the engine off.
8. Disable fuel pumps and shutdown the dyno datalogging system.
9. Continue to collect engine temperature data until the engine has reached room temperature.

Analysis:

General steps:

Synchronize and combine the dynamometer and sensor datalogs.

BSFC and engine temperature:

1. Calculate the BSFC by dividing the instantaneous fuel flow by the instantaneous horsepower.
2. Plot BSFC, exhaust gas temperature, and power vs engine temperature.

3. Select the local minimum of BSFC as the target engine temperature. If this temperature was the highest achieved, consider modifying the next test to reach a higher temperature.

Temperature time constants:

1. Plot engine temperature vs. time.
2. Determine the final and initial temperatures for the warming and cooling phases.
3. Calculate the time for the 1st and 2nd time constants for each phase.
4. Plot a 1st degree model against the data.

Areas of high heat rejection:

1. Plot the engine temperatures vs. time.
2. Cold areas are either:
 - a. Far removed from the source of heat (primarily combustion chamber)
 - b. Able to more effectively transfer heat to the surroundings
3. Hot areas are either:
 - a. Very close to the source of the heat
 - b. Have a limited ability to transfer heat to the surroundings
4. The oil pan and crankcase are relatively far from the combustion chamber, while the base of the heat fins is as close as is possible.

Appendix 12: Pulley Sizing Calculation Using Manufacturer's Catalog

$$P_t = 1 \text{ kW} \approx 1.34 \text{ hp}$$

$$K_s = 1.6$$

$$P_d = 2.144 \text{ HP @ 7000 rpm}$$

3VX Cross section

$$d = 2.20''$$

$$D = 8.00''$$

$$SR = 3.7$$

$$3VX 315 \Rightarrow C_d = 17.1$$

$$K_{HP} = 0.8$$

$$B_{HP} = 3.45$$

$$K_{BHP} = .93$$

$$T_{BHP} = (3.45 + 1.93) \cdot .8$$

$$= 3.5 \text{ HP}$$

$$\text{no. of Belt} = 2.144 / 3.5 = 0.6 = 1 \text{ belt}$$

$$V = \frac{2.2 \times 7000}{3.82} = 4031 \text{ ft/min}$$

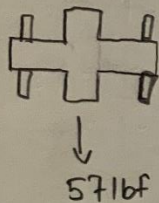
$$T_e = \frac{33000 \times 1.34}{4031} = 10.97 \text{ lbf}$$

$$T = 10.97 \left(\frac{2.2}{2} \right) = 12.1 \text{ lbf-in}$$

$$K_0 = .87$$

$$\begin{aligned} \text{Static Tension} = T_0 &= 0.9 \left\{ \frac{33000 \times 2.14}{1 \times 4031} \times \frac{2.5 - .87}{2 \times .87} + 0.07 \times 4031^2 \times 5.8 \right. \\ &\quad \left. \times 10^{-6} \right\} \\ &= 0.9 \left\{ (17.52 \times .94) + 6.6 \right\} \\ &= 20.76 \text{ lbf} \end{aligned}$$

$$\begin{aligned} F_s &= 1.5 (2 \times 20.76 \times \sin(\frac{133}{2})) \\ &= 57 \text{ lbf} \approx 60 \text{ lbf} \end{aligned}$$



Formulas for V-Belt drives design

Table 2-19

Item	Formula	Term
Design power	$P_d = P_t \times K_s$	P_d : Design power (HP) P_t : Transmission power (HP) K_s : Service factor
Service factor	$K_s = K_o + K_l + K_e$	K_s : Service factor K_o : Service correction factor K_l : Idler correction factor K_e : Environment correction factor
Power rating	$P_r = P_s + P_a$	P_r : Power rating (HP) P_s : Basic power rating (HP) P_a : Additional power rating for speed ratio (HP)
Correction power rating	$P_c = P_r \times K_L \times K_\theta$	P_c : Correction power rating (HP) P_r : Power rating (HP) K_L : Belt length correction factor K_θ : Arc of contact correction factor
Speed ratio	$SR = \frac{n_d}{n_D} = \frac{D_d}{d_d}$	SR : Speed ratio n_d : Small pulley speed (rpm) n_D : Large pulley speed (rpm) D_d : Large pulley datum diameter (in) d_d : Small pulley datum diameter (in)
Interim effective length	$L_e' = 2C' + 1.57(D_e + d_e)$	L_e' : Interim effective length (in) C' : Interim center distance (in) D_e : Large pulley effective diameter (in) d_e : Small pulley effective diameter (in)
Effective length	$L_e = 2C + \frac{\pi(D_e + d_e)}{2} + \frac{(D_e - d_e)^2}{4C}$	L_e : Effective length (in) C : Center distance (in) D_e : Large pulley effective diameter (in) d_e : Small pulley effective diameter (in) π : 3.1416
Center distance	$C = \frac{b + \sqrt{b^2 - 8(D_e - d_e)^2}}{8}$ $b = 2L_e - \pi(D_e + d_e)$	C : Center distance (in) D_e : Large pulley effective diameter (in) d_e : Small pulley effective diameter (in) L_e : Effective length (in) π : 3.1416
Arc of contact	$\theta = 180^\circ - \frac{57.3(D_e - d_e)}{C}$	θ : Arc of contact for small pulley ($^\circ$) D_e : Large pulley effective diameter (in) d_e : Small pulley effective diameter (in) C : Center distance (in)
Number of belts	$n_b = \frac{P_d}{P_c}$	n_b : Number of belts P_d : Design power (HP) P_c : Correction power rating (HP)

Item	Formula	Term
Belt speed	$V = \frac{dd \times n}{3.82}$	V : Belt speed (ft/min.) dd : Small pulley datum diameter (in) nd : Small pulley speed (rpm)
Transmission power	$Pt = \frac{Te \times V}{33000}$	Pt : Transmission power (HP) Te : Effective tension (lb) V : Belt speed (ft/min.)
Transmission power	$Pt = \frac{Tq \times n}{63025}$	Pt : Transmission power (HP) Tq : Torque (lb-in) n : Pulley speed (rpm)
Effective tension	$Te = \frac{2Tq}{dd}$	Te : Effective tension (lb) Tq : Torque (lb-in) dd : Small pulley datum diameter (in)
Effective tension	$Te = \frac{33000 \times Pt}{V}$	Te : Effective tension (lb) Pt : Transmission power (HP) V : Belt speed (ft/min.)
Torque	$Tq = Te \times \frac{dd}{2}$	Tq : Torque (lb-in) Te : Effective tension (lb) dd : Small pulley datum diameter (in)
Tight side tension	$Tt = \frac{33000 \times Pd}{nb \times V} \times \frac{2.5}{2 \times K\theta} + W \times V^2 \times 5.8 \times 10^{-6}$	Tt : Tight side tension (lb) Pd : Design power (HP) nb : Number of belts V : Belt speed (ft/min.) Kθ : Arc of contact correction factor W : Belt weight per unit (kg/m)
Slack side tension	$Ts = \frac{33000 \times Pd}{nb \times V} \times \frac{2.5 - 2 \times K\theta}{2 \times K\theta} + W \times V^2 \times 5.8 \times 10^{-6}$	Ts : Slack side tension (lb) Pd : Design power (HP) nb : Number of belts V : Belt speed (ft/min.) Kθ : Arc of contact correction factor W : Belt weight per unit (kg/m)
Tension ratio	$TR = \frac{Tt}{Ts}$	TR : Tension ratio Tt : Tight side tension (lb) Ts : Slack side tension (lb)
Minimum static tension	$To = 0.9 \times \frac{Tt + Ts}{2}$ $= 0.9 \times \left(\frac{33000 \times Pd}{nb \times V} \times \frac{2.5 - K\theta}{2 \times K\theta} + W \times V^2 \times 5.8 \times 10^{-6} \right)$	To : Minimum static tension (lb) Kθ : Arc of contact correction factor Pd : Design power (HP) nb : Number of belts V : Belt speed (ft/min.) W : Belt weight per unit (kg/m)
Static shaft load	$Fs = 1.5 \left(2nb \times To \times \sin \frac{\theta}{2} \right)$	Fs : Static shaft load (lb) nb : Number of belts To : Minimum static tension (lb) θ : Arc of contact for small pulley (°)
Span length	$Ls = \sqrt{C^2 - \frac{(De - de)^2}{4}}$	Ls : Span length (in) C : Center distance (in) De : Large pulley effective diameter (in) de : Small pulley effective diameter (in)

Appendix 13: Shaft Load Calculation for Small Pulley

Symbol	Metric	Unit	Name	Comment
S_{ut}	95000	MPa (or) psi	Ultimate Tensile Strength	
S_e'	47500	N/A		
K_a	0.98	N/A	Surface Modification Factor	MACHINED
K_b	0.879	N/A	Size Modification Factor	
K_c	1	N/A	Load Modification Factor	
K_d	1	N/A	Temperature Modification Factor	
K_e	1	N/A	Reliability Factor	
K_f	1	N/A	Miscellaneous Factor	
S_e	40917.45	MPa (or) psi	Marin Equation	
d	0.5	mm (or) in	Revised small Diameter	picked a lower standard size since the approximation is conservative already
D	2	mm (or) in	revised large diameter	assuming 1.2 for D/d for shoulder support
r	0.01	mm (or) in	fillet radius	using .02 for r/d from table 7-1
q	0.9	N/A		
K_t	2.2	N/A		
K_{ts}	2.2	N/A		
S_{ut}	95000	MPa (or) psi	Ultimate Tensile Strength	
S_e	47500	MPa (or) psi		
M_a	150	Nm (or) lbf.in		
M_m	0	Nm (or) lbf.in		
T_a	0	Nm (or) lbf.in		
T_m	72	Nm (or) lbf.in		
K_f	2.08	N/A		
K_{fs}	2.08	N/A		
1 / n	0.646491	N/A		
n	1.546811	N/A		

Appendix 14: Shaft Load Calculation for Large Pulley

Symbol	Metric	Unit	Name	Comment
S_{ut}	95000	MPa (or) psi	Ultimate Tensile Strength	
S_e'	47500	N/A		
K_a	0.98	N/A	Surface Modification Factor	MACHINED
K_b	0.879	N/A	Size Modification Factor	
K_c	1	N/A	Load Modification Factor	
K_d	1	N/A	Temperature Modification Factor	
K_e	1	N/A	Reliability Factor	
K_f	1	N/A	Miscellaneous Factor	
S_e	40917.45	MPa (or) psi	Marin Equation	
d	1	mm (or) in	Revised small Diameter	picked a lower standard size since the approximation is conservative already
D	8	mm (or) in	revised large diameter	assuming 1.2 for D/d for shoulder support
r	0.1	mm (or) in	fillet radius	using .02 for r/d from table 7-1
q	0.9	N/A		
K_t	2.2	N/A		
K_{ts}	2.2	N/A		
S_{ut}	95000	MPa (or) psi	Ultimate Tensile Strength	
S_e	47500	MPa (or) psi		
M_a	150	Nm (or) lbf.in		
M_m	0	Nm (or) lbf.in		
T_a	0	Nm (or) lbf.in		
T_m	72	Nm (or) lbf.in		
K_f	2.08	N/A		
K_{fs}	2.08	N/A		
$1/n$	0.08081141	N/A		
n	12.37449	N/A		

Appendix 15: Starter Calculations

Starter calculations followed the AGMA and bearing life methods described in *Mechanical Engineering Design* Shigley's – 10th ed. The AGMA factor choices are summarized in Table 17, and the bearing factors in Table 18. The results are summarized in Table 19.

Table 17: AGMA Input Factors

Input Factor	Value Chosen	Justification
Ko	1.5	Compression stroke is moderately nonlinear.
Qv	8	JIS n8 is comparable to AGMA Qv 8
Cmc	1	Uncrowned
Cpm	1.2	Cantilever mounted
Ce	1	Gearing is not adjusted at assembly or lapped
Kb	1	Full backup
Cf	1	Normal surface finish
Number of Cycles	120	Sim team – 30Starts/Race * 4Rev/Start
Kt	1	Less than 250°F

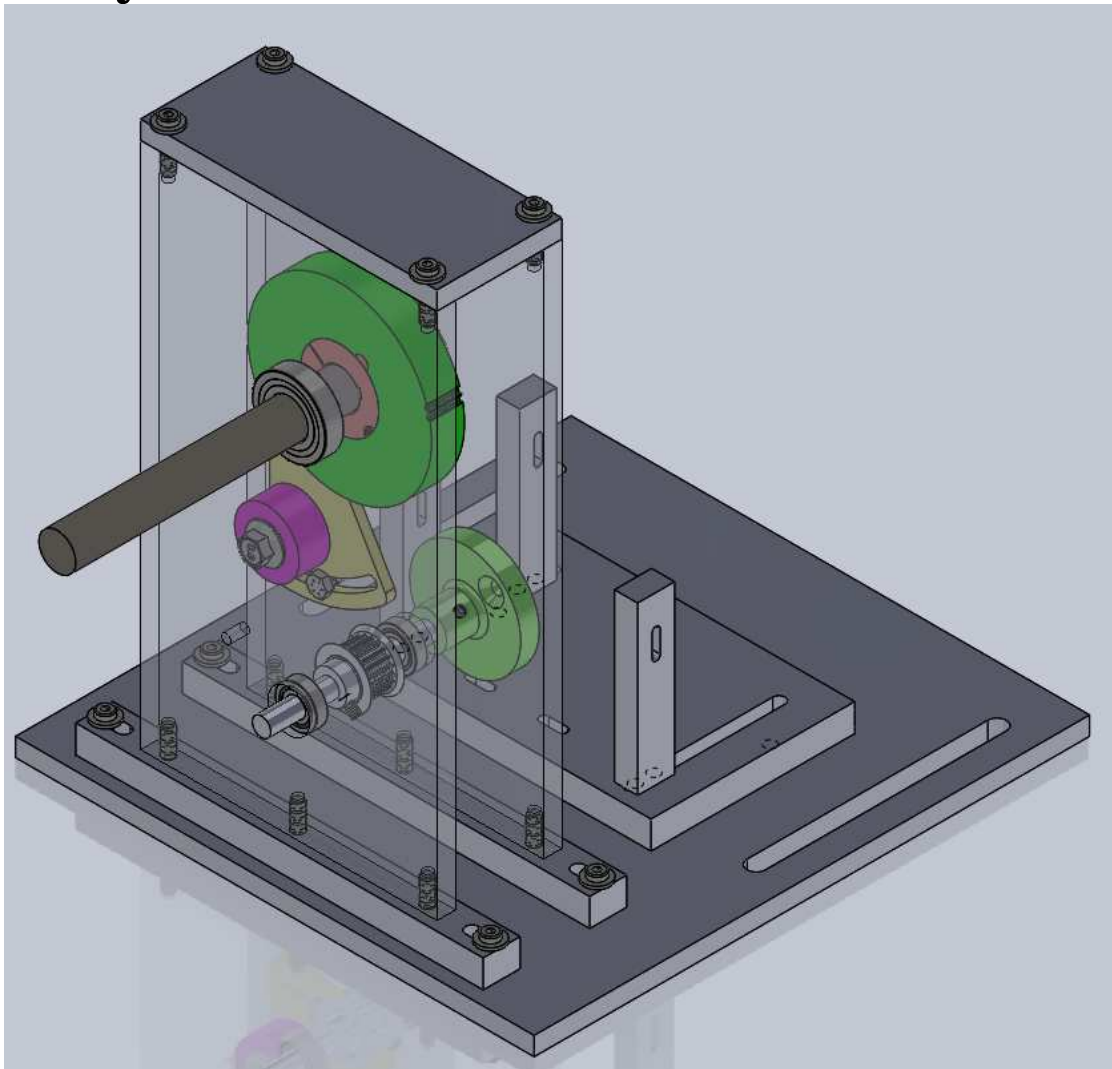
Table 18: Bearing Calculation Input Factors

Input Factor	Value Chosen	Justification
x0	0.02	Assumed – typical for Shigley's text, no better information
Θ	4.459	
b	1.5	
a	3	Ball bearings
af	1.5	Compression stroke - moderate shock

Table 19: Starter Calculation Results

Value	Result
S.F. Bending – Gear	18.8
S.F. Contact – Gear	4.4
S.F. C ₁₀ – Bearing	38.1

Dynamometer Fixture User Manual



This user manual is divided into 2 parts. In the first section, you will learn how to align the shaft to obtain desired shaft alignment. In the second section, you will learn how to tension the belt for the reduction system.

SHAFT ALIGNMENT

Tools Required: Test indicator with magnetic v-block base, standard Allen hex keys set

Step 1: After the dynamometer fixture has been assembled, visually align the output shaft of the fixture to the input shaft of the dynamometer. The tapered bushing of the dyno coupler can be used as a guide. Install the bushing midway on the dyno shaft. Align the reduction output shaft with the inner wall of the bushing. If the shafts are closely aligned, the bushing can easily slide onto both shafts.

Step 2: Put the magnetic v-block base onto the dyno shaft. Adjust the test indicator stand to move the tip of the indicator on the fixture output shaft. (Refer to figure below)

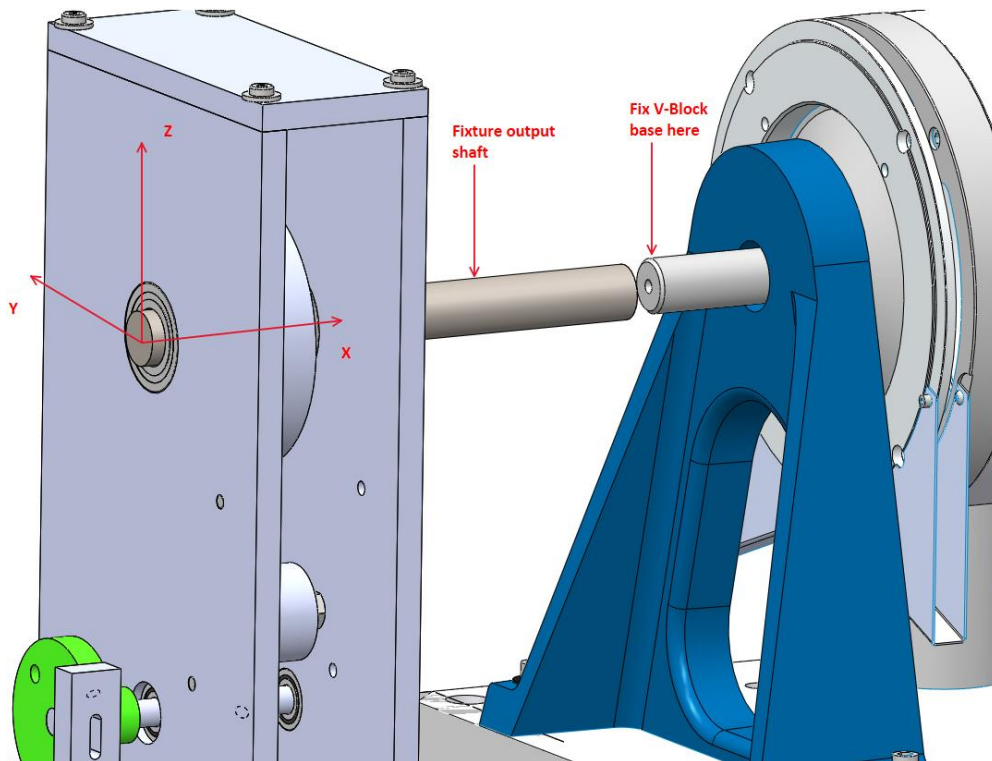
Step 3: Adjust the test indicator so that the indicator is at the middle of its range.

Step 4: Zero the test indicator and sweep the test indicator around the fixture output shaft by rotating the dyno shaft. If the tip of the test indicator loses contact or over travelled, adjust the location of the fixture along the Y direction as indicated in figure below.

Step 5: Repeat Step 4 until the desired total indicator reading is achieved (Desired TIR < .015”).

Step 6: Move the v-block base along the dyno shaft (ideally more than 1 in) and repeat step 3-5. Secure the fixture in place afterwards and verify the alignment.

Note: With the current reduction fixture design, alignment in Z direction can only be adjusted by placing shims at the bottom of the bearing plates or facing off the bearing plate bars.



BELT TENSIONING

Tools Required: 1 x ½” and 1 x 7/16” open wrenches

Step 1: Before the shafts are secured on the bearing, make sure the belt is on the shaft. (i.e. the belt is not tensioned but it is around the shaft.)

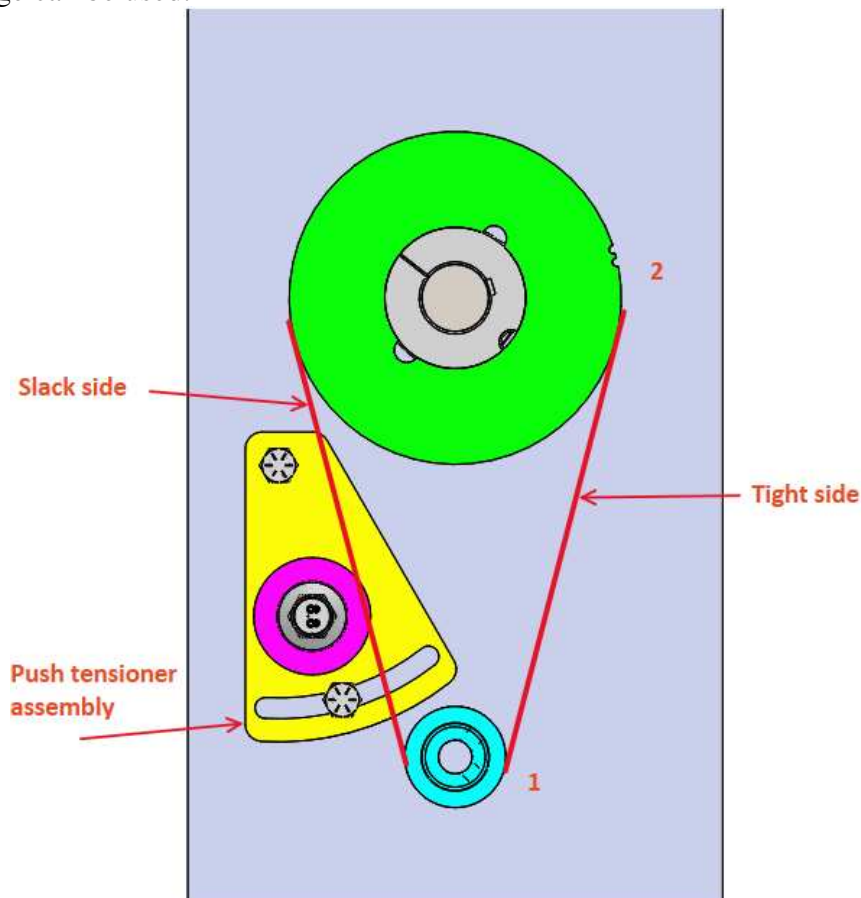
Step 2: Hold the belt at 1 and wrap the belt around the large pulley. Make sure that the belt is tight from 1 to 2. (See the figure below for reference).

Step 3: Loose the 2 x 5/16 -18 hex bolts using the wrenches. Push the tensioner in the direction indicated in figure below to tension the belt.

Step 4: After the belt is tensioned, tightened the 2 x 5/16 -18 hex while holding the belt tensioned.

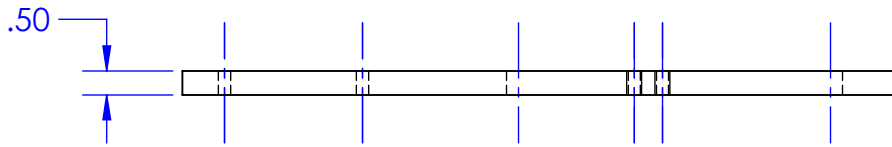
Step 5: Try and spin the large pulley. The whole reduction should turn smoothly.

Notes: In order to verify that the belt is tensioned per the manufacturer’s recommendation, a tension gauge can be used.

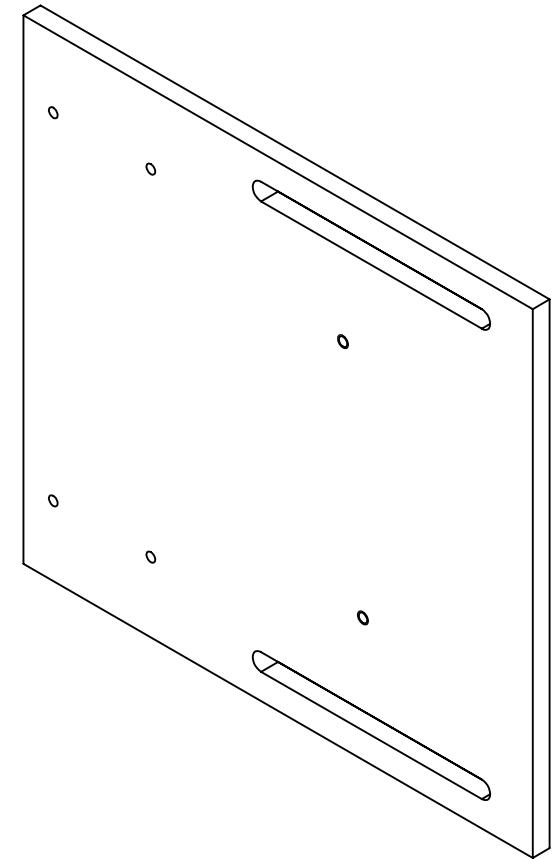
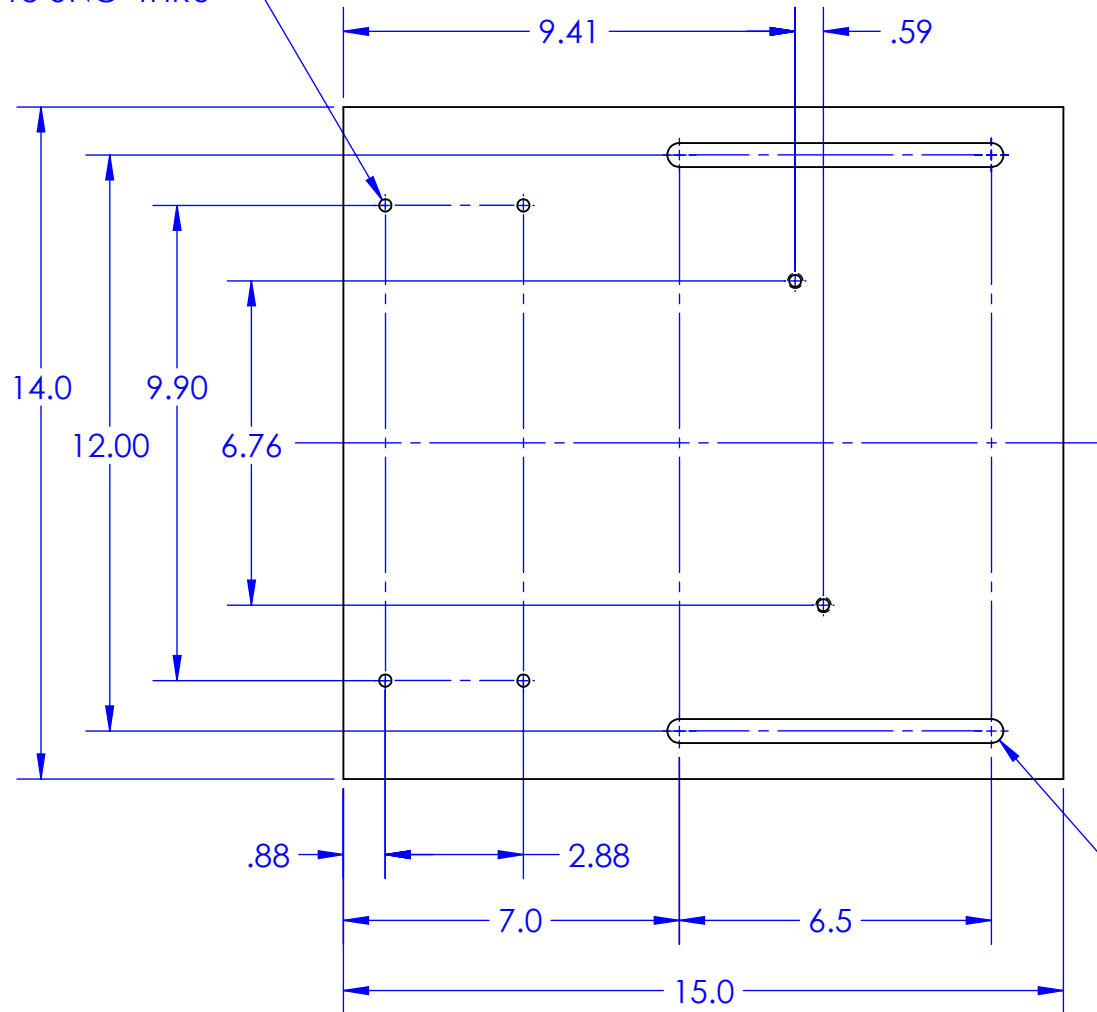


Appendix 17: Detail Drawings

The following documents are the detailed drawings for all components to be manufactured by the ICE Senior Project Team.



6X 5/16-18 UNC THRU

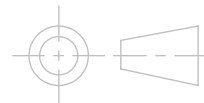


NOTE:
1. PLEASE MAKE A TEST CUT ON WATER JET TO ACCOUNT FOR THE KERF WIDTH.

4X R.25

UNLESS OTHERWISE SPECIFIED:
DIMENSIONS ARE IN INCHES
TOLERANCES:
ONE PLACE DECIMAL $\pm .1$
TWO PLACE DECIMAL $\pm .01$
THREE PLACE DECIMAL $\pm .005$

INTERPRET DRAWING
PER ASME Y14.5 2009



SMV ICE

DATE:
1/5/2020

MATERIAL:
6061-T6 ALUMINUM

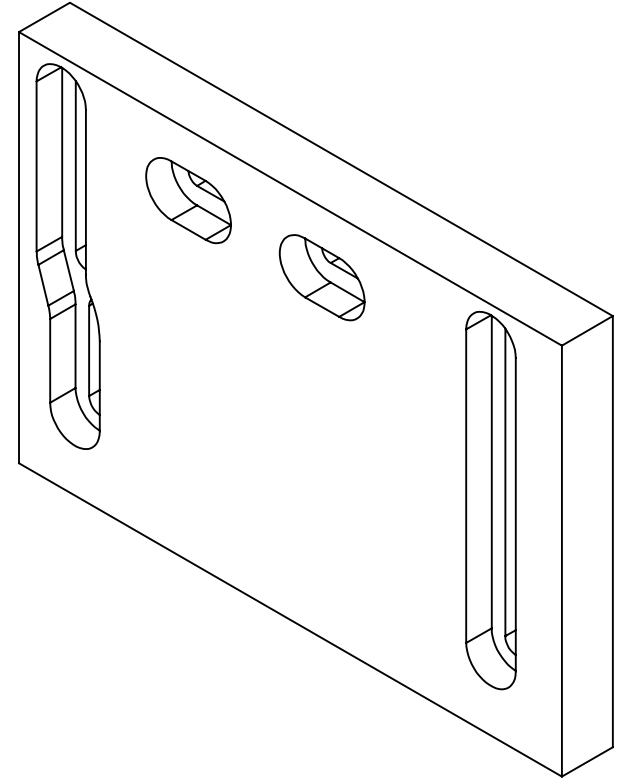
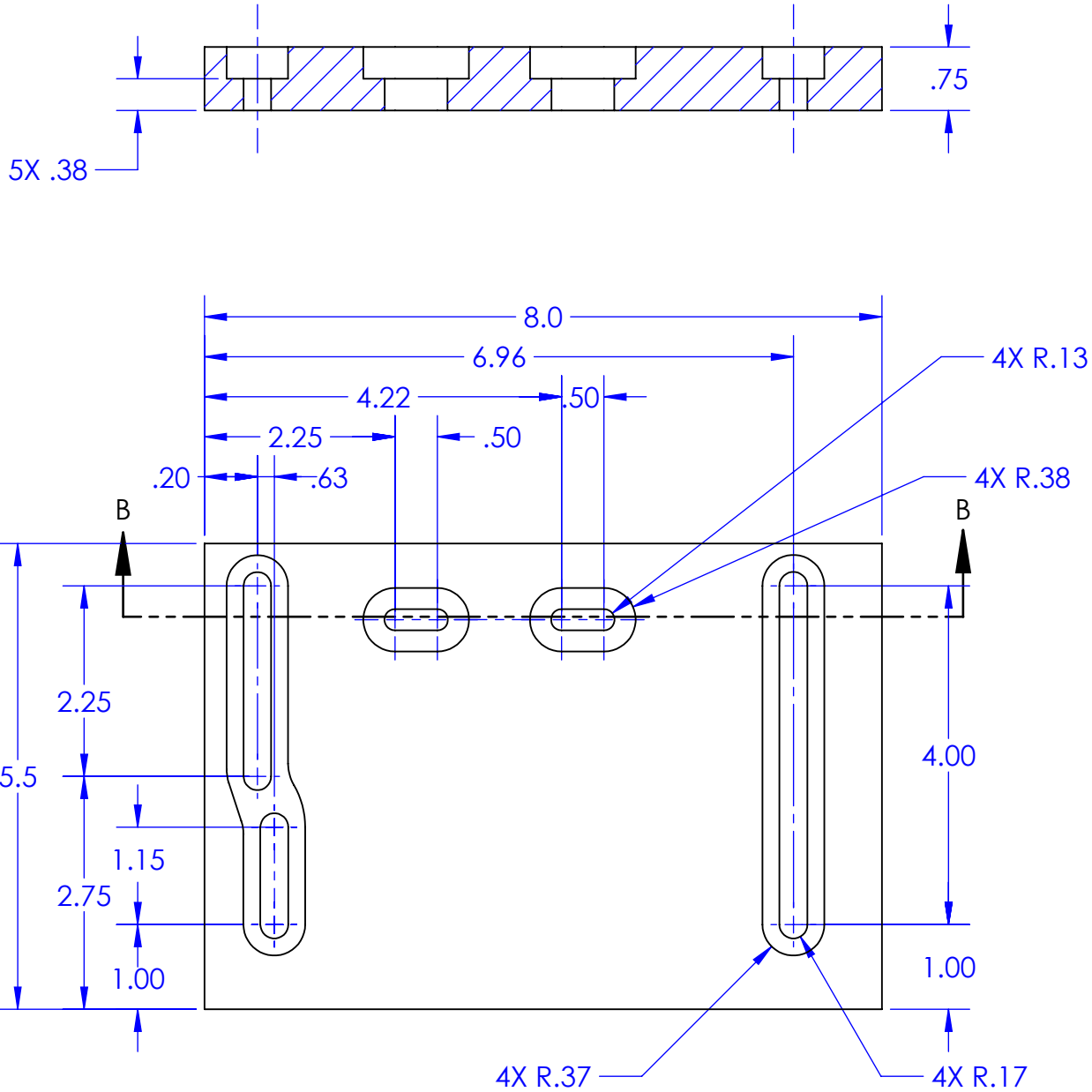
DRAWN BY:
PAING HTET LIN

TITLE:
REDUCTION BASE PLATE

SHEET 1 OF 12 SCALE: 1:4

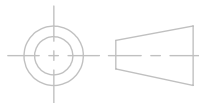
REV
B

SIZE
A



UNLESS OTHERWISE SPECIFIED:
 DIMENSIONS ARE IN INCHES
 TOLERANCES:
 ONE PLACE DECIMAL $\pm .1$
 TWO PLACE DECIMAL $\pm .01$
 THREE PLACE DECIMAL $\pm .005$

INTERPRET DRAWING
 PER ASME Y14.5 2009



SMV ICE

DATE:
 1/5/2020

MATERIAL:
 6061-T6 ALUMINUM

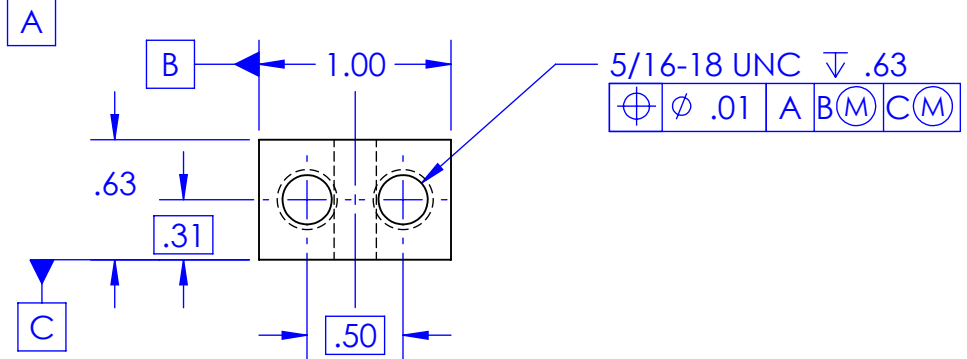
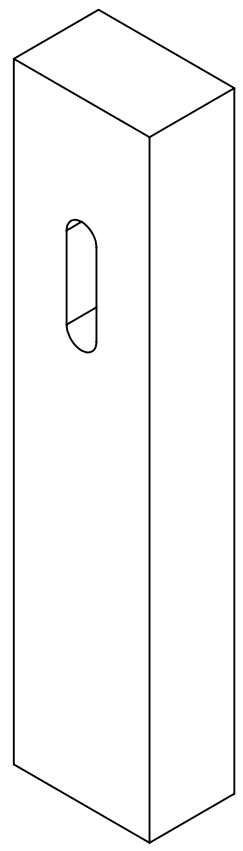
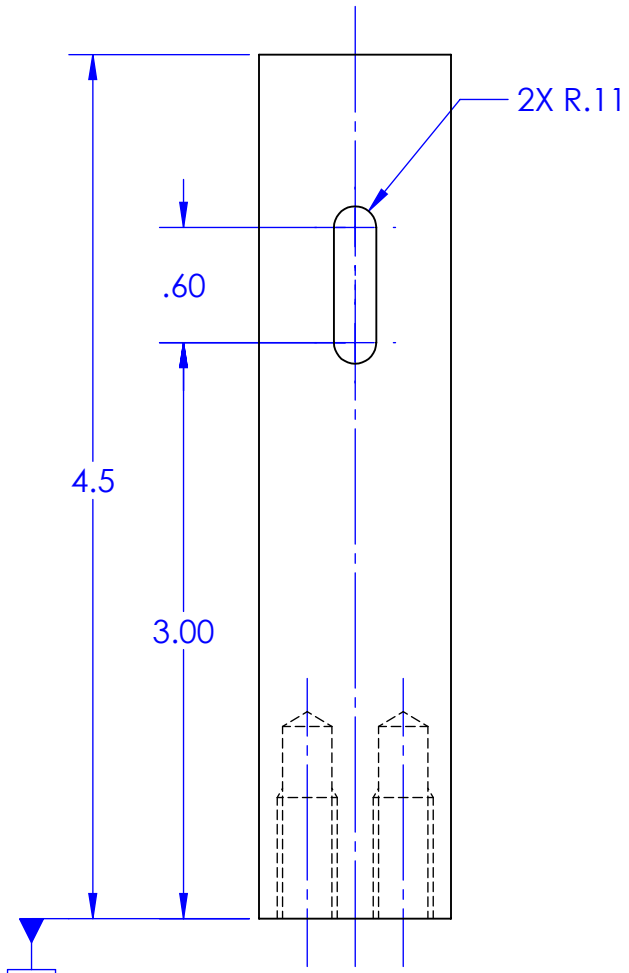
DRAWN BY:
 PAING HTET LIN

TITLE:
 ENGINE MOUNT BASE PLATE

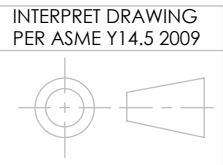
SHEET 2 OF 12 SCALE: 1:2

REV
B

SIZE
A



UNLESS OTHERWISE SPECIFIED:
 DIMENSIONS ARE IN INCHES
 TOLERANCES:
 ONE PLACE DECIMAL \pm .1
 TWO PLACE DECIMAL \pm .01
 THREE PLACE DECIMAL \pm .005



SMV ICE
 DATE: 1/5/2020

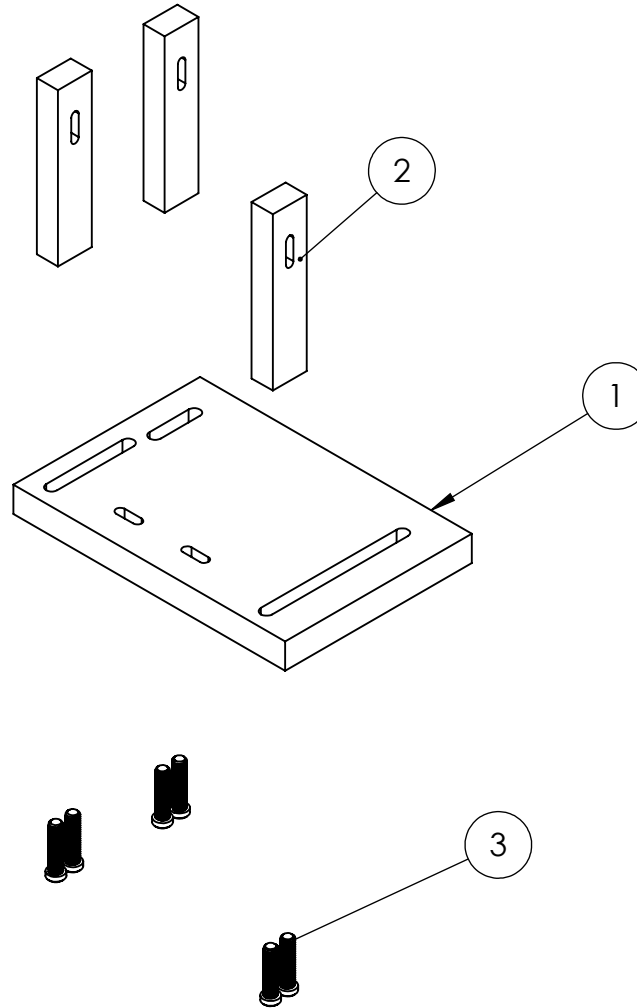
MATERIAL:
 6061-T6 ALUMINUM
 DRAWN BY:
 PAING HTET LIN

TITLE:
 ENGINE MOUNT RISER

SHEET 3 OF 12 SCALE: 1:1

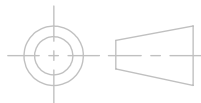
REV	SIZE
B	A

ITEM NO.	PART NUMBER	QTY.
1	ENGINE MOUNT BASE	1
2	ENGINE MOUNT RISER	3
3	5/16-18 SCREWS	6



UNLESS OTHERWISE SPECIFIED:
 DIMENSIONS ARE IN INCHES
 TOLERANCES:
 ONE PLACE DECIMAL $\pm .1$
 TWO PLACE DECIMAL $\pm .01$
 THREE PLACE DECIMAL $\pm .005$

INTERPRET DRAWING
 PER ASME Y14.5 2009



SMV ICE

MATERIAL:

TITLE:

ENGINE MOUNT SUBASSEMBLY

DATE:

1/5/2020

DRAWN BY:

PAING HTET LIN

SHEET 1 OF 1

SCALE: 1:4

REV

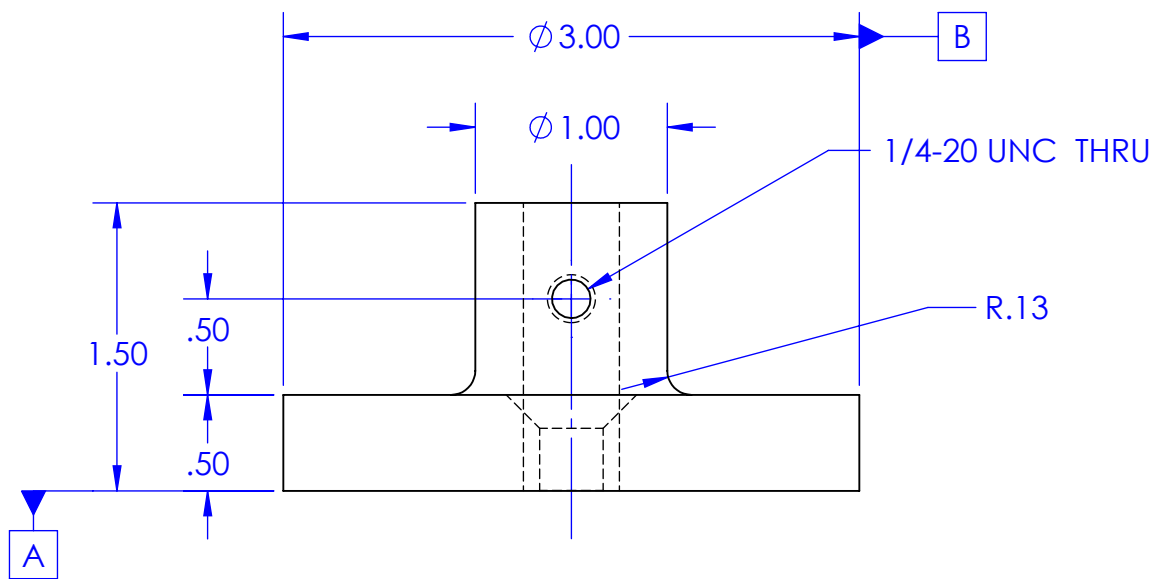
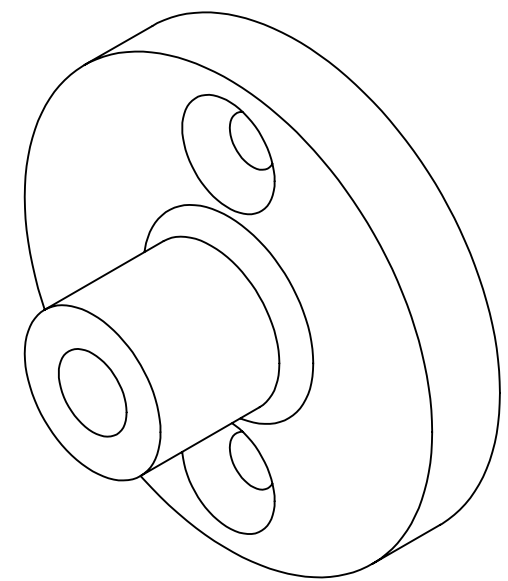
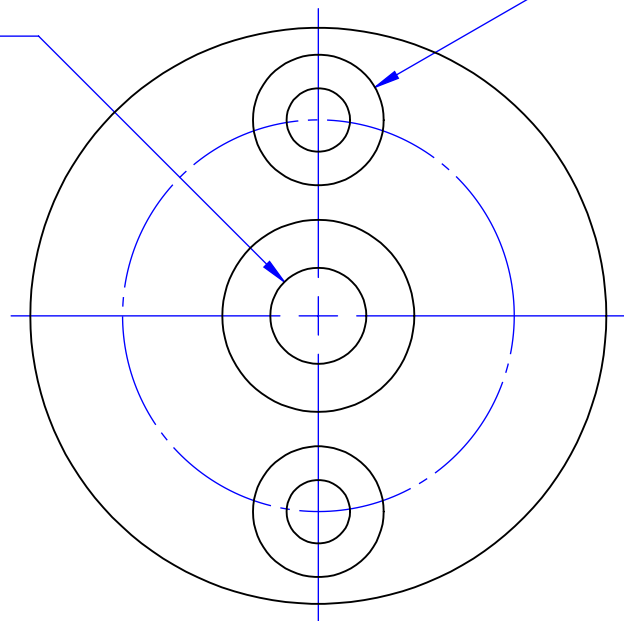
A

SIZE

A

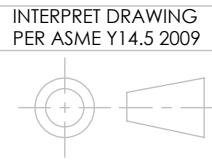
$\phi .500^{+.001}_{-.000}$
 $\phi .003$ A B

2X $\phi .33$ THRU
 $\surd \phi .68 \times 90^\circ$
 $\phi .003$ A B



NOTES:
 1. THE COUNTERSINKS ARE FOR M8-1.25 BOLTS AND THEY ARE USED TO LOCATE THE TWO THREADED HOLES ON THE FLYWHEEL OF THE ENGINE.

UNLESS OTHERWISE SPECIFIED:
 DIMENSIONS ARE IN INCHES
 TOLERANCES:
 ONE PLACE DECIMAL $\pm .1$
 TWO PLACE DECIMAL $\pm .01$
 THREE PLACE DECIMAL $\pm .005$



SMV ICE

MATERIAL:
 6061-T6 ALUMINUM

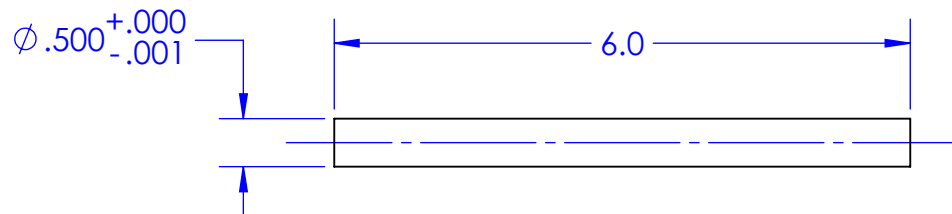
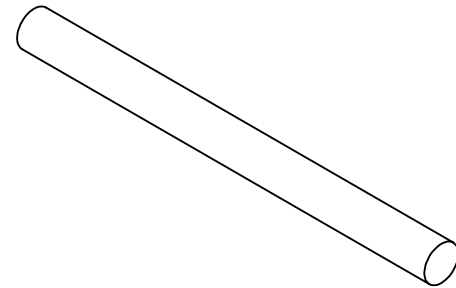
TITLE:
 ENGINE TO REDUCTION COUPLER

DATE:
 1/5/2020

DRAWN BY:
 PAING HTET LIN

SHEET 4 OF 12 SCALE: 1:1

REV **B** SIZE **A**

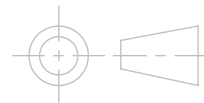


NOTES:

1. FLATS NEEDS TO BE NOTCHED AT THE LOCATIONS OF SETSCREWS IF NEEDED.
2. LOCATION OF SET SCREWS ARE DETERMINED WHILE ASSEMBLY.

UNLESS OTHERWISE SPECIFIED:
 DIMENSIONS ARE IN INCHES
 TOLERANCES:
 ONE PLACE DECIMAL $\pm .1$
 TWO PLACE DECIMAL $\pm .01$
 THREE PLACE DECIMAL $\pm .005$

INTERPRET DRAWING
 PER ASME Y14.5 2009



SMV ICE

DATE:
 1/5/2020

MATERIAL:
 AISI 4140 STEEL

DRAWN BY:
 PAING HTET LIN

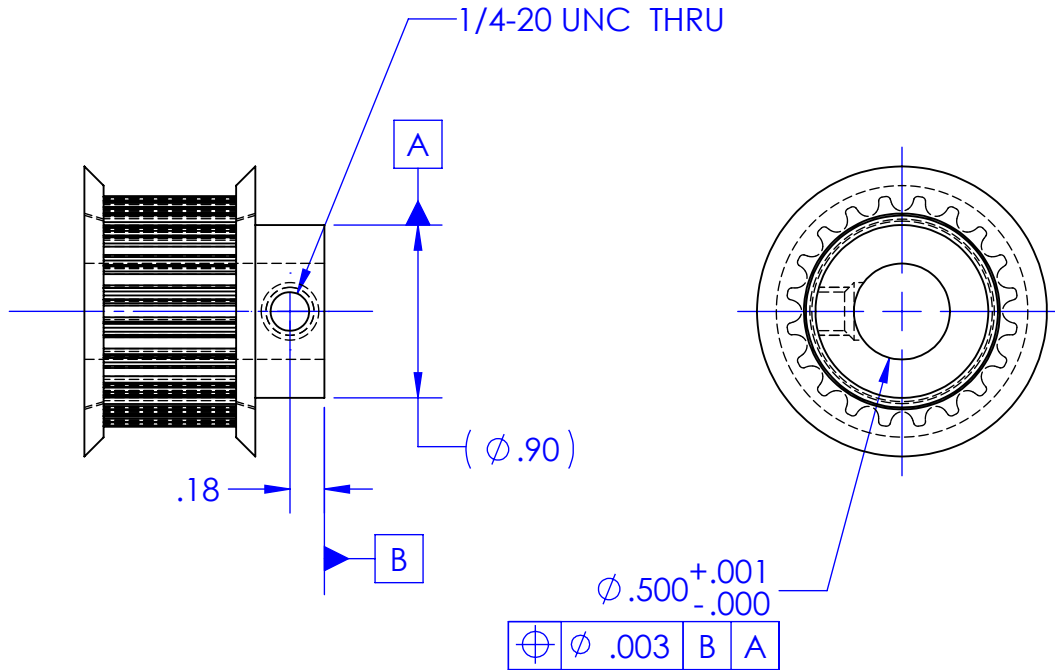
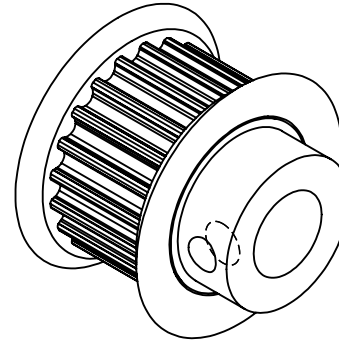
TITLE:
 SMALL SPROCKET SHAFT

SHEET 5 OF 12 SCALE: 1:1

REV	SIZE
B	A

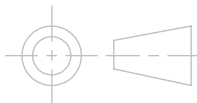
NOTES:

1. THE SPROCKET IS BOUGHT FROM AN EXTERNAL VENDOR.
2. THE $\phi .500^{+.001}_{-0}$ IS BORED ON LATHE TO GET TIGHT TOLERANCE FOR SHAFT.



UNLESS OTHERWISE SPECIFIED:
 DIMENSIONS ARE IN INCHES
 TOLERANCES:
 ONE PLACE DECIMAL $\pm .1$
 TWO PLACE DECIMAL $\pm .01$
 THREE PLACE DECIMAL $\pm .005$

INTERPRET DRAWING
 PER ASME Y14.5 2009



SMV ICE

DATE:
 1/5/2020

MATERIAL:
 AISI 4140 STEEL

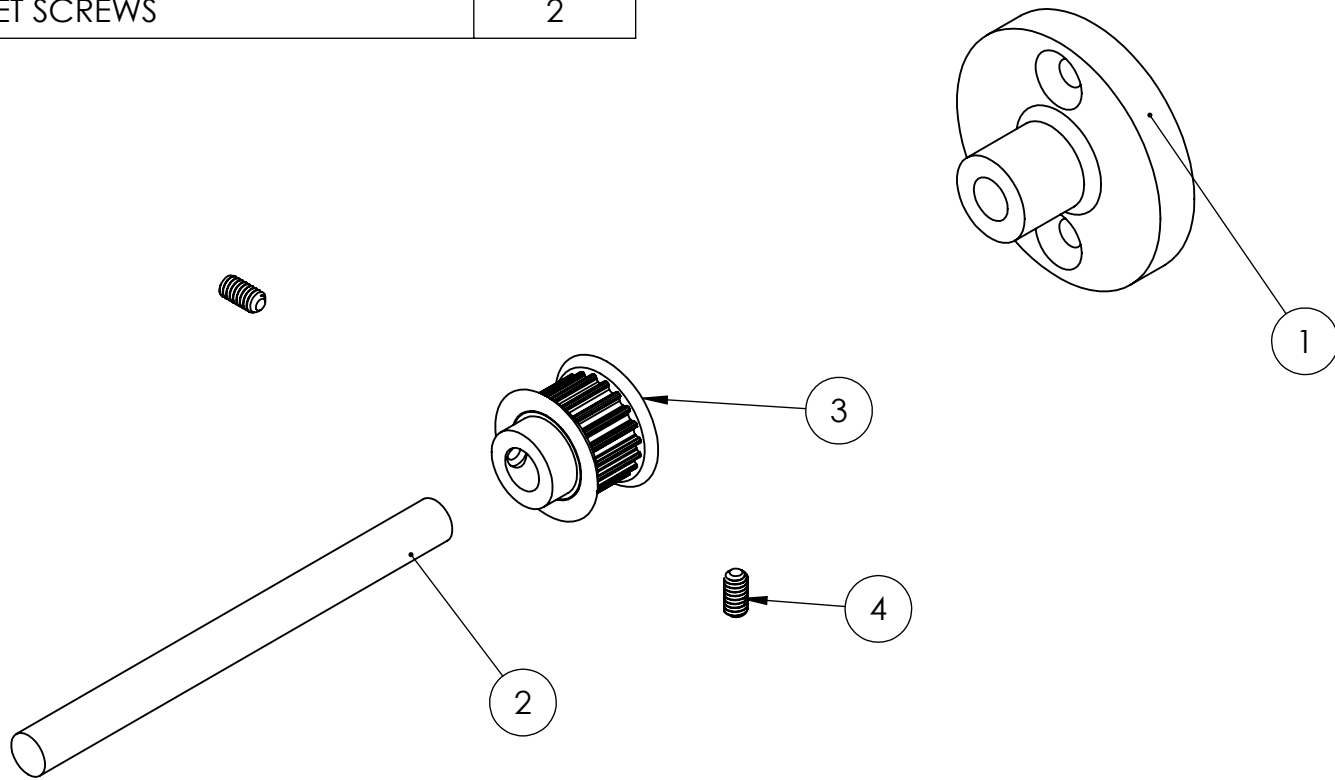
DRAWN BY:
 PAING HTET LIN

TITLE:
 SMALL SPROCKET

SHEET 6 OF 12 SCALE: 1:1

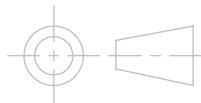
REV	SIZE
B	A

ITEM NO.	DESCRIPTION	QTY.
1	ENGINE TO REDUCTION COUPLER	1
2	SMALL SPROCKET SHAFT	1
3	GATES SMALL SPROCKET	1
4	1/4 - 20 SET SCREWS	2



UNLESS OTHERWISE SPECIFIED:
 DIMENSIONS ARE IN INCHES
 TOLERANCES:
 ONE PLACE DECIMAL ± .1
 TWO PLACE DECIMAL ± .01
 THREE PLACE DECIMAL ± .005

INTERPRET DRAWING
 PER ASME Y14.5 2009



SMV ICE

DATE:
 1/5/2020

MATERIAL:

DRAWN BY:
 PAING HTET LIN

TITLE:

SMALL SPROCKET SUBASSEMBLY

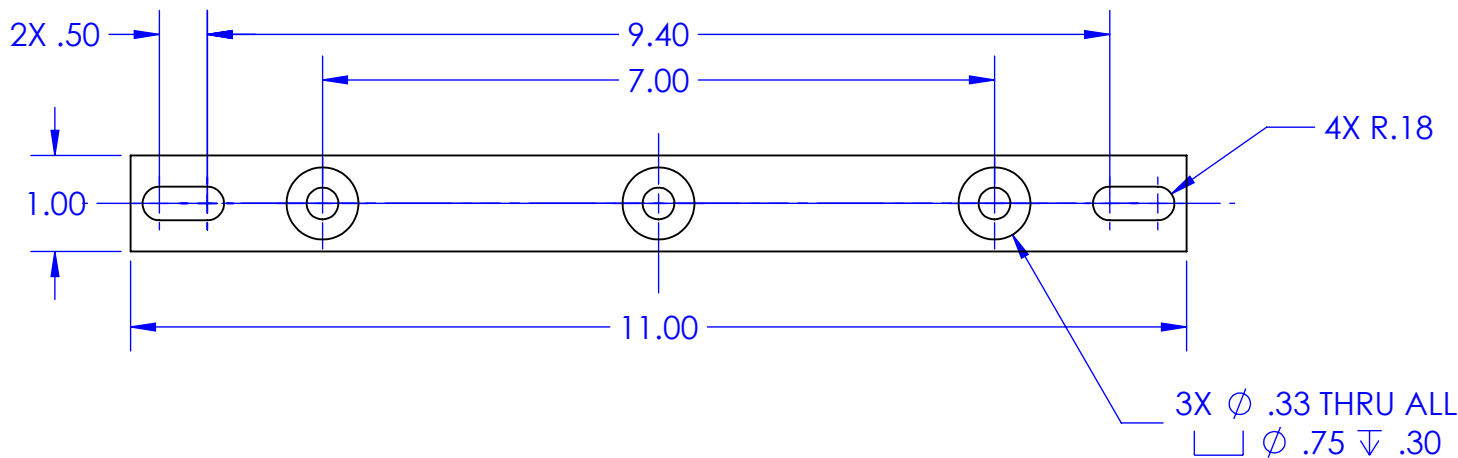
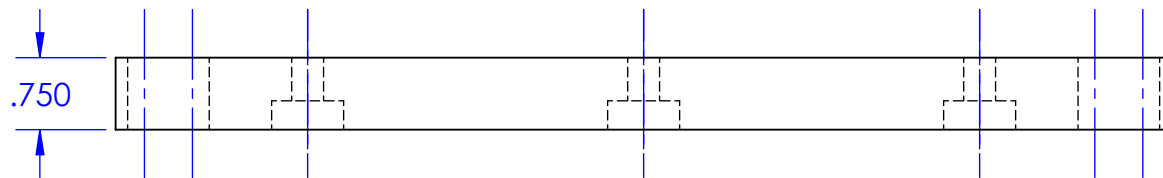
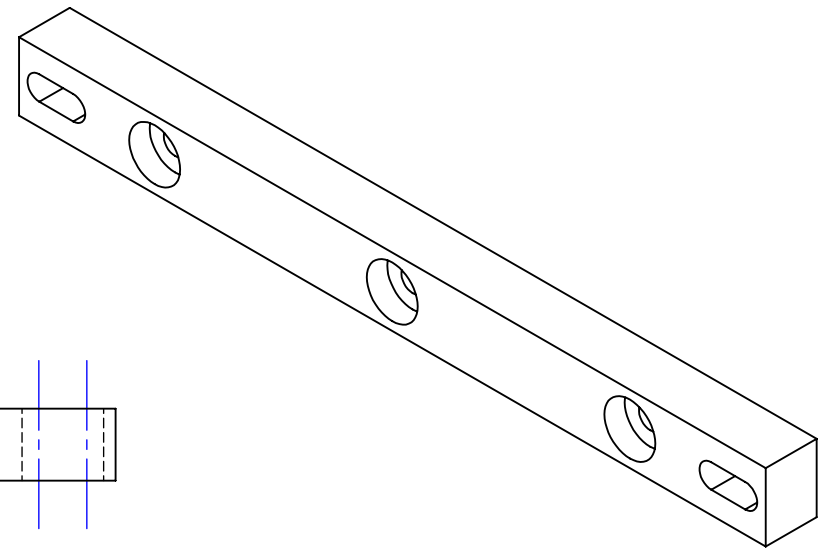
SHEET 1 OF 1

SCALE: 1:2

REV	SIZE
A	A

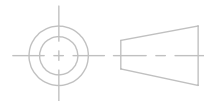
NOTES:

1. .750 THICKNESS DIMENSION IS FACED OFF BY .005 TO MAKE .745 FOR SHAFT ALIGNMENT. DEPENDING ON HOW THE BASE PLATE IS MADE, THIS DIMENSION CAN BE ADJUSTED TO GET THE REQUIRED SHAFT ALIGNMENT.



UNLESS OTHERWISE SPECIFIED:
 DIMENSIONS ARE IN INCHES
 TOLERANCES:
 ONE PLACE DECIMAL \pm .1
 TWO PLACE DECIMAL \pm .01
 THREE PLACE DECIMAL \pm .005

INTERPRET DRAWING
 PER ASME Y14.5 2009



SMV ICE

DATE:
 1/5/2020

MATERIAL:
 6061-T6 ALUMINUM

DRAWN BY:
 PAING HTET LIN

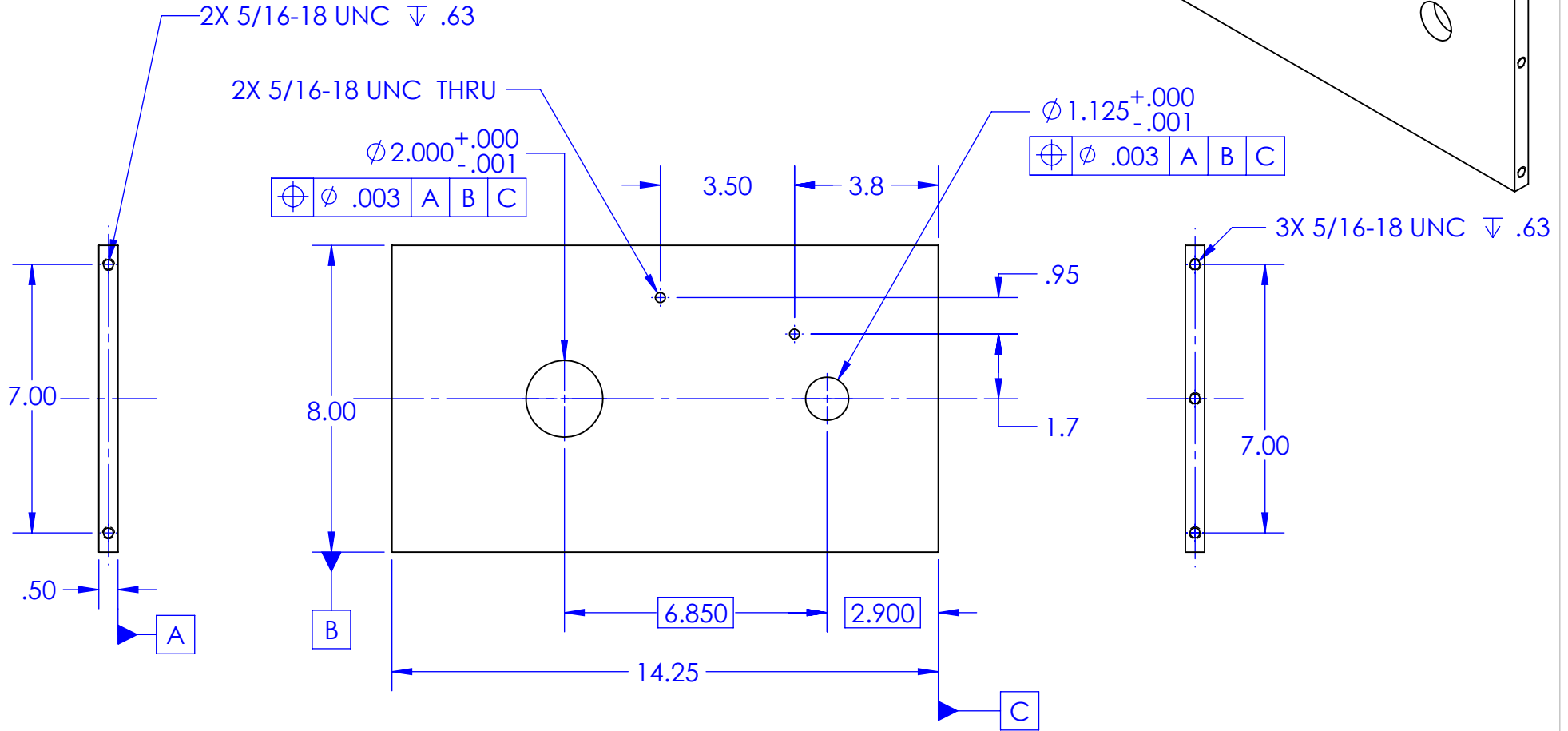
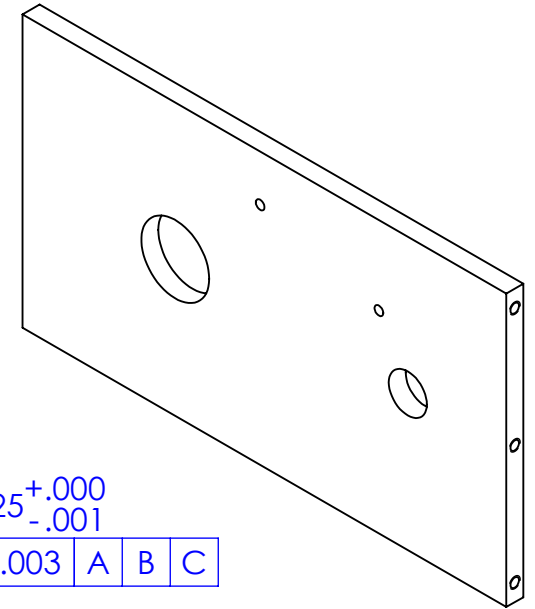
TITLE:
 BEARING PLATE BASE

SHEET 7 OF 12 SCALE: 1:2

REV	SIZE
B	A

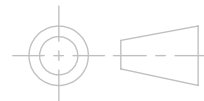
NOTES:

- 2X 5/16-18 UNC ∇ .63 HOLES ARE MADE TO BE 1/4-20 DURING TESTING SINCE THE BEARING PLATE END HOLES ARE UNDERSIZED DURING WATER JETTING.



UNLESS OTHERWISE SPECIFIED:
 DIMENSIONS ARE IN INCHES
 TOLERANCES:
 ONE PLACE DECIMAL $\pm .1$
 TWO PLACE DECIMAL $\pm .01$
 THREE PLACE DECIMAL $\pm .005$

INTERPRET DRAWING
 PER ASME Y14.5 2009



SMV ICE

DATE:
 1/5/2020

MATERIAL:
 6061-T6 ALUMINUM

DRAWN BY:
 PAING HTET LIN

TITLE:
 BEARING PLATE

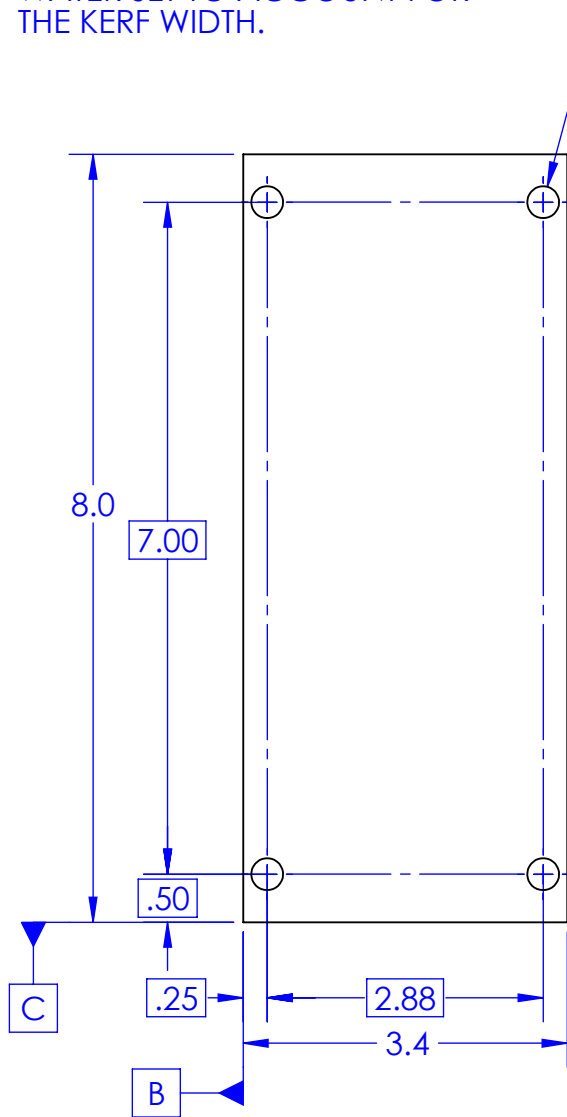
SHEET 8 OF 12 SCALE: 1:4

REV
B

SIZE
A

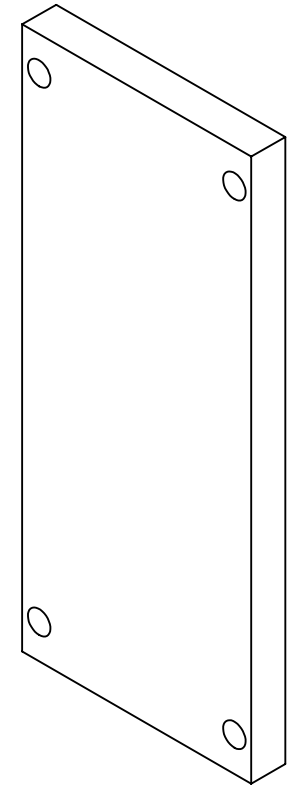
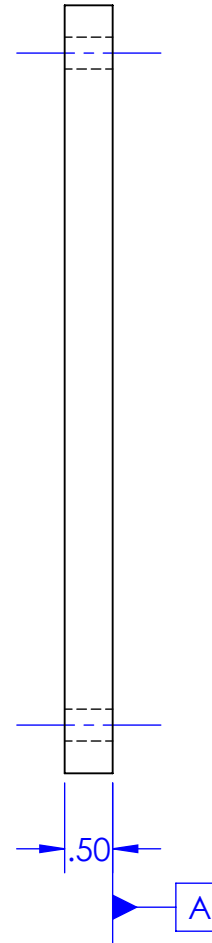
NOTE:

- PLEASE MAKE A TEST CUT ON WATER JET TO ACCOUNT FOR THE KERF WIDTH.



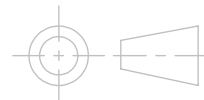
4X ϕ .33 THRU

ϕ	ϕ .02 (M)	A	B (M)	C (M)
ϕ	ϕ .01 (M)	A		



UNLESS OTHERWISE SPECIFIED:
 DIMENSIONS ARE IN INCHES
 TOLERANCES:
 ONE PLACE DECIMAL \pm .1
 TWO PLACE DECIMAL \pm .01
 THREE PLACE DECIMAL \pm .005

INTERPRET DRAWING
 PER ASME Y14.5 2009



SMV ICE

DATE:
 1/5/2020

MATERIAL:
 6061-T6 ALUMINUM

DRAWN BY:
 PAING HTET LIN

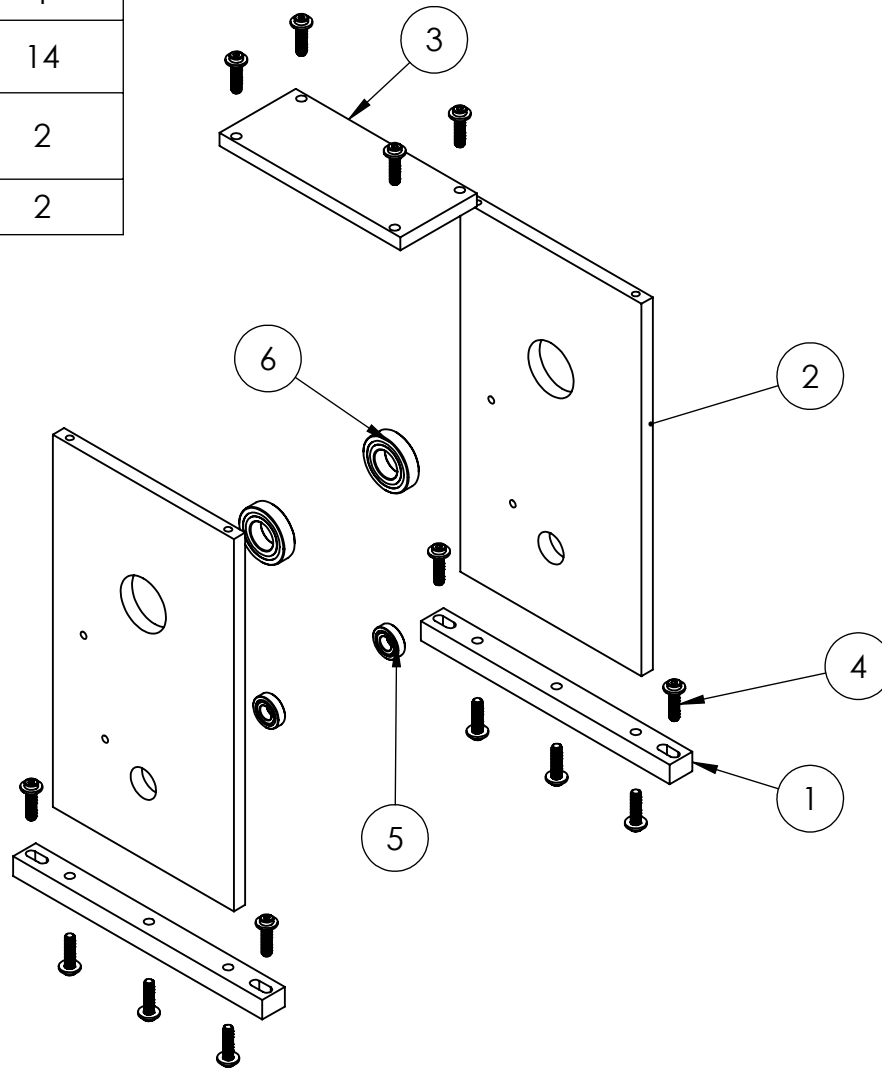
TITLE:
 BEARING PLATE END

SHEET 9 OF 12 SCALE: 1:2

REV
B

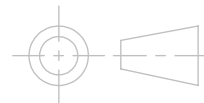
SIZE
A

ITEM NO.	DESCRIPTION	QTY.
1	BEARING PLATE BASE	2
2	BEARING PLATE	2
3	BEARING PLATE END	1
4	5/16 -18 SCREW WITH WASHER	14
5	1/2" ID, 1-1/4" OD BEARING	2
6	1" ID, 2" OD BEARING	2



UNLESS OTHERWISE SPECIFIED:
 DIMENSIONS ARE IN INCHES
 TOLERANCES:
 ONE PLACE DECIMAL $\pm .1$
 TWO PLACE DECIMAL $\pm .01$
 THREE PLACE DECIMAL $\pm .005$

INTERPRET DRAWING
 PER ASME Y14.5 2009



SMV ICE

DATE:
 10/23/2019

MATERIAL:

DRAWN BY:
 PAING HTET LIN

TITLE:

BEARING PLATE SUBASSEMBLY

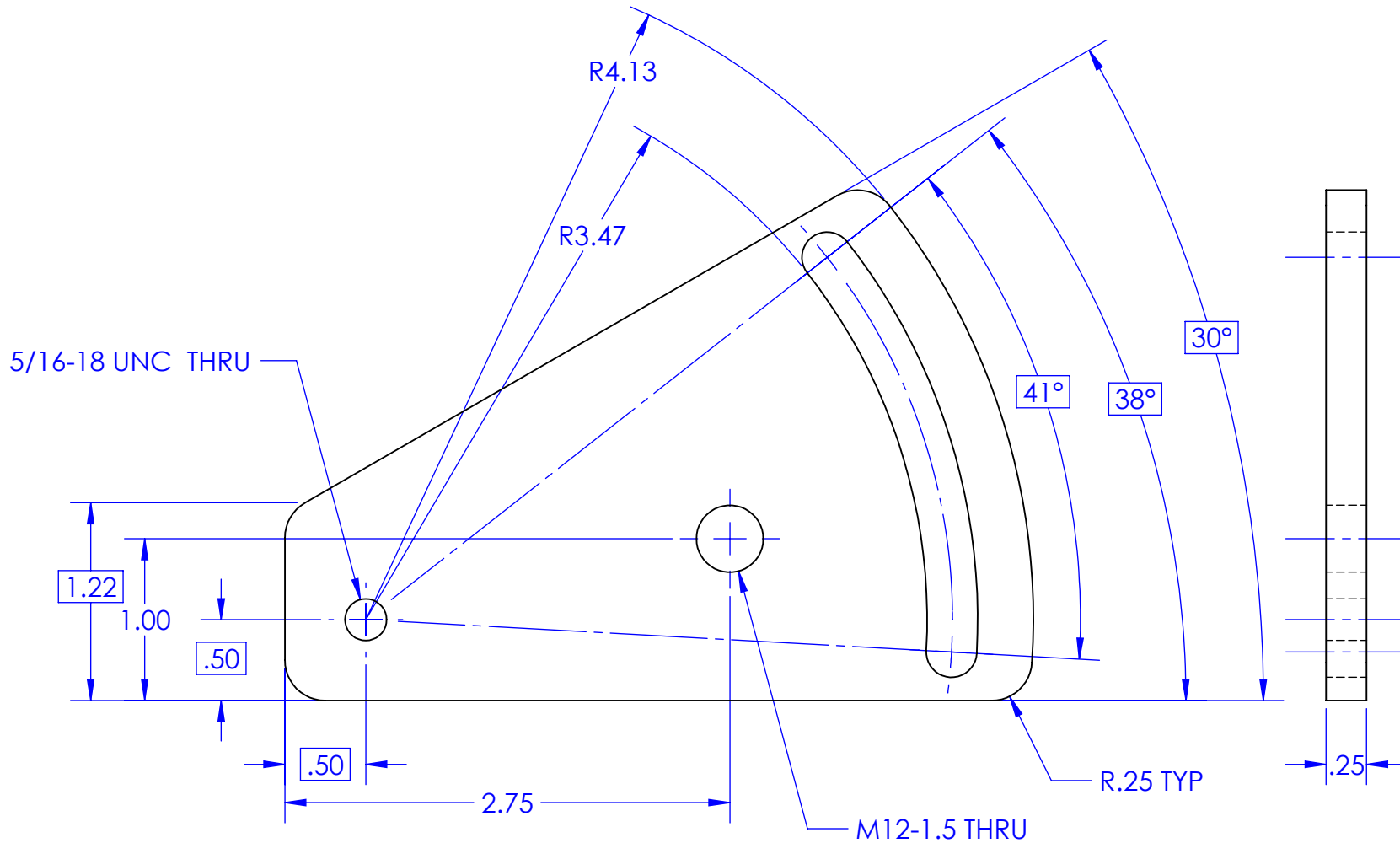
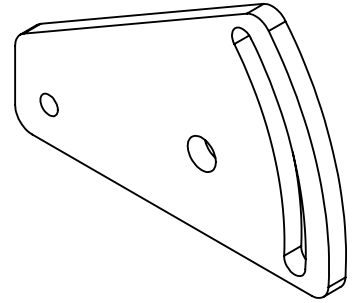
SHEET 1 OF 1

SCALE:1:6

REV	SIZE
A	A

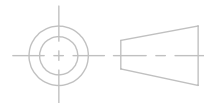
NOTE:

1. PLEASE MAKE A TEST CUT ON WATER JET TO ACCOUNT FOR THE KERF WIDTH.
2. SLOT WIDTH = .31"
3. TOLERANCES:
ANGLES = $\pm 1^\circ$



UNLESS OTHERWISE SPECIFIED:
DIMENSIONS ARE IN INCHES
TOLERANCES:
ONE PLACE DECIMAL $\pm .1$
TWO PLACE DECIMAL $\pm .01$
THREE PLACE DECIMAL $\pm .005$

INTERPRET DRAWING
PER ASME Y14.5 2009



SMV ICE

DATE:
1/5/2020

MATERIAL:
AISI 4140 STEEL

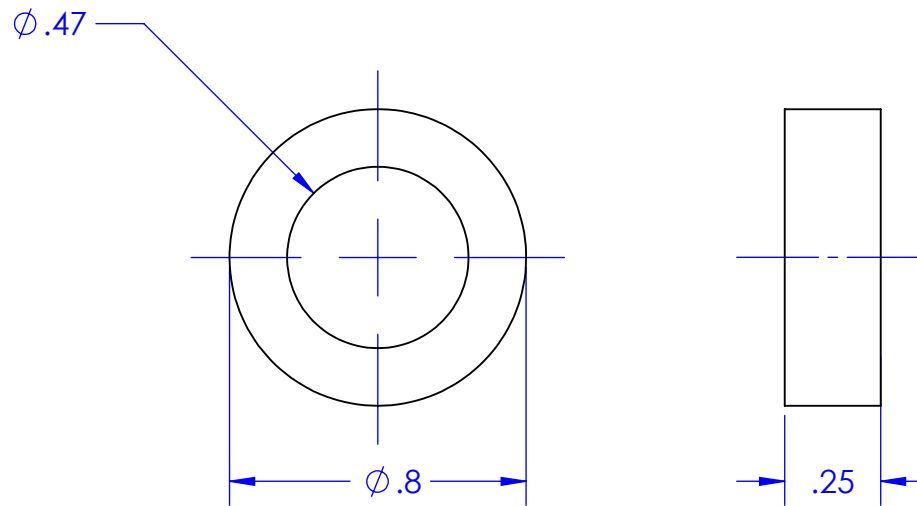
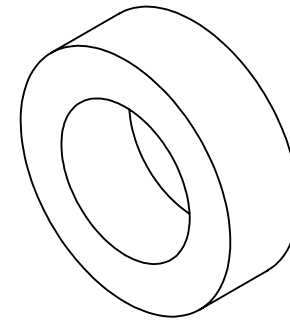
DRAWN BY:
PAING HTET LIN

TITLE:
TENSIONER BASE

SHEET 10 OF 12 SCALE: 1:1

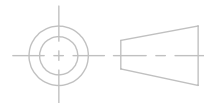
REV
B

SIZE
A



UNLESS OTHERWISE SPECIFIED:
DIMENSIONS ARE IN INCHES
TOLERANCES:
ONE PLACE DECIMAL $\pm .1$
TWO PLACE DECIMAL $\pm .01$
THREE PLACE DECIMAL $\pm .005$

INTERPRET DRAWING
PER ASME Y14.5 2009



SMV ICE

DATE:
1/5/2020

MATERIAL:
6061-T6 ALUMINUM

DRAWN BY:
PAING HTET LIN

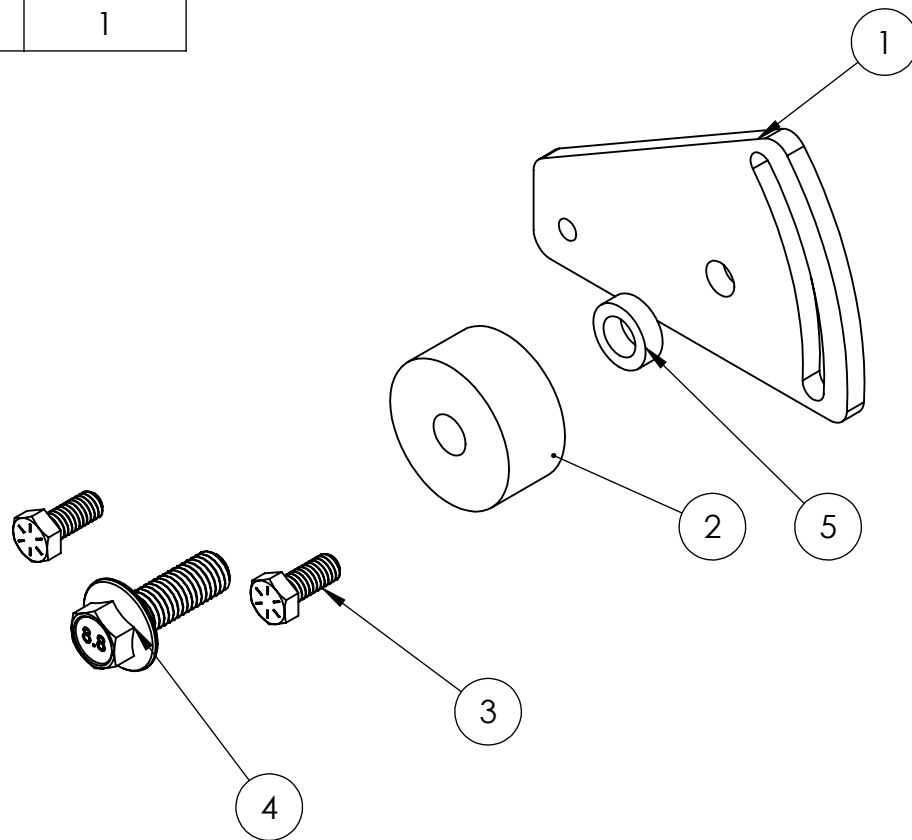
TITLE:
TENSIONER SPACER

SHEET 11 OF 12 SCALE: 2:1

REV
B

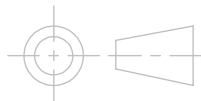
SIZE
A

ITEM NO.	DESCRIPTION	QTY.
1	TENSIONER BASE	1
2	IDLER	1
3	5/16-18 HEX BOLT	2
4	M12 - 1.5 HEX BOLT	1
5	SPACER	1



UNLESS OTHERWISE SPECIFIED:
 DIMENSIONS ARE IN INCHES
 TOLERANCES:
 ONE PLACE DECIMAL $\pm .1$
 TWO PLACE DECIMAL $\pm .01$
 THREE PLACE DECIMAL $\pm .005$

INTERPRET DRAWING
 PER ASME Y14.5 2009



SMV ICE

MATERIAL:

TITLE:

TENSIONER SUBASSEMBLY

DATE:

1/5/2020

DRAWN BY:

PAING HTET LIN

SHEET 1 OF 1

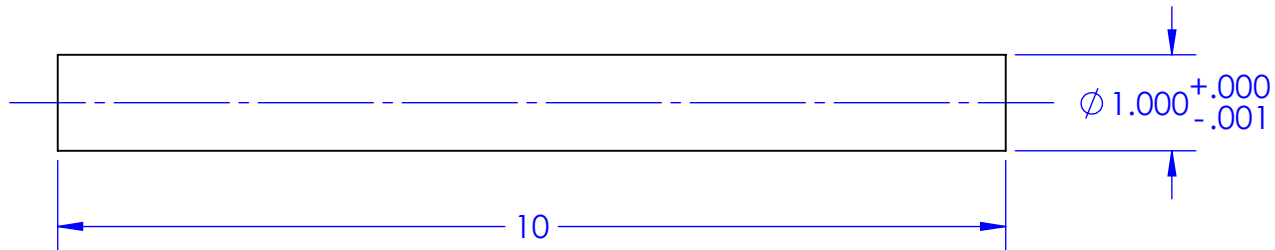
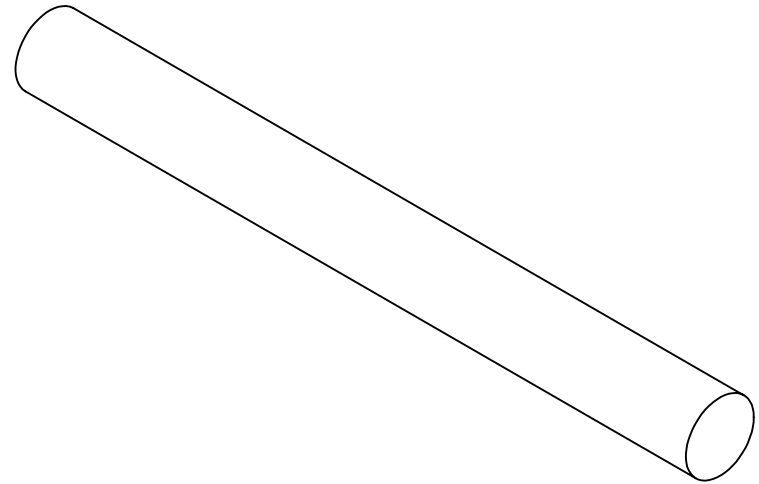
SCALE: 1:2

REV

A

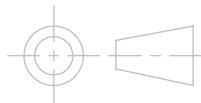
SIZE

A



UNLESS OTHERWISE SPECIFIED:
DIMENSIONS ARE IN INCHES
TOLERANCES:
ONE PLACE DECIMAL $\pm .1$
TWO PLACE DECIMAL $\pm .01$
THREE PLACE DECIMAL $\pm .005$

INTERPRET DRAWING
PER ASME Y14.5 2009



SMV ICE

DATE:
1/5/2020

MATERIAL:
AISI 4140 STEEL

DRAWN BY:
PAING HTET LIN

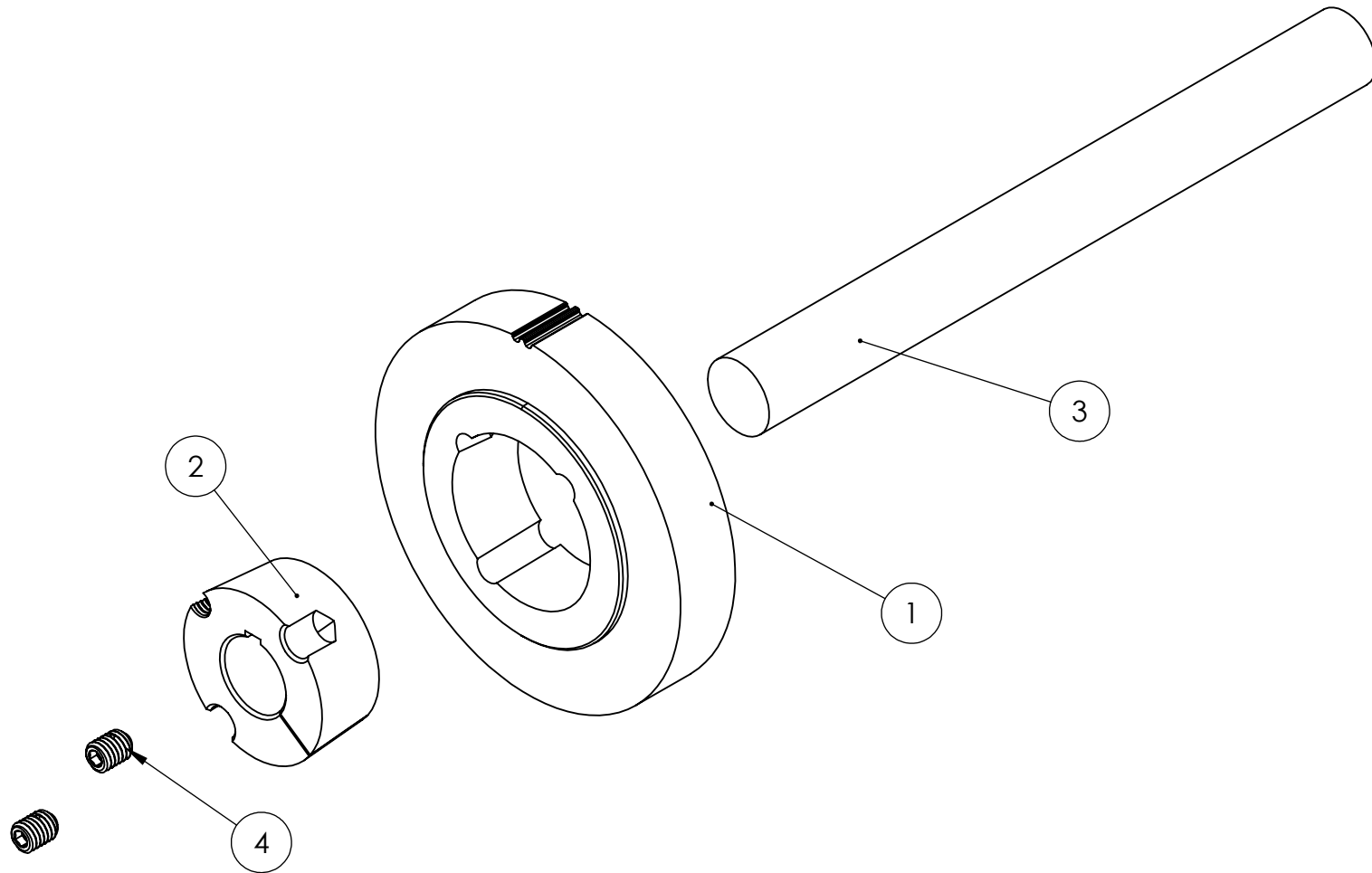
TITLE:
BIG SPROCKET SHAFT

SHEET 12 OF 12 SCALE: 1:1

REV
B

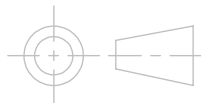
SIZE
A

ITEM NO.	DESCRIPTION	QTY.
1	GATES_TIMING_PULLEY_LAR GE	1
2	1610_BUSHING	1
3	LARGE_PULLEY_SHAFT	1
4	1610 BUSHING SET SCREW	2



UNLESS OTHERWISE SPECIFIED:
DIMENSIONS ARE IN INCHES
TOLERANCES:
ONE PLACE DECIMAL $\pm .1$
TWO PLACE DECIMAL $\pm .01$
THREE PLACE DECIMAL $\pm .005$

INTERPRET DRAWING
PER ASME Y14.5 2009



SMV ICE

DATE:
1/5/2020

MATERIAL:

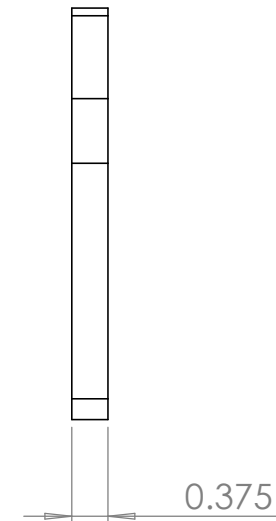
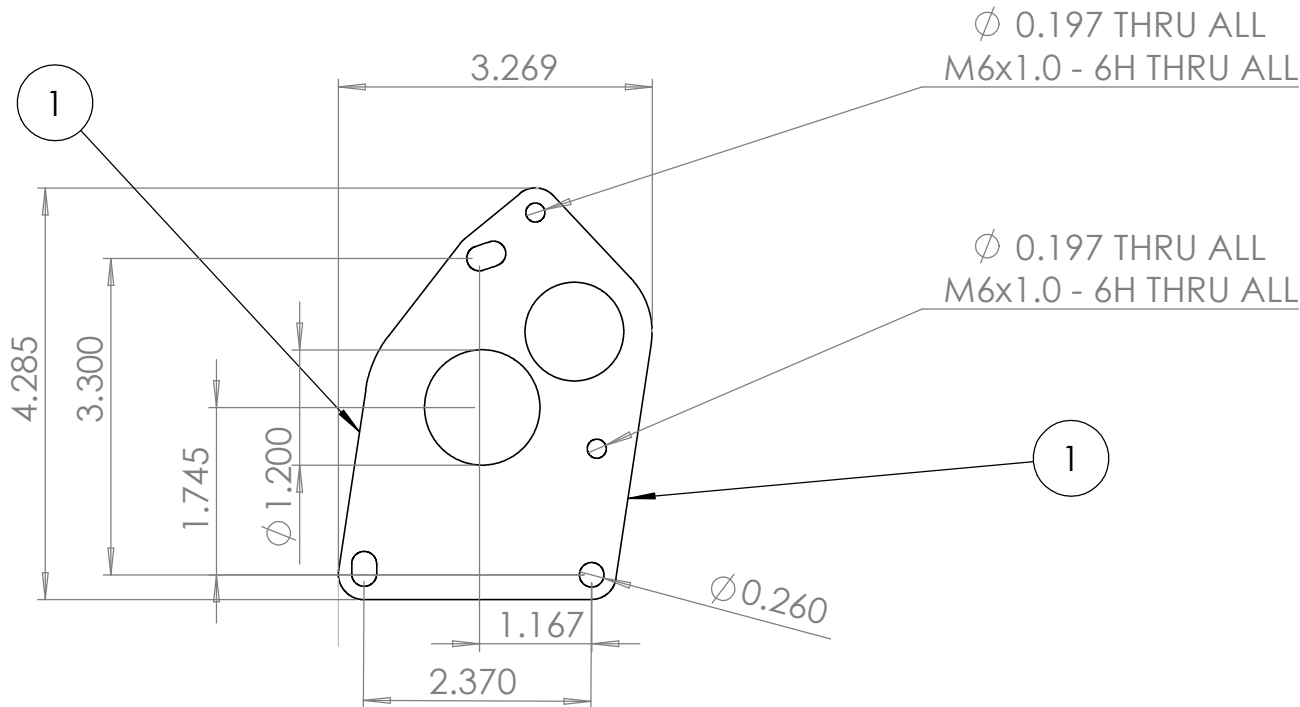
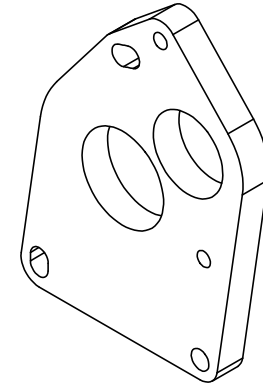
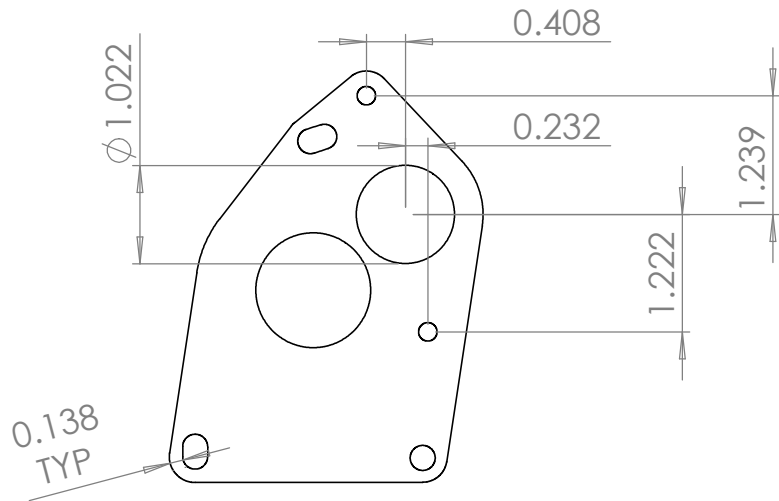
DRAWN BY:
PAING HTET LIN

TITLE: BIG SPROCKET SUBASSEMBLY

SHEET 1 OF 1

SCALE: 1:2

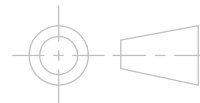
REV	SIZE
A	A



1. THESE TWO SIDES ARE PARALLEL FOR FIXTURING
2. JUST USE THE WATERJET AND THEN TAP THE HOLES

UNLESS OTHERWISE SPECIFIED:
DIMENSIONS ARE IN INCHES
TOLERANCES:
ONE PLACE DECIMAL $\pm .1$
TWO PLACE DECIMAL $\pm .01$
THREE PLACE DECIMAL $\pm .005$

INTERPRET DRAWING
PER ASME Y14.5 2009



SMV ICE

DATE:
3/7/2020

MATERIAL:

ALUMINUM

DRAWN BY:

PHILIPPE HABETS

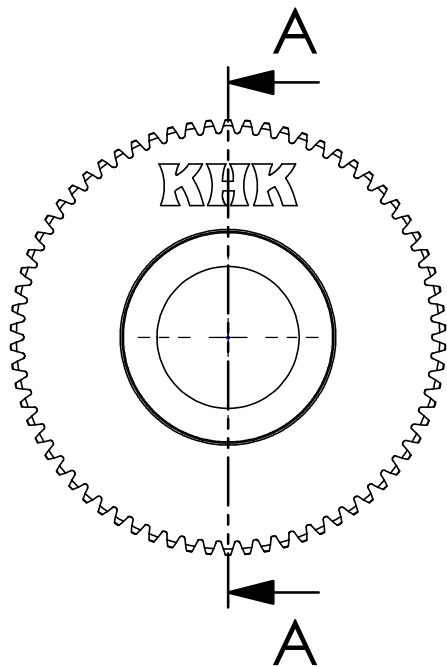
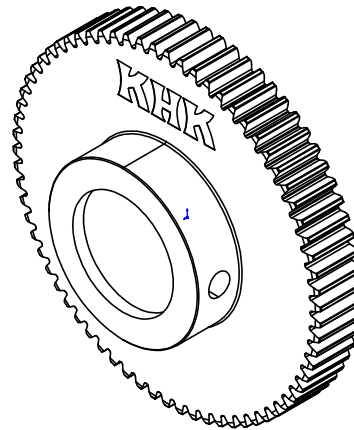
TITLE:

ESS BRACKET

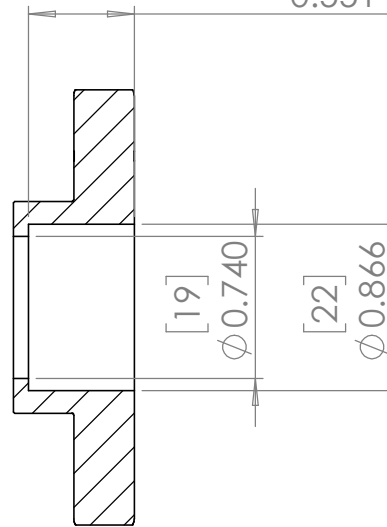
SHEET 1 OF 1

SCALE: 1:2

REV	SIZE
A	A



[14]
0.551

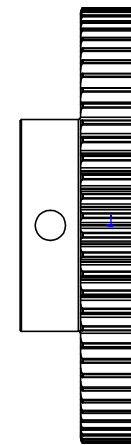


[19]

ϕ 0.740

[22]

ϕ 0.866

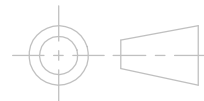


SECTION A-A

PRIMARY DIMENSIONS INCHES
SECONDARY MM

UNLESS OTHERWISE SPECIFIED:
DIMENSIONS ARE IN INCHES
TOLERANCES:
ONE PLACE DECIMAL $\pm .1$
TWO PLACE DECIMAL $\pm .01$
THREE PLACE DECIMAL $\pm .005$

INTERPRET DRAWING
PER ASME Y14.5 2009



SMV ICE

DATE:
3/7/2020

MATERIAL:

STEEL

DRAWN BY:

PHILIPPE HABETS

TITLE:

KHK GEAR MODIFICATIONS

SHEET 1 OF 1

SCALE: 1:1

REV

A

SIZE

A